NASA/CR—1999-209405

Experimental Verification of Material Flammability in Space

A.V. Ivanov
Keldysh Research Center, Moscow, Russia

Ye.V. Balashov, and T.V. Andreeva
RSC Energia, Korolev, Russia

A.S. Melikhov
All-Russian Scientific Research Institute for Fire Safety, Moscow, Russia

National Aeronautics and
Space Administration

Glenn Research Center

November 1999

Acknowledgments

The project described in this reported was conducted as a joint effort by teams in Russia and the United States. For the Russian side, material qualification, ground testing, crew training, space experiments, and data analyses were the responsibilities of teams from three organizations, as follows:

Keldysh Research Center:
A.V. Ivanov	Division Chief, Project Science Manager
V.F. Alymov	Senior Scientist
A.B. Smirnov	Senior Scientist
S.P. Shalayev	Lead Engineer
D.Ye. Belov	Intern Student (Moscow University of Physics and Technology)

RSC-Energia named after S.P .Korolev:
T.V. Andreeva	Engineer
Ye.V. Balashov	Branch Chief
A.V. Semenov	Structures Division Chief

All-Russia Scientific Research Institute for Fire Safety of Russian Ministry for Internal Affairs:

A.S. Melikhov	Chief Scientist
V.I. Potyakin	Group Lead (Scientist)
A.K. Kupchikov	Senior Scientist
I.A. Bolodyan	Division Chief

For the U.S. side, material selection, characterization, and ground testing were conducted by the NASA Johnson Space Center White Sands Test Facility under the technical management of Dr. H.D. Beeson and Dr. D.B. Hirsch. The financial and schedular management of the project was conducted by the NASA Lewis Research Center (now the NASA Glenn Research Center) under NASA Contract NAS3-97160. The technical monitors at NASA Glenn were M. Forkosh and R. Friedman.

This NASA Contractor Report is an English version of the Final Report submitted in Russian by the Russian investigators. The English translation was prepared by Natalie Goldin of Tech Trans International, Inc. Both sides express their strong gratitude to Ms. Goldin, whose service was essential to the success of the project in expediting the communications, correspondence, and reporting between the two sides of the international project team.

TABLE OF CONTENTS

EXPERIMENTAL VERIFICATION OF MATERIAL FLAMMABILITY IN SPACE

A.V. Ivanov
Keldysh Research Center
Moscow, Russia

Ye. V. Balashov, T.V. Andreeva
RSC Energia
Korolev, Russia

A.S. Melikhov
All-Russia Scientific Research Institute for Fire Safety
Russian Ministry for Internal Affairs
Moscow, Russia

SUMMARY

The flammability in microgravity of three U.S.-furnished materials, Delrin, polymethylmethacrylate (PMMA), and high-density polyethylene, was determined using a Russian-developed combustion tunnel on *Mir*. Four 4.5-mm-diameter cylindrical samples of each plastic were ignited under concurrent airflow (in the direction of flame spread) with velocities from no flow to 8.5 cm/s. The test results identify a limiting air-flow velocity V_{lim} for each material, below which combustion ceases. Nominal values are V_{lim} <0.3 cm/s for Delrin, 0.5 cm/s for PMMA, and 0.3 to 0.5 cm/s for polyethylene. These values are lower than those obtained in prior ground testing. Nevertheless, they demonstrate that flow shutoff is effective for extinguishment in the microgravity environment of spacecraft. Micro-gravity test results also show that the plastic materials maintain a stable melt ball within the spreading flame zone. In general, as the concurrent flow velocity V decreases, the flame-spread rate V_f decreases, from an average (for all three materials) of V_F = 0.5-0.75 mm/s at V = 8.5 cm/s to V_f = 0.05-0.01 mm/s at V = 0.3-0.5 cm/s. Also, as V decreases, the flames become less visible but expand, increasing the probability of igniting an adjacent surface.

INTRODUCTION

The results obtained in the third series of nonmetallic-material flammability evaluations in the combustion-tunnel apparatus *Skorost* on the Orbital Station *Mir* in space are presented here. The purpose of the work is to expand the existing database on flammability of melting flammable thermoplastic polymers in microgravity. Materials were furnished by NASA, and their selection for the flight experiment was based on the results of the ground testing in apparatuses with suppressed convection. The experiment took place on October 15-22, 1998. The ground-preparation data of the space experiment are included in the report as well.

Of late, the study of solid material combustion in zero gravity (more accurately, in microgravity) is becoming of great importance in Russia (refs. 1 to 3) and in other countries (refs. 4 to 5), especially in the U.S., where many scientific projects funded by NASA are taking place (refs. 6 and 7). The interest in this issue is explained by several reasons (ref. 8):

- first, combustion study in microgravity makes it possible to compare theoretical results against test data directly, which leads to progress in combustion theory;
- second, the effect of weak processes that are overshadowed on the ground can be investigated in microgravity due to the almost complete lack of buoyant flows, which is the most important feature of combustion in microgravity,

- finally and most important, microgravity-combustion studies can lead to the creation of advanced fire-safety systems for spacecraft applications, in particular for such complicated spacecraft as the International Space Station (ref. 9).

The fire incidents that have occurred on the Space Shuttle or the Orbital Station (OS) *Mir* demonstrate that fire is a crucial concern in spaceflight safety. The most serious operational accident in the history of manned orbital flights was the fire incident that happened on February 23, 1997 on the OS *Mir*. This fire was caused by a Solid Fuel Oxygen Generator failure as the result of the canister burnout during generator activation in the Module *Kvant*. A tragedy was avoided only due to immediate and appropriate reaction of the Russian crew. It was also helpful that the fire occurred in *Kvant* when the module was not overcrowded. The situation on *Mir* was extremely serious, and immediate resolution was necessary. The crew had either to battle the fire, or to abandon the Space Station while exit to the *Soyuz* return vehicle through *Kvant* was still possible. The flame on the Oxygen Generator was pointed in a certain direction with a length of ~0.5 m, and the temperature of the combustion products in the flame zone was extremely high due to the constant intake of pure oxygen. Sparks and drops of melting metal bright white in color burst out of the flame zone. The fire extinguished within a short period of time (~1.5 min) due to the confident actions of the Russian crew, who used three extinguishers to eliminate the fire.

For the International Space Station, the probability of fire is greater than for the spacecraft of previous generations, due to the higher power and voltage of the on-board power supplies and greater volume of scientific instrumentation with high-temperature operation.

Currently, fire safety on Russian spacecraft is achieved by prevention methods that exclude the possibility of fire through a wide range of different means, for example:

- selecting structural materials, based on the results of ground testing, with priority given to materials with higher limiting-oxygen concentrations for combustion (C_{lim}) or/and higher oxygen indices;
- specifying nonflammable materials for the working components of the electrical systems;
- maintaining low oxygen concentrations in the spacecraft pressurized compartment during the launch phase;
- decreasing the vent flow locally in the area of the electrical components that might be potential sources of fire;
- eliminating potential sources of structural material ignition by methods of current protection or by use of nonflammable instrumentation and cable harnesses; and
- preventing flame spread to materials that are flammable in an oxygen-enriched environment.

Lack of buoyant flow in the spacecraft environment reduces oxygen transfer into the combustion zone and combustion-products transfer in the opposite direction, which leads to flame extinction on the surface of solid materials when the velocity of concurrent vent flow is low. Fifty years ago, Zeldovich (ref. 10) predicted the existence of minimum and maximum flow velocities to sustain combustion. Recently, this assumption was confirmed both the theoretically (refs. 11 and 12) and experimentally (refs. 13 to 17) for the combustion of several nonmetallic materials. In particular, testing at the NASA Glenn Research Center Drop Tower (refs. 16 and 17) demonstrated that, even for a thermally thin material with a low C_{lim} of 12.5 percent (paper sheets 0.1-mm thick), a limiting flow velocity V_{lim} of 0.1 to 1.0 cm/s for combustion exists at oxygen concentrations C_{ox} of 17 to 21 percent. This is a result of the relative increase in heat losses due to radiation from the material surface and from the gas phase (refs. 11 and 12). This loss is the cause of the ignition-source suppression in microgravity at flow shutoff in the spacecraft pressurized compartment. (This conclusion differs from that of the de Ris model (ref. 18), which does not account for radiation thermal loss.) When the oxygen concentration increases up to 30 percent, the intensity of the diffusion increases as well, to the level where combustion of a thermally thin material becomes possible without imposed flows to provide oxygen intake. However, at these conditions, decreases in concurrent-flow-velocity lead to reductions in combustion intensity and flame-spread rate.

In the previous, second series of experiments in the *Skorost* apparatus on OS *Mir* (ref. 3), the existence of the limiting velocity V_{lim} for combustion was confirmed for PMMA and glass-epoxy-composite strip samples 2-mm thick at $C_{ox} = 21.5$ percent. It was concluded that V_{lim} depends on C_{ox}. For PMMA, with a low oxygen index of 15.5 percent, the limiting flow velocity is less than 0.5 cm/s; and for glass-epoxy composite, with a high oxygen index of 19 percent, the limiting flow velocity is greater than 15 cm/s. When the concurrent-air-flow velocity decreases but is not less than V_{lim}, the combustion intensity decreases in microgravity, similar to a thermally thin

material phenomenon. Combustion of the PMMA sample occurs from the front edge in the concurrent-flow velocity of 4.5 cm/s. The flame has a lengthened dome shape, and its front zone is white due to the presence of soot particles. Downstream, the flame color is orange. The ejection of the bright products of material destruction is observed. When the flow velocity is reduced to 2 cm/s, the flame size decreases noticeably, and the shape of the flame changes to a hemisphere. Combustion becomes less violent, and ejection intensity and brightness decrease. When the flow velocity is close to the limiting flow velocity V_{lim} of 0.5 cm/s, the pattern of combustion changes drastically. The hemispherical flame acquires a pale-blue color and becomes almost invisible. The lengths of the material-destruction and boiling zones decrease. Combustion becomes unstable, which causes the flame extinction in flow velocities greater than zero.

The described characteristic of nonmetallic-material combustion enables the potential development of a fire-safety system for a space station that is based on air-flow shutoff in the space-station compartment. This system is reliable at a low oxygen concentration (C_{ox} = 21 percent). This ecologically safe fire-safety and fire-alarm system (*i.e.*, one that does not automatically release an atmospheric-polluting agent for suppression) has been implemented on the *FGB* module of the International Space Station.

As of now, only those materials that maintain their integrity during combustion have been investigated. Materials that disintegrate when burning present more danger for fire safety because the flame can spread further with parts of the burning structure, ejected melt drops, *etc.* Materials such as polyethylene are of great interest since they form a lengthy melt zone, which might be a source of melt drops that promote faster flame spread compared to usual combustion.

Preliminary results of polyethylene-insulation flammability in microgravity were obtained in the NASA Wire Insulation Flammability (WIF) experiment during the Space Shuttle flight STS-50 (refs. 19 and 20). Tests were performed in a glovebox apparatus at an oxygen concentration of 21 percent on the combustion of polyethylene insulation 0.375-mm thick on a NiCr wire with a diameter of 0.75 mm and a length of 110 mm. The samples, installed in a miniature wind tunnel, were heated by Joule heating to relatively high temperatures (75 to 80 °C) and ignited from one of the ends. Combustion was studied in opposed and concurrent flows of 10 cm/s.

Photographic and video observations provided the unique result that, in microgravity, the flame stabilizes on the molten ball in both concurrent and opposed flows. The diameter of the molten ball is 3.0 to 4.5 mm, *i.e.*, 2 to 3 times greater than the initial diameter of the sample. In concurrent flow, the molten ball is ellipsoidal, and the oscillating flame stabilizes in front of the ball. The bright yellow flame is followed by the thin flame zone of a blue color, and the flame color changes gradually to red downstream. The melted material accumulates asymmetrically on the NiCr wire and moves slowly downstream. Pictures taken during the test show that the material surface close to the flame is discolored and opaque. The flame-spread rate of the downstream flame edge is higher (1.6 mm/s) than the flame-spread rate of the upstream flame border (1.2 mm/s); therefore the length of the flame increases over time. However, the results of the analysis presented in (ref. 18) predict a stationary pattern of the flame spread.

In opposed flow, the spherical melt drop becomes steady only in 15 to 18 sec after the ignition. Then, the flame-spread rate is constant at 0.66 to 0.70 mm/s, approximately one-half the rate in concurrent flow.

Formation of the bubbles of the gaseous products of material destruction inside was also observed during the test. These bubbles collapse, ejecting burning particles of the material and causing flame disturbances.

A lot of interesting data was collected during the WIF test program, for example, information regarding soot formation. However, one of the most important results is that, in microgravity, the extinction of the polyethylene occurs almost immediately when the flow of relatively low oxygen concentration (C_{ox} = 21 percent) stops. As mentioned above, this feature of material combustion in microgravity, which was also observed in the second series of flammability experiment with PMMA and glass-epoxy in the *Skorost* apparatus on OS *Mir*, provides a basis for a fire-safety system for space station. The new system will be based on the fire suppression at flow shutoff in the ventilated microgravity environment of orbiting spacecraft.

This is the Final Report for the joint project under Contract NAS3-97160, "Experimental Verification of Material Flammability in Space" between the NASA Glenn Research Center and Johnson White Sands Test Facility (U.S.A.) and the Keldysh Research Center (Russian Federation). The report was written in Russian by the Russian principal investigators. This NASA Contractor's Report is an English translation prepared by Natalie Goldin of TechTrans International, Houston TX. The English version is identical to the Russian original in organization, data presentation, and conclusions. The summary section of the Contractor's Report is written by the project monitor, Robert Friedman of the NASA Glenn Research Center.

1. GROUND TESTING FOR THE SPACE EXPERIMENT ON MATERIAL FLAMMABILITY

The Contract NAS3-97160 Statement of Work states that the main objective of the "Material Flammability Evaluation In Space" U.S./Russia Joint Project is to assess the effect of air flow of low velocity on the combustion of selected U.S. materials in long-duration microgravity in the *Skorost* apparatus on OS *Mir*. Material combustion during the testing occurs in concurrent flow (with respect to the flame-propagation direction). The following tasks are to be accomplished:

- Define a minimum limiting flow velocity (V_{lim}) to sustain material combustion.
- Define how the flame-spread rate (V_F) depends on the concurrent flow velocity (V).
- Review the results obtained in space experiment against the ground-testing results.

The experience of the first and second series of *Skorost* apparatus operations in 1994 and 1996 showed that the apparatus cannot be used to obtain combustion parameters (V_{lim}, V_F) for a wide range of materials due to its limitations. Measurements of V_{lim} and V_F are possible in the microgravity environment of spacecraft, however, if the material is flammable in the given oxygen concentration in the spacecraft compartment at the time of the space experiment and if the flow velocity in the apparatus chamber is higher than a limiting velocity for the material. These conditions may be summarized by the following: $C_{ox} \geq C_{lim}$; and $V \geq V_{lim}$. C_{ox} (%) is the oxygen concentration in the spacecraft compartment atmosphere and, hence, in the *Skorost* apparatus; C_{lim} (%) is the limiting oxygen concentration for the material; V (cm/s) is the flow velocity in the apparatus chamber; and V_{lim} (cm/s) is the limiting velocity for the material.

Seven materials provided by the NASA Glenn (formerly Lewis) Research Center (USA) were considered for the space flammability evaluation. The materials of interest were furnished as strip, flat, or cylindrical samples. These materials were polyethylene of high density, polyethylene of low density, PMMA (polymethylmethacrylate), Delrin (polyacetal), rigid polyurethane, and glass-epoxy composite. The ground testing showed that all materials named above melt while burning with the exception of glass-epoxy. The U.S. PMMA appeared to melt as well, which is not typical of Russian-made PMMA.

Based on ground measurements of C_{lim} and V_{lim}, three of seven materials were selected on the following criteria:

- The material shall be flammable at an oxygen concentration of 21% ($C_{lim} < 21$ percent).
- The material shall not disintegrate while burning—*i.e.*, the burning pieces do not separate from the burning sample.
- The zone of melted material shall be minimal.
- The sample shall not deform while burning.

1.1 The *Skorost* Test Apparatus

The space *Skorost* apparatus was developed and built at RSC-Energia in cooperation with Keldysh Research Center and the All-Russian Institute for Fire Safety to study the combustion of strip and cylinder samples of non-metallic materials in microgravity in concurrent flows of given velocities and at given oxygen concentrations.

Two series of the space experiments conducted in 1994 and 1996 confirmed the *Skorost* functionality but indicated a need to minimize the flow velocity and to improve other flow parameters inside the combustion chamber, such as uniformity and steadiness. To accomplish this, *Skorost* was modified. The modifications included mesh installation at the fan outlet, fairings to cover the igniters, removal of the protruding parts of thermocouple attachments from the flow core path, *etc*.

1.1.1 Skorost Schematic.—Figures 1.1 and 1.2 show schematic and general views of the *Skorost* apparatus. The apparatus consists of the combustion chamber, two carousels with test samples installed, filters, flow-rate meter, fan, pipelines, control panel, and cameras.

The combustion chamber is the most important part of the apparatus. The combustion chamber is an aluminum-alloy wind tunnel, 320-mm long, with a rectangular cross-section (150×80 mm). C_{ox} cannot be controlled independently in *Skorost* because air from the spacecraft compartment is purged through the chamber, and oxygen concentration depends on the atmospheric chemical composition in the spacecraft at the time of the test. To avoid

the contamination of the spacecraft compartment, the apparatus is equipped with two sets of filters. Filter operation was evaluated on the *Mir* full-scale mock-up (core module) during the ground preparation for the experiment.

Two carousels are located symmetrically inside the combustion chamber. Six samples of tested materials can be mounted as cantilevers on each carousel. A sample is 60 mm long. (A strip sample is no more than 3 mm thick, and a cylindrical sample has a diameter up to 5 mm.) To comply with crew-safety requirements, the test sample is selected and put in the test position along the chamber centerline by rotation of the carousel using an external lever only. A crew member is not allowed to open the combustion chamber. The sample free end is ignited inside the chamber, and then combustion occurs in a concurrent uniform flow, which is parallel to the sample axis. Adjacent samples are separated by distances of 25 to 27 mm, measured along their longitudinal axes.

The prime and redundant igniters are built-in devices that consist of a NiCr heating coil located on the bracket. The igniter coil wire diameter is 0.3 mm, and it is heated by direct current. The heating coil is powered through the end terminals when it approaches the sample, and it will ignite only the sample that is placed along the combustion-chamber centerline. The igniter drive is supplied with springs to return the igniter to its initial position. The heating coil can be heated up to minimum, nominal, and maximum temperatures, as desired to provide a reliable ignition.

The flow velocity is the most important parameter that can be controlled in the test apparatus. *Skorost* means "velocity" in Russian, and it gave the apparatus its name. The velocity can be changed within a wide range (from 20-30 to 0.3 to 0.5 cm/s) during the test by adjusting the flow-rate meter knob position and the fan-motor voltage drop, according to ground flow calibrations performed prior to the tests.

To assure flow uniformity, meshes are installed at the combustion-chamber inlet and outlet. In a contingency situation, the combustion-chamber inlet can be closed with a metal shutter. A heat exchanger installed at the combustion-chamber outlet cools the air heated by the burning sample. The experiment is monitored and recorded by *HI-8* and *Betacam* cameras through two rectangular PMMA windows, 100 × 60 mm in size, that are located on the side and on the top of the combustion chamber. Pressure and oxygen concentration measured by the standard monitoring instrumentation in the spacecraft compartment are recorded at the time of the test.

1.1.2 Flow Calibration in the Skorost Combustion Chamber.—Flow calibration was performed after the installation of the igniter fairings at the Keldysh Research Center, using a laser technique according to the diagram shown on figure 1.3. A laser beam was transformed into a plane ~ 0.5-1.0 mm thick for smoke visualization. Smoke was fed into the chamber from a box located at the combustion-chamber inlet. The velocity of the flow is actually the velocity of the stable smoke blobs flowing through the chamber. Smoke-blob movements are referenced to a scale grid, located on the background and recorded by the video camera. The distance between gridlines is 10 mm. Measurements are done along the 30- to 40-mm distance with an error of 1 to 2 mm. The accuracy of the time measurement that a selected smoke fragment takes to pass a distance between the gridlines is defined by the camera frame rate of 25 frames/sec. This error δt is less than 0.04 sec. The test was repeated, and the flow-velocity measurement error appears to be less than 10 to 15 percent.

For calibration purposes, the combustion chamber was filled with smoke before the fan was turned on. The smoke visualization demonstrated that, when the flow velocity is above 3 to 4 cm/s, flow in the middle part of *Skorost* combustion chamber (flow core) is fairly uniform. The rear border of a smoke cloud is practically undisturbed when smoke passes through the combustion chamber, which confirms flow uniformity. (The smoke moves from the mesh at chamber inlet to the point of sample location and farther—see fig. 1.4.) When the flow velocity is lower (less than 3 cm/s), the smoke cloud rear border is disturbed, which might be an indication of flow-core degeneration and Blasius velocity-profile formation at small Reynolds numbers.

Due to problems that occurred at the filter delivery to the OS *Mir*, the flight *Skorost* was equipped only with two filters instead of four. Therefore, one of two parallel combustion-chamber outlets was sealed on orbit. The ground calibration was performed with two filters instead of four, at the *Mir* nominal voltage (27 V) and at the lower voltage of 25.9 V that was on the Space Station at the time of the experiment, when the high power-consuming "Electron" electrolysis system was working. The lower voltage supplied to the *Skorost* control board permits the control of a lower range of flow velocities.

The flow calibration results by smoke visualization are shown on figure 1.5. The airflow velocity V in the *Skorost* is plotted versus φ for two U settings, where φ is a flow-rate meter knob position on the control board, and U is a voltage supplied to the control board and the *Skorost* air-pump motor. The flow-velocity range from 0.3 to 10 cm/s covers that desired for the space experiment.

1.2 Material-Flammability Evaluation by C_{lim} Method

The limiting oxygen concentration C_{lim} that sustains material combustion was determined to evaluate material flammability in an oxygen-enriched environment in normal gravity. Limiting oxygen concentration is evaluated for the most hazardous situation—where a flame propagates upward. A different technique is used in the U.S. for material-flammability evaluation in buoyancy-driven flows—the so-called LOI evaluation (limiting oxygen index). LOI is the minimum volumetric concentration of the oxygen/nitrogen mixture to sustain "candle-like" material combustion with downward flame propagation, obtained using standard test methods (refs. 21 to 22).

1.2.1 Apparatus Schematic.—An apparatus shown in figure 1.6 was used for C_{lim} evaluation. The apparatus consists of the working chamber, a cylinder 140-mm in diameter and 500-mm high. A sample is mounted in the holder attached to the upper lid of the chamber. The chamber has an observation window to monitor combustion. A gaseous mixture supplied to the working chamber is prepared in a mixer. The mixer can maintain oxygen concentrations in the chamber with deviations of less than 0.5 percent (total). Oxygen concentration is monitored by a gas analyzer of the "Zircon" type. A set of meshes installed in the chamber is used for flow stabilization to provide a steady flow and a uniform velocity field. The flow rate through the chamber is controlled by a flow-rate meter of the PC-5 type. A vacuum pump and control valves are used to create a vacuum and to set a prescribed pressure in the chamber. A gas burner with propane fuel from the bottle is used to ignite the sample. Gas is ignited by a heating coil connected to a power supply.

1.2.2 Test Methodology and Results.—For C_{lim} evaluation, samples 150 mm long and 5 mm wide are used. Material thickness is the same as in the space test. Below is the description of the test procedure:

The sample is secured in the holder and inserted into the chamber. The air flow of prescribed oxygen concentration is purged through the chamber in an upward direction. After the desired flow rate and pressure are obtained in the chamber, the sample is ignited. When combustion is stabilized, the igniter is moved away to the wall of the test chamber and turned off. If the flame spreads along the entire length of the sample, the material will be considered flammable in the prescribed conditions. Then the parameters are modified to be less favorable for combustion. If the flame does not spread along the entire length of the sample, the material is assumed as being nonflammable in the prescribed conditions. Therefore, the limiting combustion parameters are identified in a series of tests.

The results of limiting oxygen concentration C_{lim} determined at the All-Russia Institute for Fire Safety for the selected U.S. materials are shown in table 1.1. The tests confirmed that all provided materials are flammable in the gaseous media with oxygen concentrations between 11.2 to 19.8 percent; therefore, steady combustion in the *Skorost* flow can be predicted for the space experiment on *Mir* where the oxygen concentration is at least 21 percent. However, the steady combustion of the provided materials in oxygen concentrations of 21 percent has differing behaviors. All the selected materials melt during combustion. When melting is fast and dripping of the molten non-viscous matter is intense, the melting transfers heat out of a flame zone; therefore, higher oxygen concentration is required to sustain combustion, *i.e.*, C_{lim} increases. The tests showed that upward combustion of the polyurethane and nylon samples is unstable at $C_{ox}= 21$ percent. Higher oxygen concentrations (25 and 22 percent respectively) are required to sustain steady upward combustion of the free-mounted samples of these materials (no other elements involved). To obtain an actual limiting oxygen concentration for these materials, the testing employed a well-known technique—a thin mica back-plate (about 0.3 mm thick) is used to support the ignited heated material. The resulting C_{lim} appears to be significantly lower than C_{lim} identified for the original monolithic samples—19.8 and 18.9 percent for polyurethane and nylon, respectively. Other materials do not demonstrate the same drastic effect of melting on C_{lim} values, which might be explained by the higher viscosity of the burning molten material.

Delrin has the lowest C_{lim} of 11.2 percent, which might be explained by its chemical composition, in particular, by a high content of oxygen in the monomer CH_2O, which is 53 percent of the material mass. The U.S.-made PMMA has a limiting oxygen concentration of 16.8 percent, which is a little higher than $C_{lim} = 15.5$ percent of the Russian-made PMMA (not included in table 1.1). This might be explained by either the tendency of the U.S.-made PMMA to melt, or by a difference in chemical compositions (softener addition, for example). Other materials have C_{lim} within the range of 17.1 to 19.8 percent.

Table 1.1 also shows limiting oxygen concentration C_{lim} and limiting oxygen indices LOI obtained at the NASA White Sands Test Facility. For upward flame propagation (C_{lim}), the strip samples used were 100 mm long (instead of 150 mm) and 5 mm wide. The concurrent flow velocity was 4 cm/s. The burning criterion for this test is either a length of the burnt sample (no less than 50 mm), or a duration of self-sustained combustion (no less than 3 min). The discrepancy in C_{lim} evaluation between the U.S. and Russian tests for most of the fuels is less than

ΔC_{lim} = 1 percent. The more significant difference in C_{lim} results for nylon and polyurethane is explained by the mica back-plate used during the Russian testing.

For the LOI test procedure at White Sands (candle-like combustion, downward flame propagation), the sample length was increased to 150 mm. The opposed flow velocity was again 4 cm/s. The burning criterion is the same as described above for C_{lim}—either a length of the burnt sample of at least 50 mm, or a duration of self-sustained combustion of at least 3 min. For all materials, with the exception of polyethylene, C_{lim} is less than LOI; therefore, upward combustion on the ground is more of a fire hazard than "candle-like" combustion where the flame propagates downward.

Based on the C_{lim} evaluation and on the pattern of combustion in the limiting-oxygen-concentration apparatus, three materials were selected for the space experiment, PMMA, Delrin, and high-density polyethylene.

1.3 Evaluation of Limiting Flow Velocity for Combustion in Apparatuses with Suppressed Convection

It is well known that the natural convection in a thin layer of gas is suppressed if the Rayleigh (or Grashof) number does not exceed a critical value (see refs.14, 15, 23 and 24). Based on this principle, in order to simulate microgravity conditions (namely, the absence of natural convection), two apparatuses with reduced natural convection were built to calculate V_{lim}:

- Horizontal Narrow-Channel apparatus (fig. 1.7, All-Russia Institute For Fire Safety);
- Vertical Combustion Chamber (fig. 1.8, Keldysh Research Center).

1.3.1 Narrow-Channel Apparatus Schematic.—The Narrow-Channel apparatus and pertinent test procedure for material-flammability evaluations in a suppressed convection environment that partially models the space environment were patented in Russia; the patent license has number 2116093, October 12, 1995.

The schematic of the Narrow-Channel apparatus for V_{lim} evaluation is shown on figure 1.7. A set of meshes is installed in the chamber of the apparatus to provide a uniform flow across the chamber cross-section. The working chamber is a flat channel between two massive copper plates heavy enough to assure a uniform wall temperature. A distance h_c between upper and lower plates is variable. The sample is mounted on the shaft. The shaft can be moved backward and forward by a drive, keeping the sample in the midline of the channel. A gaseous flow with prescribed oxygen concentration prepared in a mixer flows into the channel. The flow rate is determined by a flow-rate meter (PC-3), and the oxygen concentration is measured by a gas analyzer (Zircon-M). The sample edge is kept at a prescribed distance from the meshes by the drive. The sample is ignited outside before its insertion into the channel.

To maintain the prescribed flow velocity, a flow calibration in the Narrow Channel was performed. The flow velocity was defined using a smoke-visualization technique—the movement of a small smoke blob (size of about 5 mm) over a certain distance in the location of the sample.

1.3.2 Procedure and Results of Narrow Channel Testing.—The Narrow Channel test in the apparatus on figure 1.7 evaluates material flammability in terms of V_{lim} determined at a prescribed oxygen concentration C_{ox} (greater than C_{lim}), through the following steps:

- define h_c based on C_{ox} (a vertical distance between horizontal plates is calculated using a special formula);
- mount a sample on the shaft using a special fixture (samples of monolithic materials that maintain their shape and do not melt are strips 1 mm × 5 mm × 20 mm; samples of melting materials are mounted using mica back-plates 0.3-mm thick; back-plate size is 6 × 60 mm); all samples are installed in the channel midline, i.e.,the distance from the sample to upper and to lower plate shall be the same;
- create a oxygen-nitrogen mixture flow of prescribed velocity and oxygen concentration in the Narrow Channel (the gaseous mixture is prepared in the mixer);
- ignite the sample outside the channel in the flow of gaseous mixture from the channel outlet; when combustion becomes stable (wait for at least 3 sec), insert the sample into the channel with a 10-mm distance from the burning front edge to the mesh;
- monitor combustion closely; record sample shape changes; maintain the combustion zone in the channel midline;

- define V_{lim} for materials burning without rigid char formation as the flow velocity where the duration of self-sustained combustion is at least 20 sec;
- define V_{lim} for materials burning with rigid char formation as the flow velocity where the duration of self-sustained combustion is at least 10 sec.

Ordinarily, to eliminate the effect of residual natural convection, the apparatus is mounted horizontally. However, a new methodology was developed to minimize a discrepancy between V_{lim} obtained in the space experiment on *Mir* and V_{lim} evaluated in the Narrow Channel. To accomplish this, the Narrow-Channel test is done twice—in a horizontal and a vertical position of the apparatus, and the lesser value of the two results is accepted as the best estimate of the unknown limiting flow velocity.

Limiting flow velocities were evaluated in the Narrow-Channel apparatus at oxygen concentrations of 21 and 23 percent, which correspond to the actual oxygen concentration on *Mir* during the space testing of 1994 and 1996. The results obtained are in table 1.2, which shows that, as oxygen concentration increases, V_{lim} for all tested materials decreases. Limiting flow velocities for the selected materials range from 0.5 to 16.9 cm/s at $C_{ox} = 21$ percent, and from 0.3 to 6.8 cm/s at $C_{ox} = 23$ percent.

The Narrow-Channel tests showed that, in agreement with the limiting oxygen concentration results, six of seven tested materials have a tendency to melt. When the flow velocity is close to V_{lim}, a ball of melt forms on the front edge of the sample, and it grows with time.

1.3.3 Vertical Combustion Chamber Apparatus Schematic.—The Narrow Channel test disadvantage is the small size of the sample, which is about 2-mm thick. Therefore, the combustion study may be complicated, especially for the coarse-grained materials. The scale effect on combustion cannot be evaluated.

To study the combustion of relatively massive samples, the Keldysh Research Center developed and built an apparatus with a vertical combustion chamber (ref. 25). The apparatus is designed to evaluate a limiting flow velocity in a suppressed-convection environment for cylindrical samples of about 10-mm diameter (fig. 1.8). The apparatus consists of a vertical combustion chamber, which is closed at the bottom. The combustion chamber has a square cross-section (15 × 15 mm) and is 250 mm high. Two opposite walls of the chamber are built of quartz, which provides an opportunity to monitor combustion closely. Other components of the apparatus are a mechanism for camera vertical translation with a four-step gear; a sample mounted in a stationary holder; an igniter; and visualization system to monitor combustion.

The gap between the sample side surface and the chamber interior wall is very small; thus combustion occurs only on the lower edge of the sample in the flow of 21 percent of oxygen concentration. Sample movement creates a flow, and the velocity of sample translation defines the velocity of the flow. Since the distance between the flame and the bottom surface of the sample is small (2 to 3 mm), the convection in the heated layer of gas is suppressed (refs. 23 and 24), and a limiting flow velocity can be evaluated.

1.3.4 Procedure and Results of Keldysh Center Tests.—The bottom surface of the sample is ignited outside the chamber, and then the sample is inserted into the chamber. The sample is moving with the prescribed velocity from 0.2 to 10.0 cm/s, which can be adjusted by the translation mechanism operation and voltage changes. With optical equipment, the flame or its extinction at a given relative velocity of the sample is observed visually.

The U.S.-provided materials selected for the *Mir* tests were tested in this apparatus. The experiments were conducted at four different velocities created by the sample-chamber relative movement, 0.4, 1.1, 3.1, and 6.0 cm/s. Delrin and PMMA combustion stops at the chamber inlet when the velocity is 0.4 cm/s; however, samples still burn at V = 3.1 cm/s. When velocity is 1.1 cm/s, both combustion and extinction are observed. Therefore, the limiting flow velocity for Delrin and PMMA is close to 1.1 cm/s. The high-density polyethylene samples do not sustain combustion when the flow velocity is less than 6.0 cm/s. Therefore, a limiting flow velocity for the high-density polyethylene is ~4.5 cm/s. The results obtained at Keldysh Research Center and at All-Russia Institute for Fire Safety agree in general ranking, despite some differences in the numerical values.

1.4 Flame Propagation Along the Material Surface in the Narrow Channel Apparatus

Thermoplastic polymer testing in the Narrow-Channel apparatus showed that a collar of melting material forms on the edge of the sample. The molten material accumulates, and its mass increases during the test. The time τ_D from the moment of material ignition to the moment when the drop of molten material touches the lower plate of the Narrow Channel is important. This time characterizes indirectly the viscosity of the melt and helps to predict material

behavior during the space test. The time τ_{t_1} is higher for materials that have lower V_{lim} at a given oxygen concentration. This finding is verified for the tested polymers. For high-density polyethylene, Delrin, and PMMA, τ_{t_1} is 15 to 20, 45 to 50, and 20 to 25 sec, respectively.

The length of the melting portion of the material and the mass of the melt drop are smallest for Delrin, due to the low V_{lim} for Delrin compared to polyethylene and PMMA. The previous testing on *Mir* showed that if the flow velocity is small, a flame will be shorter; and, consequently, the heated and melted portion of the sample will be shorter. Besides, the Narrow-Channel testing demonstrated that the viscosity of molten Delrin is higher than the viscosity of molten PMMA. Based on all these factors, the tests showed Delrin to be a most appropriate material for the space experiment, with space testing starting at a low velocity flow—about 2-3 cm/s.

Compared to the Russian PMMA, the U.S. PMMA melts, which makes the Russian material more suitable for the testing. The Russian PMMA burns without rigid char formation, undergoes complete pyrolysis, and maintains its shape when the flow velocity is close to V_{lim}. All these properties make PMMA a model material for polymer combustion study in Russia.

Both low-density and high-density polyethylene have limiting flow velocities greater than those of Delrin and PMMA. Therefore, the experiment has to start at a relatively high flow velocity. Polyethylene forms a ball of molten material in 10 to 15 sec, because of fast formation of a lengthy melting zone (10 mm).

In summary, the results of the ground testing in the Narrow-Channel apparatus with suppressed convection demonstrate that Delrin, high-density polyethylene, and PMMA have a relatively steady combustion zone; and, therefore, these materials are suitable for the space experiment.

One of the objectives of the space experiment on *Mir* is to analyze the flame-spread rate over the surface of the selected materials. As a part of flame-propagation study, an average flame-spread rate was measured in the Narrow-Channel apparatus. Measurements were taken for the initial phase of combustion, the period from sample insertion into the Channel to when the molten material drop touches the lower plate of the Channel. The flow velocity was from 1 to 4 cm/s above V_{lim} at $C_{ox} = 21$ percent and from 3 to 11 cm/s above V_{lim} at $C_{ox} = 23$ percent.

The results of flame propagation rate (V_f) measurements for the three selected materials are presented in table 1.3. Delrin has the lowest V_f (0.12 to 0.16 mm/s), and polyethylene has the highest V_f (0.52 to 0.60 mm/s).

A flame-spread rate might be a function of a number of material characteristics, such as material reactivity, melting temperature, surface tension, viscosity, *etc.* Besides, materials were tested in flows of different velocities, which is another obvious explanation of a difference in V_f values. A higher flow velocity will promote a longer flame zone. The longer the flame zone, the longer the portion of the sample that is heated up to a melting temperature, which will define a rate of molten material drop formation and a rate at which material is leaching out from the sample. The analysis showed that, for selected materials, a flame spread due to melting prevails over a flame spread due to material escaping from the front edge of the sample.

The rates of material burning-out for Russian-made PMMA and polyethylene are less than 0.05 mm/s at a flow velocity $V = 10$ cm/s and $C_{ox} = 21$ percent, *i.e.*, 5 to 10 times lower than the flame-spread rates measured for the melting materials that were tested. Therefore, it can be predicted that the diameter of a drop formed by the molten material will be growing during the flight experiment on *Mir*.

1.5 *Skorost* Ground Testing

Based on the results of the previous testing in the apparatuses with suppressed convection and accounting for C_{lim}, only three materials, Delrin, high-density polyethylene, and PMMA, were tested in *Skorost* on the ground. The samples were 1.5 mm × 8 mm strips and 4.5-mm diameter cylinders, 60 mm long. The samples were tested in *Skorost* in both vertical (downward combustion, in concurrent flow) and horizontal orientation. Below is a timeline for the *Skorost* testing:

- ignition of the sample at the nominal current with the heating coil;
- sample combustion in a flow of 8 cm/s;
- sample combustion at flow shutoff, *i.e.*, when the flame propagated through half of the sample, the fan was tuned off, and the inlet was closed.

The experiment was videotaped by two Panasonic video cameras from two perpendicular perspectives. Extensive video information was collected and processed. The data on the flame size and shape, flame-propagation rate, and time of flame quenching at flow shutoff are available.

1.5.1 Skorost Testing – Combustion-Chamber Vertical Orientation.—Figures 1.9 to 1.11 show examples of sample combustion when Skorost is oriented vertically with downward combustion. Flame shape and color are visible on these figures. The flame has a candle-like shape; therefore, combustion is sustained primarily by natural convection, and the effect of forced flow (8 cm/s) is secondary. Only when the flow velocity is increased up to its maximum (above 20 cm/s), does the flame have a mushroom shape, which is typical for the space environment as observed in the experiments of 1994 and 1996. The Delrin flame has a blue color (complete combustion of pyrolysis products), while the high-density polyethylene and PMMA flames are white, due likely to the presence of soot particles.

All tests showed sample deformation. The heated portion of the sample loses its rigidity and bends downstream, carrying along the flame zone (in a form of droplets or jets of the viscous melt). The strip samples start to bend 15 to 20 sec after the ignition, while the cylindrical samples maintain their shape longer, up to 90 sec. Therefore, a cylindrical shape is the recommendation for the space-flammability evaluation on *Mir*.

Table 1.4 shows the results of the flame-spread rate V_f measurements along the surface of the samples when they are positioned vertically. These measurements were obtained during the initial phase of combustion (the first 15 to 20 sec after ignition), when the samples still keep their original shape. For Delrin, V_f is 1.5 to 2 times lower for cylindrical samples than for strip samples. For polyethylene and PMMA, V_f differences with shape are much less.

The video tapes provide the following information: τ_1 - the time from ignition to a moment when the flame front propagates through a half of a sample; and τ_2 - the time of flame quenching at flow shutoff (zero flow velocity). Both times depend on sample thermal deformation. Deformation promotes flame-spread rate increase in the downstream direction, which leads to a flame-size increase. The Delrin sample has the longest quenching time τ_2, about 2 min, while the size of the flame zone stays small.

1.5.2 Skorost Testing – Combustion-Chamber Horizontal Orientation.—Figures 1.12 and 1.13 show examples of sample combustion when Skorost is oriented horizontally. The flame shape during the initial phase of combustion is close to that observed in the space experiment (although asymmetrical due to buoyancy). In comparison to that observed in the Skorost vertical orientation, the sample deformation starts earlier and progresses faster. In 10 to 15 sec after ignition, the heated portion of the sample bends down under the effect of gravity. The sample bending completely changes the combustion and flow pattern around the sample. However, some V_f data have been obtained during the initial phase of combustion. Thus, a flame-propagation rate for Delrin, when the gravity force is perpendicular to the sample axis and flow-velocity vector, increases to 0.8 mm/s for the strip sample and to 0.35 to 0.4 mm/s for the cylindrical sample, i.e., a flame-propagation rate almost twice compared to the rate when the chamber is oriented vertically. The time τ_2 for Delrin is one-third that of the vertical-orientation case, which may be explained by the larger size of the flame. Similarly, high-density polyethylene and PMMA samples show qualitative reductions in combustion and extinguishment times in the horizontal orientation compared to those in the vertical orientation.

1.6 Selection of Materials, Sample Shape, and Test Modes for the Space Experiment

Material-flammability evaluation in space is feasible if, firstly, a sample can be ignited and sample combustion is stable until a prescribed amount of sample material is consumed at the oxygen concentration on the *Mir* atmosphere; and, secondly, the flow velocity in the combustion chamber is higher than a limiting velocity V_{lim} for this material. Hence, all materials shall be flammable at $C_{ox} = 21$ percent and a flow velocity less than 20 cm/s, or:

$$C_{ox} > C_{lim} \text{ and } V > V_{lim};$$

where C_{ox} (percent) is the oxygen concentration in the *Mir* compartment, C_{lim} (percent) is the limiting oxygen concentration to sustain material combustion, V (cm/s) is the velocity of the flow in the combustion chamber, and V_{lim} (cm/s) is the limiting velocity of the flow to sustain material combustion. Figure 1.14 shows a relation among velocities, mentioned above. The shaded area describes the environment that is most likely to occur during the flight: a

V range from near zero to 25 cm/s, and a C_{ox} range from 21 to 23 percent. Data and the extrapolations shown on figure 1.14 are based on the results of the Narrow-Channel tests, table 1.2.

Figure 1.14 shows that Delrin (data curve 1), PMMA 3, and high-density polyethylene 4 characteristics are within this shaded area; therefore, the space experiment is possible on *Mir*, and a limiting flow velocity V_{lim} and a flame-spread rate V_f for these materials can be obtained. As noted, the cylindrical samples maintain their shape longer; therefore, this shape is preferred for the space experiment.

The results of the previous *Skorost* testing of PMMA on *Mir* suggest that values shown in table 1.2 and on figure 1.14 may be higher than actual data obtained in *Skorost* during the space test. However, V_{lim} from table 1.2 was taken as the first approximation for the flow velocity setting in the *Skorost* combustion chamber on *Mir* for V_{lim} evaluation.

Table 1.5 describes in general the space test procedure on *Mir* for the three selected materials, Delrin, high-density polyethylene, and PMMA at an oxygen concentration of 21 percent in the *Mir* compartment. The material ignition occurs at flow velocities 2 to 3 cm/s higher than V_{lim} from table 1.2. The first set of samples were tested according to *Skorost* ground testing timeline, described above. The flame-spread rate and time of flame decay at flow shutoff were measured accordingly. Three samples of each material were used to evaluate V_{lim} accurately for the material.

1.7 *Skorost* Special Testing

The objectives of the *Skorost* special testing with four filters was:

- to familiarize the crew with the apparatus;
- to develop the space-experiment test procedure; and
- to assess crew fire and toxicology safety.

The space-experiment test-procedure development and fire- and toxicology-safety assessment were performed in accordance with RSC-Energia programs and standards. *Skorost* was oriented vertically for this test to avoid contaminating the observation window with soot particles. The induced flow in the combustion chamber was in the downward direction. Two Delrin samples were burned for training purposes (one by the main crew, and another one by the back-up crew). Crew training was successful, and the crew had no comments.

During the fire- and toxicology-safety assessment, the air-purification system of the *Mir* module mock-up was turned off to eliminate its effect on the air quality and to evaluate the *Skorost* filter system. Six people were in the working compartment of the mock-up for one hour, and only one comfort fan was on. For the fire- and toxicology-safety assessment, one sample of each material was burned (PMMA, Delrin, polyurethane, nylon, polyethylene, glass-epoxy). The samples were ignited at their free end, and half of each sample was burned in the flow. Then the flow was shut off, and the samples burned until completely quenched.

Samples of the compartment atmosphere were taken through probes for analysis at four times —before the test, half a minute after each sample ignition, after each sample extinguishment, and at the end of the test. The gaseous environment at the *Skorost* air-pump outlet was analyzed during sample combustion. The *Skorost* combustion chamber was purged for five minutes between sample burns.

The gaseous environment was analyzed for the presence of: oxygen, carbon monoxide, carbon dioxide, unsaturated hydrocarbons (total), and saturated hydrocarbons (total). The gaseous chromatograph "Tsvet 560" was used for the toxicology analysis. Table 1.6 shows the results of the gaseous environment analysis at the *Skorost* outlet and in the Space Station compartment (mock-up), when the Space Station air-quality control system is not working. The performed analysis confirmed that maximum allowable concentrations for a flight of long duration (up to 180 days) are not exceeded, and carbon monoxide is not detected. Therefore, the *Skorost* filter system is in compliance with crew safety requirements for the *Mir* Space Station. Later, the analyses and testing were repeated for the apparatus with one set of filters (two filters total), and they found that impurity concentrations at the *Skorost* outlet are also within allowable limits.

2. SPACE EXPERIMENTS IN *SKOROST* ON ORBITAL STATION (OS) *MIR*

The *Skorost* apparatus was accepted for the flight test after ground preparation, which included:

- space-experiment procedure development,
- *Skorost* special testing for safety assessment, and
- *Skorost* electrical system development and checkout.

On October 14, 1998, the OS *Mir* crew 26 (Cosmonauts G. Padalka and S. Avdeev) assembled and prepared the flight *Skorost* apparatus. It was connected to the Kvant Module power and telemetry systems, and the control board was checked out. *Skorost* functionality and readiness were confirmed. The apparatus was prepared for microgravity flammability evaluation of selected nonmetallic structural materials, *i.e.*, the thermoplastic polymers, Delrin, PMMA, and high-density polyethylene.

Twelve samples were installed in the *Skorost* combustion chamber (four of each material; cylindrical samples 4.5-mm in diameter and 60-mm long). Samples were mounted rigidly on two carousels according to the following arrangement:

- Delrin (Samples #1, #2, #3, and #4) and PMMA (Samples #5 and #6) were mounted on the first carousel;
- PMMA (Samples #7 and #8) and polyethylene (Samples #9, #10, #11, and #12) were mounted on the second carousel.

The flight *Skorost* apparatus was equipped with only one set of filters instead of two. Therefore, one of the two parallel outlets was sealed during the assembly procedure.

Four test cycles were accomplished successfully in *Skorost* on *Mir* on October 15-22, 1998. Each test cycle covered combustion of three samples (one of each material). The first test cycle was performed on October 15, 1998, with Samples #1, #5, and #9; the second test cycle was performed on October 19, 1998, with Samples #2, #6, and #10; the third and fourth test cycles were performed on October 22, 1998, with Samples #3, #8, and #11 and #4, #7, and #12 respectively.

The experiment was monitored and recorded by *HI-8* and *Betacam* cameras. Since the video recording was performed outside the times of the communication window between the ground and the Space Station, real-time monitoring of the combustion experiment was not feasible.

Oxygen concentration in the *Mir* compartment was measured and recorded. It was higher than the expected 21 percent (total), ranging from 22.5 to 25.4 percent. The power supplied to *Skorost* was off-nominal as well. Therefore, part of the flow-velocity selection in the test program (table 1.5) had to be modified. Table 2.1 of the report shows the changes that were implemented into the test program as determined during communication sessions with the OS *Mir* crew before the beginning of each test cycle.

2.1 Delrin Testing

2.1.1 Sample #1.—The space experiment was done on October 15, 1998. The space-compartment environment was characterized by a total pressure p_{ATM} of 709 mm Hg (94.5 kPa); an oxygen partial pressure p_{O_2} of 160 mm Hg (21.3 kPa, or 22.5 percent of the total pressure); a water partial pressure p_{H_2O} of 7.4 mm Hg (0.99 kPa); a carbon-dioxide partial pressure p_{CO_2} of 5.2 mm Hg (0.70 kPa); and a temperature T = 20 °C.

The sample was ignited at a velocity V of 2 cm/s. An attempt to ignite the sample by two igniters at nominal temperature failed after 54 sec, and then two igniters at maximum temperature ignited the sample in 22 sec. The sample length was divided into two halves by a concentric mark in the middle. The first half of the sample was burned in a flow velocity of 1 cm/s, and then the flow was stopped. The duration of combustion was 3 min and 33 sec. After the flow shutoff, the Delrin sample #1 continued to burn for 2 min:10 sec, until combustion finally ceased.

The combustion chamber observation windows were foggy initially. The heat from the Delrin sample #1 combustion distorted the adjacent PMMA sample #7 and bent it toward the combustion chamber window. The Polyethylene sample #12 was also deformed by heat.

<u>2.1.2 Sample #2</u>.—The space experiment was done on October 19, 1998. The space-compartment environment was characterized by p_{ATM} = 722 mm Hg (96.3 kPa); p_{O2} = 171 mm Hg (22.8 kPa, or 23.6 percent of total); p_{H2O} = 7.8 mm Hg (1.04 kPa); p_{CO2} = 5.8 mm Hg (0.77 kPa); and T = 20 °C.

The sample was ignited at V = 4 cm/s. (Based on the first test results, the flow velocity for ignition was increased.) The ignition time was 5 sec. The sample length was divided into three equal parts. The first portion of the sample was burned in a flow velocity of 1 cm/s, and the combustion time from ignition to the moment when the fan was switched was 2 min:37 sec. The second portion of the sample was burned at V = 0.5 cm/s for 3 min:20 sec, and when the flow was stopped, combustion decayed and ceased in 24 sec.

<u>2.1.3 Sample #3</u>.—The space experiment was done on October 22, 1998. The space-compartment environment was characterized by p_{ATM} = 715.5 mm Hg (95.4 kPa); p_{O2} = 182 mm Hg (24.3 kPa or 25.4 percent of total); p_{H2O} = 8 mm Hg (1.1 kPa); p_{CO2} = 6.3 mm Hg (0.84 kPa); and T = 20 °C.

The sample was ignited at V = 4 cm/s. The ignition time was 12 sec; the sample was ignited on the second attempt (after the igniter was applied to the sample for the second time). The sample length was divided into three equal parts. The first portion of the sample was burned at V = 2 cm/s, and the combustion time from ignition to the moment when the fan was switched was 1 min:45 sec. The second portion of the sample was burned at V = 0.3 cm/s for 3 min:49 sec.

During Delrin sample #3 combustion (~1 sec after combustion of the second portion of the sample started), a piece of the PMMA sample #5 floated, struck, and remained attached to the flame zone, and the two materials burned together. When the flow was stopped, combustion ceased in 13 sec.

<u>2.1.4 Sample #4</u>.—The space experiment was also done on October 22, 1998, and the space-compartment environment was the same as that reported for Delrin sample #3. The sample was ignited at V = 4 cm/s. The ignition time was 14 sec; the sample ignited on the second attempt.

The sample length was divided into three equal parts. The first portion of the sample was burned at V = 7 cm/s, and the combustion time from ignition to the moment when the fan was switched was 51 sec. The second portion of the sample was burned at V = 0.3 cm/s for 2 min:19 sec. When the flow was stopped, combustion ceased in 19 sec.

2.2 PMMA Testing

<u>2.2.1 Sample #5</u>.—The space experiment was done on October 15, 1998, and the space-compartment environment was the same as that reported for Delrin sample #1. The sample was ignited at V = 2 cm/s. The ignition time was 9 sec; the sample ignited on the second attempt.

The sample length was divided into two halves by a concentric mark in the middle. The first half of the sample was burned at a flow velocity of 2 cm/s, and then the flow was stopped. The first half of the sample burned for 2 min:3 sec. When the flow was stopped, combustion ceased in 4 sec.

<u>2.2.2 Sample #6</u>.—The space experiment was done on October 19, 1998, and the space-compartment environment was the same as that reported for Delrin Sample #2. The sample was ignited at V = 2 cm/s. The ignition time was 23 sec.

The sample length was divided into three equal parts. The first portion of the sample was burned at V = 1 cm/s, and the combustion time from ignition to the moment when the fan was switched was 58 sec. The second portion of the sample was burned at V = 0.5 cm/s for 1 min:21 sec, and combustion ceased before the flame front propagated to the second concentric mark. Hence, the flame extinguished prior to flow shutoff.

<u>2.2.3 Sample #7</u>.—The space experiment was done on October 22, 1998, and the space-compartment environment was the same as that reported for Delrin sample #3. PMMA sample #7 was burned last, because it was distorted during Delrin sample #1 combustion, as noted. The sample was bent, and it was ignited on the side. The sample was ignited at V = 2 cm/s. The ignition time was 22 sec. The front part of the sample created a loop with a large drop of melting material formation.

The sample length was divided into three equal parts. The first portion of the sample was burned at V = 8.5 cm/s, and combustion time from ignition to the moment when the fan was switched was 31 sec. The second portion of the sample was burned at V = 0.5 cm/s for 3 min:26 sec. When the flow was stopped, combustion ceased in 15 sec.

<u>2.2.4 Sample #8</u>.—The space experiment was done on October 22, 1998, and the space-compartment environment was the same as that reported for Delrin sample #3. The sample was ignited at V = 4 cm/s. The ignition time was 11 sec; the sample ignited on the third attempt.

The sample length was divided into three equal parts. The first portion of the sample was burned at V = 4 cm/s, and combustion time from ignition to the moment when the fan was switched was 48 sec. The second portion of the sample was burned at V = 0.75 cm/s for an unknown period of time, because of missing data on the video tape. The combustion time from the first concentric mark was 2 min:28 sec. PMMA sample #8 reignited Delrin sample #1.

2.3 High-Density Polyethylene Testing

<u>2.3.1 Sample #9</u>.—The space experiment was done on October 15, 1998, and the space-compartment environment was the same as that reported for Delrin sample #1. The sample was ignited at V = 8.5 cm/s. The ignition time was 10 sec; the sample ignited on the second attempt.

The sample was divided into two halves by a concentric mark in the middle. The first half of the sample was burned at a flow velocity of 8.5 cm/s, and then the flow was stopped. The first half of the sample burned for 1 min 3 sec. When the flow was stopped, combustion ceased in 13 sec. A fog formed in the combustion chamber upon extinguishment, but it dispersed after purging.

<u>2.3.2 Sample #10</u>.—The space experiment was done on October 19, 1998, and the space-compartment environment was the same as that reported for Delrin sample #2. The sample was ignited at V = 8.5 cm/s. The ignition time was 5 sec.

The sample length was divided into three equal parts. The first portion of the sample was burned at V = 4 cm/s, and combustion time from ignition to the moment when the fan was switched was 59 sec. The second portion of the sample was burned at V = 2 cm/s for 1 min:34 sec. The third portion of the sample was burned at V = 1 cm/s for 51 sec. After flow shutoff, combustion ceased immediately. A fog formed in the combustion chamber upon extinguishment, but it dispersed after purging.

<u>2.3.3 Sample #11</u>.—The space experiment was done on October 22, 1998, and the space-compartment environment was the same as that reported for Delrin sample #3. The sample was ignited at V = 8.5 cm/s. The ignition time was 7 sec; and, due to minor deformation of the sample, the crew had to rotate the carousel to move the sample closer to the igniter.

The sample length was divided into three equal parts. The first portion of the sample was burned at V = 2 cm/s, and combustion time from ignition to the moment when the fan was switched was 57 sec. The second portion of the sample was burned at V = 1 cm/s for 1 min:34 sec. The third portion of the sample was burned at V = 0.5 cm/s for 26 sec. After flow shutoff, combustion ceased immediately. A fog formed in the combustion chamber upon extinguishment. The fog disappeared after purging.

<u>2.3.4 Sample #12</u>.—The space experiment was done on October 22, 1998, and the space-compartment environment was the same as that reported for Delrin sample #3. The sample was ignited at V = 8.5 cm/s. The ignition time was 7 sec.

The sample length was divided into three equal parts. The first portion of the sample was burned at V = 1 cm/s, and combustion time from ignition to the moment when the fan was switched was 58 sec. The second portion of the sample was burned at V = 0.5 cm/s for 1 min:39 sec. The third portion of the sample was burned at V = 0.3 cm/s for 48 sec. After flow shutoff, combustion ceased immediately. A fog formed in the combustion chamber upon extinguishment. The fog disappeared after purging.

3. TEST RESULTS AND DISCUSSION ON COMBUSTION OF SAMPLES IN MICROGRAVITY

According to the test timeline, test conditions were changed when the flame front propagates the given fraction of the sample length l, either $(1/2) \times l$, $(1/3) \times l$, or $(2/3) \times l$, depending on the sample number and combustion mode. The flow velocity during the test was changed from highest to lowest, or to zero. The points where the fan was to be switched was indicated by concentric marks on the samples. When the front of the flame got to the last mark, the flow was stopped, $i.e.$, the fan was turned off, and the shutter at the combustion chamber inlet was closed. Then the sample quenching time τ_2 was measured.

Unfortunately, oxygen concentration, which is an important environmental property that defines material combustion, was elevated at the time of the space experiment. Moreover, oxygen concentration was different for all three test days, or C_{ox} = 22.5, 23.6, and 25.4 percent, which complicates the test data analysis.

3.1 Verification of Ground Calibration of Flow in *Skorost* by Vortex Movement in the PMMA Flame

Usually, four filters at the *Skorost* outlet are used to avoid space compartment contamination with hazardous combustion products, namely, two sets of gas mask filters (of "M" and "BKF" type), connected in series. However, due to technical problems during delivery, the flight *Skorost* used for the space experiment was equipped with two filters (one set) only. Therefore, one of the *Skorost* exhaust outlets was sealed during the apparatus assembly on orbit. Additional safety testing verified that *Skorost* with two filters is still in compliance with crew safety requirements, but the flow velocity in *Skorost* combustion chamber decreased significantly.

Figure 1.5 shows the results of flow calibrations, which were repeated on the ground with the test *Skorost* apparatus equipped with two filters. The flow velocity was measured at a low power supplied to *Skorost* from the *Mir* Power Supply System (25.9 V), as was the case on *Mir* during the space experiment. To have the hydraulic resistance in the test *Skorost* as close to the hydraulic resistance in the flight *Skorost* as possible, the sets of meshes in the test *Skorost* combustion chamber underwent special thermal treatment to clean away the combustion-product residue left after the previous testing. Nevertheless, because the test *Skorost* apparatus was used for ground calibration instead of the flight one, a velocity-field identity became a concern.

It is known that, in microgravity with no buoyancy, a velocity of vortices on the flame border characterizes an air-flow velocity. The most stable vortices are formed in the PMMA sample flame. The computer-aided processing of the videotape provided real-time information on the flow velocity during the test. Figure 1.5 includes a comparison of ground calibration data and real-time data obtained from the video. The discrepancy is within the error of measurement (10 to 15 percent); therefore, ground calibration data on the flow velocity during the space experiment are applicable.

3.2 Concurrent Flow Effects in the Flame Zones of Burning Nonmetallic Materials in Microgravity

The samples tested in the space experiment are symmetrical. Therefore, only one video camera *Betacam* was used to record sample combustion through the window on the top of the combustion chamber. The other camera recorded the control board to show conditions during the test (power to the fan motor, flow-rate meter knob position, and the number of the sample in the midline).

Figures 3.1 to 3.12 show the results of computer-aided processing of the video information obtained from orbit for all 12 samples. The combustion parameters that characterize a flame and a melting zone are a diameter and "length" of the molten drop (d_D, l_D), a diameter and length of the flame (D_F, L_F), a gap between the flame and the sample surface (δ_x), coordinates of the front and rear border of the flame (X_F^+, X_F^-), and the heat wave-front coordinate (l_{hw}), all shown as functions of time τ. All lengths on figures 3.1 to 3.12 are dimensionless, normalized by dividing by the sample initial diameter $(d_0 = 4.5$ mm$)$. Time τ starts from the moment when the igniter moves away from the sample after ignition. The flame-front coordinate time history provides information on V_F^+, which is a flame front-border propagation rate, and V_F^-, which is a flame rear-border propagation rate, or a material-destruction rate. In figures 3.1 to 3.12, the flame coordinates are shown with arbitrary starting points. For the front border of the flame X_F^+, the position is shown increasing in a negative direction. For the rear border of the flame X_F^-, the position is shown increasing in a positive direction. Lines through the points indicate the slopes that determine V_F^+ as the time rate of change of X_F^+, and V_F^- as the time rate of change of X_F^-.

3.2.1 Delrin Sample #1.—This was the first sample. The cosmonauts did not notice a weak flame, because they expected to see a bright one. Thus, they continued to ignite the sample for 54 sec at nominal current through the ignition coil, and then for another 22 sec at maximum current. Due to the prolonged and unreasonable ignition, adjacent samples #7 (PMMA) and #12 (polyethylene) were heated and deformed.

The Delrin combustion occurred with the formation of a spherical melt ball, which bubbled vigorously (fig. 3.13). Combustion dynamics for Delrin sample #1 are shown in figure 3.1. The diameter of the ball d_D is constant (about 1.6) during almost the entire first part of the test (V = 1 cm/s). Its length l_D increases from 2.0 at

$\tau = 180$ sec to a maximum of 2.9 at $\tau = 255$ (the time of flow shutoff) and then decreases to 2.25 at $\tau = 310$ (in the time period when the sample continues to burn even though V is zero).

For Delrin sample #1, the flame-propagation rate V_F^+ increases greatly from 0.053 to 0.092 mm/s at $\tau = 180$ sec. The material-destruction rate V_F^- is constant and low at 0.036 mm/s. However, when the flow stops, the material-destruction rate increases to 0.060 mm/s. It is still unknown why Delrin sample #1 continued to burn for 130 sec after flow shutoff until finally extinguishing.

3.2.2 Delrin Sample #2.—Combustion dynamics for Sample #2 are shown in figure 3.2. This sample was ignited at a higher flow velocity (V = 4 cm/s instead of 2 cm/s). The higher flow velocity and the experience gained during Delrin sample #1 combustion helped the cosmonauts to ignite the sample in only 5 sec. Figure 3.2 indicates that the diameter of the melt ball d_D increases from the initial 1.0 at $\tau = 0$ to 2.15 at 140 sec during the first mode of the test (V = 1 cm/s). By the end of the experiment, d_D reaches 2.5. The melt-ball length l_D (not shown) is 2.55 at first, and then it increases during the second mode of the test (V = 0.5 cm/s), but not rapidly. Flame diameter and length increase from $D_F = 2.0$ and $L_F = 1.75$ at $\tau = 0$ to $D_F = 3.9$ and $L_F = 5.3$ at 115 sec.

Figure 3.2 also shows the amplitude of sample rear-edge oscillations (coordinate X_F^-). These oscillations are caused by formation and eruption of big bubbles with gaseous products of material destruction inside. Despite the growing size of the melt ball, the material-destruction rate V_F^- is constant at 0.105 mm/s for both V = 1 and 0.5 cm/s, which is three times higher than the rate of 0.036 mm/s measured for Delrin sample #1. The flame-front propagation rate V_F^+ (not shown in fig. 3.2) is 0.13 mm/s at V = 1 cm/s and 0.10 at V = 0.5.

A flame of a light blue color was observed during the test when the flow velocity was 1 cm/s. The flame became almost transparent when the flow velocity decreased to 0.5 cm/s. The flame and melt ball at the latter time are illustrated in figure 3.14.

3.2.3 Delrin Sample #3.—Combustion dynamics for Delrin sample #3 are shown in figure 3.3. The size of the melt drop increases rapidly during the first mode, similar to that of Delrin sample #2, up to $d_D = 2.0$ at $\tau = 90$ sec. The size of the flame increases as well and reaches $D_F = 4.4$ and $L_F = 4.8$ at $\tau = 90$ s, with a rate of change of the flame length shown as 0.21 mm/s. The gap between the flame and sample surface δ_F is 1.0 to 1.15 (not shown in fig. 3.3). The material-destruction rate V_F^- shown in the figure remains the same at 0.175 mm/s for the V = 2 and 0.3 cm/s conditions, but it decreases by almost a factor of two (0.075 cm/s) after $\tau = 150$ sec, when a piece of the PMMA sample #5 stuck to the Sample #3 and the two samples started to burn together. The flame-front propagation rate V_F^+ (not shown) decreases by almost a factor of three (i.e., from 0.25 to 0.085 mm/s) when the flow velocity changes from 2 to 0.3 cm/s.

3.2.4 Delrin Sample #4.—The last Delrin sample was tested at a maximum flow velocity of 7 cm/s. Combustion dynamics for Delrin sample #4 are shown in figure 3.4. The diameter of the boiling melt drop d_D increases constantly from an initial 1.0 to 2.0 at $\tau = 60$ sec (the end of the first mode) to 2.4 at $\tau = 160$ (near the end of the second mode). The size of the flame reaches $D_F = 4.5$ and $L_F = 6.5$ at $\tau = 60$. The flame-front propagation rate V_F^+ is 0.4 cm/s during the first mode (not shown in the figure). The material-destruction rate V_F^- of 0.185 is the same for both modes, about half of the flame-propagation rate.

A bright flame of a light blue color was observed when the flow velocity was 7 cm/s (fig. 3.15). The brightness of the flame decreased when the flow velocity was reduced to 0.3 cm/s (fig. 3.16).

3.2.5 PMMA Sample #5.—A picture of the PMMA flame when V = 2 cm/s is shown on figure 3.17. The rear part of the flame was of a white color with well-defined border, but the front part of the flame was unstable, red-orange in color, with a poorly-defined border. Soot particles were ejected from the flame, forming strands. Bright spurts were also visible. A high-temperature zone, visualized by tiny bubbles appearing in the transparent PMMA material, was located in front of the main swollen collar of melting material. Tiny drops of molten material were noticeable within this zone. These drops moved away from the sample axis; but, being unable to overcome a sur-face-tension force, they returned to the points of their origin (fig. 3.18).

Combustion dynamics for PMMA sample #5 are shown in figure 3.5. The melt-drop diameter d_D increases gradually and reaches 2.0 by $\tau = 70$ sec. Simultaneously, both the diameter and length of the hemispherical flame increase from 2.0 at $\tau = 0$ to 4.0 at 40 sec. After that time, the flame diameter remains constant at 4.0 to 4.1, but the length of the flame continues to increase at a small rate. The flame-front propagation rate is a constant for the entire test at $V_F^+ = 0.26$ mm/s, but the material-destruction rate V_F^- increases from 0.06 mm/s measured during the time interval of $\tau = 20$ to 45 sec to 0.2 after $\tau = 45$.

3.2.6 PMMA Sample #6.—PMMA sample #6 was tested at a lower flow velocity than PMMA sample #5. After about 50 sec of the second part of the test (V = 0.5 cm/s), the transparent flame extinguished when the fan was still working. The short part of the sample before the second concentric mark remained in the initial conditions, without bubbles in the transparent PMMA material.

Combustion dynamics for PMMA sample #6 are shown in figure 3.6. During the initial period of combustion ($\tau < 20$ sec) at V = 1 cm/s, the drop of melting material swells rapidly to a diameter of 2.0 at $\tau = 50$ sec. Simultaneously, both the diameter and length of the flame increase. The gap between the flame and sample surface δ_i appears to be constant at a value of about 1.2, as shown in figure 3.6.

The analysis of D_f, δ_i, and d_D shows that at $\tau < 50$ sec:

$$D_1 = d_D + 2\delta_i$$

Hence, an increase in the PMMA melt-ball diameter d_D leads to an increase in the flame diameter D_f.

From figure 3.6, the calculated flame-front propagation rate at V = 1 cm/s appears to be constant and equal to 0.35 mm/s at $\tau = 0$ to 30 sec, which is higher than the rate of 0.26 mm/s for Sample #5 at V = 2 cm/s. This discrepancy might be explained by higher oxygen concentration at the test times (23.6 percent instead of 22.5 percent).

The gaseous bubbles formed inside the transparent PMMA sample in front of the flame zone demonstrate the thermal-wave propagation. This process was video recorded. The thermal-wave propagation, V_{HW}, at V = 1 cm/s is shown in figure 3.6 as 0.43 mm/s. When the flow velocity decreases from 1 to 0.5 cm/s at $\tau = 80$ sec, both V_{HW} and V_f^- decrease. (The thermal-wave propagation went to 0.09 mm/s; the material-destruction rate went to 0.066 mm/s.)

During the first mode of the test, the flame was white and opaque with soot formation; and the edge of the sample was visible only in the moments of bright spurts. During the second mode, the flame became blue and transparent, and the edge of the sample was visible; but the low contrast of the video did not show confidently the border of an almost invisible flame. Simultaneously, the color of the flame changed from white-orange to blue.

3.2.7 PMMA Sample #7.—This sample was burned last, because it was damaged. The sample was bent; and, therefore, it was ignited from the side. However, after ignition the flame propagated upstream and in 7 sec reached the front edge of the sample. Under the effect of concurrent flow, the front part of the sample created a loop with a large drop of melting material formed. Then the sample became straight again, and combustion was similar to that following a normal ignition (see fig. 3.19).

Combustion dynamics for PMMA sample #7 are shown in figure 3.7. In the first mode, the flow V is a maximum of 8.5 cm/s. The flame diameter and length reach values of 4.4 and 7.4, respectively. The average flame-front propagation rate V_f^* is 0.73 mm/s, and the material-destruction rate V_f^- of 0.135 is several times lower. In the second mode, a new measurement of the coordinates of the melting front along the sample surface X_M is included. The slope of these positions determines the melt-front propagation rate V_M, which has a constant value of 0.095 mm/s. The material-destruction rate V_f^- decreases during the second mode to 0.105 mm/s. Combustion continues for more than 200 sec at the V = 0.5 cm/s mode

3.2.8 PMMA Sample #8.—The sample was tested in three different modes, but it is unclear due to loss of some video data when the flow velocity changed for the third mode. The flame extinguished at $\tau = 205$ sec (approximately), when the flow velocity was apparently 0.5 cm/s. Just before that time, the sample ignited the adjacent remainder of Delrin sample #1. Both samples burned together for a while.

Combustion dynamics for PMMA sample #8 are shown in figure 3.8. During the first mode, the flame diameter and length increase greatly by about factors of three. The flame-front propagation rate is 0.42 mm/s, and the material-destruction rate is 0.24 mm/s. During the second mode, the material-destruction rate decreases to about half the original rate. As also reported for PMMA Sample #7, a melt-front propagation rate V_M, is determined, which is of the order of 0.13 to 0.16 mm/s.

3.2.9 Polyethylene Sample #9.—In general, the flame was white in color, due to soot particles, and elongated (fig. 3.20). When the fan was turned off and the flow velocity decreased from 8.5 cm/s to zero, the flame length decreased rapidly, especially in the portion of the flame that is white. By $\Delta\tau = 3$ sec, the flame was blue and transparent with $L_f = 2.8$ and $D_f = 2.6$; i.e., it acquired a shape close to a hemisphere. The flame also oscillated longitudinally with a frequency of about 1.2 Hz before combustion decayed at $\Delta\tau = 10$ sec after flow shutoff. After extinguishment, the combustion chamber was filled with a thick white smoke, which consists of the products of polyethylene thermal destruction.

Combustion dynamics for Sample #9 are shown in figure 3.9. About 25 sec after ignition, the flame becomes steady. D_1 is 2.5, while L_1 increases at a constant rate shown to be of the order of 0.35 mm/s, almost until flow shutoff. Within the period $\tau = 8$ to 50 sec, the flame-front propagation rate V_F^* is constant at 0.48 mm/s and the material-destruction rate V_1^- is also constant at the lower rate of 0.185 mm/s.

3.2.10 Polyethylene Sample #10.—Combustion dynamics for Sample #10 are shown in figure 3.10. The diameter of the melt ball d_1 increases from 1.7 to about 2.0 during the first mode and remains nearly constant thereafter. The relatively small δ_F might be explained by a sharpened shape of the sample edge. The flame size increases during the first mode, reaching $D_F = 2.6$ and $L_F = 4.8$. The flame-front propagation rate V_F^* is 0.13 mm/s during the first mode. The flame-front propagation rate V_F^* is 0.37 mm/s during the second mode and part of the third mode. The material-destruction rate V_1^- is low during the first mode (0.13 mm/s), highest during the second mode (0.49), and intermediate during the third mode (0.27).

3.2.11 Polyethylene Sample #11.—Polyethylene sample #11 had a slightly bent shape prior to the test. The free end of the sample deviated from the axis by about 10 percent of the sample radius at $\tau = 40$ sec. When the flow velocity decreased to 0.5 cm/s, the brightness of the flame decreased as well, and the flame became almost invisible. Oscillations of the flame at a frequency of 2.5 Hz started, and, in $\Delta\tau = 22$ sec, the flame extinguished while the fan was still working. As in the previous polyethylene tests, after extinguishment, the combustion chamber was filled with a thick white smoke, which consists of the products of polyethylene thermal destruction.

Combustion dynamics for Sample #11 are shown in figure 3.11. The flame length increases rapidly at a rate of 0.21 mm/s during the first mode. For each test mode, the flame-propagation rates are constant but different. The flame-front propagation rate decreases from 0.3 mm/s during the first mode to 0.18 during the second.. The material-destruction rate is 0.076 mm/s, only one-fourth the flame-propagation rate during the first mode, and it increases to 0.18 mm/s during the second mode, which is an indication that the polyethylene combustion is quasi-stationary.

3.2.12 Polyethylene Sample #12.—Polyethylene sample #12 was heated and deformed during the prolonged ignition of Delrin sample #1. The flame was white at ignition ($V = 8.5$ cm/s), then became light blue ($V = 1$), and then became dark-blue, almost invisible ($V = 0.5$). At $\tau = 80$ sec, the flame oscillated longitudinally at a self-sustained frequency of 2.3 Hz. The oscillations continued during the third part of the test ($\tau > 145$ sec, $V = 0.3$ cm/s). Then, in about 40 sec, the flame extinguished while the fan was still working. As in the previous test, after extinguishment the combustion chamber was filled with a thick white smoke, which consists of the products of polyethylene thermal destruction.

Combustion dynamics for Sample #12 are shown in figure 3.12. The melt-ball diameter is constant at about 1.4 during the second mode. The flame diameter and length increase during the first mode, but appear to be nearly constant during the second mode. The flame-front propagation rate V_F^* is 0.20 mm/s during the first mode and 0.13 during the second mode. The material-destruction rate is nearly uniform at 0.14 to 0.11 mm/s during these two modes.

3.2.13 Flame-Front Propagation-Rate Summary.—Figure 3.21 presents the results of the space experiment in terms of the variation of the flame-front propagation rate V_F^* with the changes in the velocity of the flow V for the 12 samples of Delrin, PMMA, and polyethylene. V_1^* decreases rapidly from 0.5-0.75 to 0.05-0.10 mm/s when the flow velocity decreases from $V = 8.5$ to $V = 0.3$-0.5 cm/s. This pattern leads to a conclusion that damping of the vent flow in the space station compartment will suppress the fire source in microgravity.

Figure 3.21 also shows the flame-front propagation rate (melting front) data that were obtained in the Narrow Channel apparatus (table 1.3). The flame-propagation rate V_F^* obtained in the ground testing appeared to be lower than V_F^* from the space experiment on *Mir*. This phenomenon can be explained by the fact that the flame does not surround the whole drop of melt in the Narrow Channel, which decreases the heat flux to the sample and the flame-propagation rate.

3.3 Characteristics of Limiting Combustion Modes

At an oxygen concentration of 22.5 percent, the Delrin sample #1 was still burning at $V = 1$ cm/s. The ground testing of material flammability in the Narrow Channel apparatus showed that at $C_{ox} = 21$ percent, $V_{lim} = 0.50$ cm/s and at $C_{ox} = 23$ percent, $V_{lim} = 0.30$. When the oxygen concentration increased to $C_{ox} = 23.6$ percent and 25.4 percent in the space experiment, Delrin combustion did not stop at $V = 0.5$ cm/s (Sample #2) and $V = 0.3$ cm/s (Samples #3 and #4), respectively. Therefore, in these conditions, V_{lim} for Delrin is less than 0.3 cm/s. Table 3.1 shows the results of τ_2 measurements, where τ_2 is the time of flame extinction at flow shutoff in the *Skorost*

combustion chamber. With the exception of the first Delrin sample (Sample #1, which might be overheated), $\tau_2 = 13$ to 24 sec for Delrin, which is several times lower than the extinction time in the ground test ($\tau_2 = 115$ sec).

A limiting flow velocity V_{lim} has been identified for PMMA. When the oxygen concentration C_{ox} was 23.6 and 25.4 percent, V_{lim} was close to 0.5 cm/s. The flame did not decay when the flow velocity was 2 cm/s at $C_{ox} = 22.5$ percent (i.e., $V_{lim} < 2$ cm/s), nor when the flow velocity was 0.75 at $C_{ox} = 25.4$ percent ($V_{lim} < 0.75$ cm/s). The limiting flow velocity obtained in the ground testing is higher: at $C_{ox} = 21$ percent, $V_{lim} = 3.3$ cm/s, and at $C_{ox} = 23$ percent, $V_{lim} = 2.3$ cm/s. The time τ_2 of sample extinction at flow shutoff in microgravity was about 11 to 15 sec, which is less than half of the extinction time in the ground test ($\tau_2 = 30$ sec).

A limiting flow velocity V_{lim} has been identified for high-density polyethylene as well. When the oxygen concentration was 25.4 percent, V_{lim} was about 0.3 to 0.5 cm/s, while at $C_{ox} = 23.6$ percent, combustion was still going at $V = 1$ cm/s, (i.e., $V_{lim} < 1$ cm/s). The following values for a limiting flow velocity for polyethylene were obtained in the ground testing in the apparatuses with suppressed convection: at $C_{ox} = 21$ percent, $V_{lim} = 8.3$ cm/s, and at $C_{ox} = 23$ percent, $V_{lim} = 3.6$ cm/s. The elevated limiting-flow-velocity data from the Narrow Channel test might be explained by high thermal losses from the flame to the cooled copper plates that formed the Channel (ref. 3). Table 3.1 shows that τ_2 for polyethylene is very short ($\tau_2 < 10$ s). That means that, in microgravity at low oxygen concentrations ($C_{ox} = 21$ percent), diffusion is not sufficient to sustain combustion, and additional oxygen intake by forced convection is required.

3.4 Non-Steadiness and Other Characteristics of Combustion in Microgravity

The nonsteadiness of polymer combustion observed in the space experiment might be explained by two reasons: (1) the formation of the melt drop, which is almost spherical for Delrin and PMMA (see figs. 3.14 and 3.18) or ellipsoidal for polyethylene (see fig. 3.20), and (2) a violent (especially for Delrin and PMMA) boiling within the volume of molten material.

Figures 3.1 to 3.12 show (whenever possible) the dimensionless diameter and length of the melt drop, d_D and l_D, measured at the time of the experiments. The drop size is not enough to achieve steadiness even after 100 to 150 sec. Therefore, for flammability evaluations of these types of materials, the length of the sample and the time of the experiment should be increased. The dimensionless drop diameter increases rapidly in the beginning of the experiment, and the diameter of the flame and length of the flame increase as well. By the end of the experiment, the diameter of the melt ball is 2 to 2.5 times greater than the initial diameter of the cylindrical sample, and the shape of the sample changes drastically during combustion. The gas dynamics of combustion changes as well, which should be accounted for in the analysis and comparison with the test data.

Polyethylene has the most stable and steady combustion. Although the gaseous bubbles formed inside the melt, there is no significant ejection of material from the fuel surface. However, in the quenching mode, intense longitudinal oscillations of the flame occur. Figure 3.22 shows the results of flame-length measurements and presents the dynamics of the Polyethylene sample #9 extinction, when the flow velocity changed from 8.5 cm/s to 0. The length of the part of the flame that is white due to the presence of soot particles decreases rapidly ($\tau = 60$ to 63 sec); and, in three seconds, the entire flame becomes blue and transparent, with $L_1 = 2.8$ and $D_1 = 2.6$, i.e., it acquires a shape close to a hemisphere (see fig. 3.23). The flame maintains this shape until extinction 10 seconds after the fan is turned off ($\tau = 71$ sec). Combustion is stationary. However, along with the stationary process, flame fluctuations are observed ($\tau = 64$ to 71 sec). The flame wave moves from $x = 0$ (edge of the sample) to $x = 6.3$ (the front of the flame when the fan was turned off) with a frequency of 1.3 to 1.4 Hz (see figs. 3.23 and 3.24). The accumulation of flammable gases next to the surface of the sample in the area where stationary combustion has already occurred and the inability of diffusion to provide enough oxygen to the fuel without forced convection might explain these self-sustained flame fluctuations. There are about ten fluctuations of the flame front within 7 sec ($\tau = 64$ to 71 sec) with periods of 0.72 sec (fig. 3.22). The velocity of flame-wave movement in the downstream direction is about 60 mm/s, i.e., more than 100-times higher than the flame-spread rate of 0.48 mm/s that is noted for quasi-stable combustion at the maximum concurrent flow velocity of 8.5 cm/s. Gradually, the brightness of the flame decreases, and the flame decays beginning at its upstream end. In a short time, a thick white smoke that consists of the cooled products of polyethylene pyrolysis fills the chamber—a reliable indication that combustion of polyethylene has stopped.

Oscillations of this type with the frequency of 2.3 Hz were observed during Polyethylene sample #11 combustion when the flow velocity is close to limiting ($V = 0.5$ and 0.3 cm/s at $C_{ox} = 23.6$ percent). The similar process was

observed before for candle-flame extinguishment in the *Glovebox* experiments (*Candle Flame*) on Space Shuttle and OS *Mir* (refs. 26 and 27).

Delrin combustion in microgravity is accompanied by the violent boiling inside the foamy melt drop. The size of the gaseous bubbles inside the drop is comparable to the size of the drop itself. Spurts of gaseous fuel ten times longer than the initial diameter of the sample are formed when the bubbles collapse. When the spurts are ignited, they look like the long tails of flame moving in the upstream direction (Fig. 3.25). The flame-tail velocity is much higher than the flame-spread rates V_F^* and V_F^- shown on figures 3.1 to 3.4, for example.

PMMA combustion is also accompanied by ejection of gaseous products of material destruction. The spurts ignite and form flame tails of various length and brightness (see fig. 3.26).

The data on the flame-color change when the flow velocity is close to the limiting velocity are of great interest. During PMMA combustion, the flame is white at $V > 1$ cm/s, due to the presence of soot particles, and it becomes dark-blue and almost invisible at $V = 0.75$ to 0.5. A similar phenomenon is observed during the polyethylene and Delrin testing, although the flame color is light blue instead of white when the flow velocity is high. Disappearance of the burning soot in the flame indicates a flame temperature decrease (ref. 8). This phenomenon may promote the suppression of fire sources and the extinction of solid nonmetallic-material fires at flow shutoff.

4. PRACTICAL RESULTS

The results of the completed testing are significant for fire-safety assurance in the pressurized compartments of orbiting spacecraft.

All tests conducted with the three different melting materials showed that fire decayed upon the shutoff of vent flow in the combustion chamber. Taking into account the fact that the spherical melt drops of the material are burning prior to flow shutoff, one finds this phenomenon to be very important. It is known that microgravity is the most favorable environment for heat and mass transfer in case of spherical symmetry. Therefore, material extinguishment occurs in the most favorable conditions for combustion. Hence, the possibility of effectively suppressing fire on the surface of thermoplastic polymers by vent flow shutoff is confirmed.

The adjacent Delrin sample #1 was ignited during PMMA sample #8 combustion. The large diameter of the flame at the low flow velocity is the probable cause. Therefore, a flame-size assessment shall be done for two combustion modes:

(a) If combustion occurs at a flow velocity close to limiting, the flame will have a minimum length, but a maximum diameter. This mode might be the most dangerous one, because the probability to ignite an adjacent element is high.

(b) If combustion occurs at a flow velocity that is high enough, the flame will have a maximum length, but a minimum diameter. Therefore, elements located downstream might be ignited.

At flow shutoff, the size of the flame will change by decreasing in the downstream direction and increasing in the lateral direction. This effect shall be considered in the design of configurations for flammable components in the spacecraft compartment. However, this issue should be analyzed further.

An important result of the experiment is that the drop of molten material stays attached reliably to the solid base.

The experience with melting polymer materials demonstrates the high fire hazard associated with their use. In normal gravity, the size of fire increases rapidly due to hot melt flowing down and igniting nonmetallic structural elements located below the fire. For example, a fire might spread down a cable harness, after ignition of polyethylene insulation. If the cable harness is vertical, a fire can spread with a velocity of tens of centimeters per second.

For fire-safety reasons, the use of melting polymers in spacecraft is strictly limited. It has been assumed that the burning melt drops can separate from the material and create numerous sources of a fire. The conducted experiment did not confirm this assumption for the orbital flight. In microgravity, the burning drops of melt do not separate from the material in the air flow with velocities below 10 cm/s. The drop of melt stays attached to the base solid material. This result may ease the limitations on the use of polymer materials in the ventilated environment of orbiting spacecraft.

The limiting flow velocities (V_{lim}) obtained in the test appears to be low, which was predetermined by test-material selection. Priority was given to the most flammable materials, which are not widely used in spacecraft.

5. RECOMMENDATIONS ON CONTINUING RESEARCH ON FLAMMABILITY OF NONMETALLIC MATERIALS IN MICROGRAVITY

As was noted in reference 9, the main obstacle to creating a reliable fire-safety system in the pressurized compartments of International Space Station modules is the limited understanding of the unusual characteristics of the process of combustion of solids in microgravity. Combustion of thermally thin layers of fuel (sheets of paper ~0.1-mm thick) has been the primary study in experiments. This is due to the short time τ, during which it is possible to maintain a state of weightlessness in free fall in ground facilities ($\tau < 10$ sec in drop towers and $\tau < 25$ sec in laboratory aircraft). The data obtained are undoubtedly of great theoretical interest, but as a rule, materials in the form of thermally thick layers are used in real structures. For combustion tests, these require a much longer duration of weightlessness, which can only be provided during expensive and comparatively rare flights of sounding rockets ($\tau = 6$ to 10 min) and spacecraft ($\tau \to \infty$).

Therefore, in all, only six materials in the form of specimens with a sufficiently large cross-section have been tested to date under conditions of prolonged weightlessness (refs. 2, 3, 28 to 30), and three of these were tested in the last series of combustion experiments on the *Skorost* experimental unit aboard the *Mir* Space Station. The results are analyzed in this report and are presented as reports to the Fifth International Microgravity Combustion Workshop held in May 1999 in Cleveland U.S.A. (refs. 29 and 30). As was noted in reference 30, ground facilities with a reduced natural-convection effect (the Narrow Channel experimental unit) can apparently be used only for comparative testing of the flammability of materials.

Most often, experiments in weightlessness have investigated the combustion of a reference or model material (PMMA, polymethylmethacrylate), the thermal and kinetic characteristics of which have been studied in the greatest detail. Planar specimens (plates with width $b = 8$ mm and thicknesses $h = 1, 2,$ and 3 mm) were tested in the first series of space experiments on the *Skorost* experimental unit aboard the *Mir* Space Station (ref. 2). It was observed that the flame was not extinguished at a velocity V of the oncoming flow that (as per updated data) exceeded 5 cm/s. The flame was extinguished only when the flow decayed after the fan had been switched off. In the second series of space experiments on the same apparatus aboard the *Mir* Space Station, burning planar specimens of PMMA ($b = 2$ mm) were extinguished when the air-flow rate with an oxygen concentration $C_{ox} = 21.5$ percent decreased to V = 0.5 cm/s. This agrees with the results of this study, which find that a limiting velocity $V_{lim} = 0.5$ cm/s at $C_{ox} = 23.6$ percent for cylindrical specimens with diameter $d = 4.5$ mm. A tendency for extinction of a flame on the surface of a PMMA specimen with thickness $h = 3.2$ mm in a stagnant atmosphere with a very high oxygen concentration $C_{ox} = 50$ percent at $p = 202$ kPa (2 atm) was observed in experiments under the Solid Surface Combustion Experiments program (ref. 28).

Thus, at least for the reference material (PMMA), the results of the space experiments confirmed the presence of a lower velocity limit for combustion V_{lim} predicted by the theory (refs. 11 and 12). However, it should be noted that the velocity V_{lim} only characterizes the combustion limit for specimens made of the same material and with the same geometrical shape.

Figure 5.1 presents the results of numerical calculations from (ref. 11) on the combustion limits of PMMA in the vicinity of the stagnation point of the oncoming flow of a gaseous mixture containing oxygen. The results are in the form of a map of the mass concentration of oxygen C_{ox} in the oncoming gas flow as a function of the velocity gradient of the external flow at the critical (stagnation) point a (the derivative of the tangential component of the gas velocity u calculated in the direction of the axis of the streamlined body), which characterizes the flow in the vicinity of the critical point. The velocity at the border of the boundary layer increases linearly with the distance x from the critical point, *i.e.*, $u = ax$.

The values of the inverse dimensionless diagnostic variable, the Damköhler number

$$\mathbf{Da} \cong \beta / a$$

are actually plotted along the x-axis of the graph in figure 5.1, where β is the modified pre-exponential factor in the expression for the rate of the chemical reaction (ref. 11). The Damköhler number is the ratio of the characteristic gas-dynamic time, which is proportional to $1/a$, to the characteristic chemical-reaction time, which is proportional to $1/\beta$. If the value of β is fixed, which corresponds to the combustion of any one selected material, then the following relation is valid,

$$\mathbf{Da}^{-1} \sim a$$

The results of the calculations show that the relative role of heat losses to radiation from the surface of the solid body increases as the velocity gradient a decreases. This leads to a decrease in the temperature of the flame and extinction of the flame as a result of the decrease in the rate of the chemical reaction. If there is no radiation from the surface (emissivity $\varepsilon = 0$), then only the upper velocity limit of combustion is observed—the flame is extinguished at low Damköhler numbers because the time that the reacting particles remain in the reaction zone becomes negligible with respect to the characteristic chemical-reaction time ("flame blowout").

The velocity gradient a at the critical point is a function of both the velocity of the oncoming flow V and the characteristic dimension d and shape of the streamlined body. For example:

- For a streamlined sphere, $a = 3V/d$;
- For a streamlined cylinder perpendicular to its generatrix, $a = 4V/d$;
- For a streamlined disk along the normal to its plane, $a = \pi V/2d$.

As the calculation results given in figure 5.1 show, at a given oxygen concentration C_{ox}, the flame is extinguished in the vicinity of the critical point at a definite, fixed value a. Hence, it follows that the combustion velocity limit V_{lim} changes proportionally to the characteristic dimension of the upstream side of the streamlined body. This means that V_{lim} is not constant for a material at a given concentration of oxidizer, but rather it is dependent on the streamlining conditions and the characteristic linear dimension of the body (the scale factor), in particular.

As is noted above, little reliable experimental data are available to date on the combustion limits of non-metallic materials in microgravity in order to generalize them to obtain a theoretical Damköhler number. Space experiments should be continued with variation of the Damköhler number through selection of materials with different combustion reaction-rate constants and variation of the cross-section of the specimens.

Above all, it is necessary to study the effect of the scale factor. For this purpose, flammability tests should be conducted on cylindrical specimens with various diameters ($d = 2$ to 8 mm). Here, based upon the results of ground experiments, it is necessary to select materials for which the velocity limit for combustion V_{lim} is higher than those of the melting thermoplastic polymers tested in this work. As the results from the second series of experiments on the *Skorost* experimental unit aboard the *Mir* Space Station show (ref. 3), the fiberglass and fabric-based laminates used extensively in the pressurized compartments of the ISS modules may be suitable for this purpose.

A study of the combustion of nonmetallic materials with only frontal ventilation of the specimens could be conducted on the *Skorost* experimental unit. Of course, this is the most hazardous mode of streamlining from the fire standpoint, but questions regarding the outbreak of fire on the lateral surface structural elements are also of great interest. It has been demonstrated in theoretical works that two flame fronts are formed immediately after ignition, and these fronts spread in opposite directions along the surface of a thermally thin layer of fuel. The trailing edge of the flame, which moves downstream, is less intense than the leading edge, and it soon degenerates because of insufficient oxygen inflow into this area. As a result, at a certain time after ignition, the flame spreads only in the direction opposite to the slow-moving flow of oxidizing gas (ref. 31).

The theoretical results presented need to be verified by experiments under natural conditions; but, to do so, the *Skorost* experimental unit must be modernized by expanding its experimental capabilities and by eliminating the circuit and structural deficiencies that were revealed during the operations of the present model.

In order to make the modernized *Skorost-M* unit universal and suitable for conducting studies on combustion in a downstream flow in microgravity both on the front and the lateral surfaces of specimens, the design of the igniting devices will be changed, and these devices will be tucked into special niches to increase the uniformity and stability of the flow.

When the combustion chamber of the *Skorost* experimental unit is modernized, it is proposed that the diameter of the rotating drums be increased by a factor of 1.5 (from 60 to 90 mm), and accordingly, the cross-section of the combustion chamber be increased by a factor of 1.5 (from 80×150 to 110×200 mm). This will make it possible to prevent the undesirable heating effect of a burning specimen on neighboring specimens as observed in these experiments, and it will also make it possible to expand the flow nucleus in the combustion chamber. An increase in the distance between specimens by a factor of 1.5 is also necessary to expand the field of view of the compact interferometer with a laser-light source proposed for *Skorost-M*, in order to determine the temperature fields in the flame zone of specimens burning in microgravity. This will markedly increase the information that can be derived from expensive space experiments.

CONCLUSION

The third series of space experiment in the *Skorost* apparatus was conducted and videotaped in October of 1998 on the Orbital Station *Mir*. The combustion of twelve selected cylindrical samples of three plastic materials, Delrin, PMMA, and high-density polyethylene, was observed in microgravity. The diameter of each sample was 4.5 mm, the flow velocity was from 0.3 to 8.5 cm/s, and oxygen concentration was elevated (ranging from 22.5 to 25.4 percent).

The characteristics of melting material combustion were identified in microgravity for the modes close to limiting. The limiting flow velocities were obtained for tested materials:

- for PMMA, $V_{lim} = 0.5$ cm/s at $C_{ox} = 23.6$ percent;
- for polyethylene, $V_{lim} = 0.3 - 0.5$ cm/s at $C_{ox} = 25.4$ percent;
- for Delrin, $V_{lim} < 0.3$ cm/s at $C_{ox} = 25.4$ percent.

The values for a limiting flow velocity obtained in the space experiment appear to be lower that the values obtained in the ground testing with apparatus with suppressed convection (horizontal Narrow Channel).

It has been demonstrated that at flow shutoff the extinction in microgravity occurs in 5 to 20 s, which is significantly lower than the extinction time obtained during the ground testing. The shorter extinction time is favorable for fire-safety system operation in space compartments, where the fire-system response is based on vent-flow shutoff.

It has been shown that, if the concurrent flow velocity V decreases, the flame-spread rate V_f will decrease, from $V_f = 0.5$ to 0.75 mm/s at V = 8.5 cm/s to $V_f = 0.05$ to 0.01 mm/s at V = 0.3 to 0.5 cm/s.

Based on the analysis of data obtained on nonmetallic material flammability in space, it is proposed to continue the space-experiment program in *Skorost* and *Skorost*-M.

REFERENCES

1. A.Yu. Belyaev, S.D. Egorov, A.V. Ivanov, *et al.:* Main Trends of Investigations of Materials' Combustion in Reduced Gravity for Orbital Station Fire Assurance. *Proc. Microgravity Science and Appl. Sess./Inter. Aerospace Cong.,* Moscow, 1995, pp. 237–240.
2. S.D. Egorov, *et al.:* Fire Safety Experiments on "MIR" Orbital Station, in H.D. Ross, ed.: *Third International Microgravity Workshop,* NASA CP–10174, Aug. 1995, pp. 195–199.
3. A.V. Ivanov, V.F. Alymov, A.B. Smirnov, *et al.:* Study of Materials' Combustion Processes in Microgravity. *Proc. Joint Tenth European and Sixth Russian Symp. on Phys. Sci. in Microgravity,* Moscow, vol. 1, 1997, pp. 401–408.
4. M. Shipp, H. Spearpoint: Fires in Microgravity. *Fire Safety Eng.,* vol. 1, no. 4, Aug. 1994, pp. 41–45.
5. K. Ito, O. Fujita: Research of Ignition and Flame Spread of Solid Materials in Japan. in H.D. Ross, ed.: *Third International Microgravity Workshop,* NASA CP–10174, Aug. 1995, pp. 201–206.
6. M.K. King and H.D. Ross: Overview of the NASA Microgravity Combustion Program. *AIAA Jour.,* vol. 35, 1998, pp. 1337–1345.
7. M.K. King: NASA Microgravity Combustion Program, in K.R. Sacksteder, ed.: *Fourth International Microgravity Combustion Workshop.* NASA CP–10194, May 1997, pp. 3–20.
8. H.D. Ross: Combustion and Fire Safety in Microgravity, in R.K. Crouch, V.I. Polezhaev, eds.: *Proc. Microgravity Sci. and Appl. Sess./Inter. Aerospace Cong.,* Moscow, 1995, pp. 225–236.
9. R. Friedman: Fire Safety in Spacecraft. *Fire and Materials,* vol. 20, 1996, pp. 235–243.
10. Ya.B. Zeldovich: Unmixed Gases Combustion Theory. *Tech. Physics Magazine,* vol. XIX, rev. 10, 1949, pp. 1199–1210.
11. J.S. T'ien: Diffusion Flame Extinction at Small Stretch Rate: The Mechanism of Radiative Loss. *Comb. and Flame,* vol. 65, 1986, pp. 31–34.
12. S.S. Rybanin: The Multi-Dimensional Theory of Macro-Heterogeneous Systems Combustion. *Chem. Sci. Diss.,* Institute of Chemical Physics, 1987 (in Russian).
13. A.S. Melikhov, V.I. Potyakin: Limit Modes for Solid Materials Combustion in Microgravity. Chemical Physics of Combustion and Explosion. *Proc. VI All-Union Symp. on Comb. and Explosion,* Alma-Ata, 1980, pp. 48–51.

14. A.S. Melikhov, V.I. Potyakin, A.M. Ryzhov, B.A. Ivanov: Limit Modes for Polymer Material Combustion in Suppressed Convection. *Comb. Explosions, and Shock Waves*, vol. 19, 1984, pp. 393–395.

15. A.S. Melikhov, I.N. Nikitenko, A.V. Shtepa: Material Smoldering Study. Condensed Systems Combustion (Chemical Physics Of Combustion And Explosion). *Proc. XI All-Union Symp. on Comb. and Explosion*, Suzdal, November 19–24, 1989, pp. 110.

16. S.L. Olson, P.V. Ferkul and J.S. T'ien: Near-Limit Flame Spread over a Thin Solid Fuel in Microgravity. *Twenty Second Symposium (International) on Combustion*, The Combustion Institute, Pittsburgh, 1988, pp. 1213–1222.

17. G.D. Grayson, K.R. Sacksteder, P.V. Ferkul, J.S. T'ien: Flame Spreading over a Thin Fuel in Low Speed Concurrent Flow: Drop Tower Experimental Results and Comparison with Theory. *Microgravity Sci. and Technol.*, vol. VII, 1990, pp. 187–195.

18. J.N. de Ris: Spread of a Laminar Diffusion Flame. *Twelfth Symposium (International) on Combustion*, The Combustion Institute, Pittsburgh, 1969, pp. 241–252.

19. P.S. Greenberg, K.R. Sacksteder and T. Kashiwagi: Wire Insulation Flammability Experiment: USML-1 1 Year Post Mission Summary, in N. Ramachandran, *et al*, eds.: *Joint Launch + One Year Science Review of USML-1 and USMP-1 with the Microgravity Measurement Group*. NASA CP–3272, vol. II, May 1994, pp. 631–655.

20. P.S. Greenberg, K.R. Sacksteder and T. Kashiwagi: The USML-1 Wire Insulation Flammability Glovebox Experiment, in H.D. Ross, ed.: *Third International Microgravity Workshop*, NASA CP–10174, Aug. 1995, pp. 25–30.

21. C.J. Hilado: Flammability Handbook for Plastics, Fourth Ed., Technomics Publ., Lancaster, PA, 1990.

22. Test Method for Measuring the Minimum Oxygen Concentration to Support Candle-Like Combustion of Plastics (Oxygen Index). ASTM D 2863–97.

23. B. Gebhart, Y. Jaluria *et al.*: Buoyancy-Induced Flows and Transport. 1998, chapters 13, 14.

24. V.G. Gershuni, Ye.N. Zhukhovitski: Convective Stability of Non-Compressed Fluids. Moscow, 1972, pp. 32–61.

25. V.F. Alymov, A.N. Batov, G.S. Glushko, A.V. Ivanov, A.S. Melikhov: Apparatus With the Suppressed Convection for Material Flammability Evaluation at Near-Limit Modes. *Russian Federation Patent* No. 2106166, Nov. 30, 1995.

26. D.L. Dietrich, H.D. Ross, J.S. T'ien: Candle Flame in Non-Buoyant and Weakly Buoyant Atmospheres. *AIAA Paper* 94–0429, 1994.

27. D.L. Dietrich, H.D. Ross, D.T. Frate, J.S. T'ien, Y. Shu: Candle Flame in Microgravity, in K.R. Sacksteder, ed.: *Fourth International Microgravity Combustion Workshop*, NASA CP–10194, May 1997, pp. 237–242.

28. R.A. Altenkirch, *et al*: Reflight of the Solid Surface Combustion Experiment: Flame Radiation Near Extinction, in K.R. Sacksteder, ed.: *Fifth International Microgravity Combustion Workshop*, NASA CP–1999-208917, May 1999, pp. 27–30.

29. A.V. Ivanov, *et al.*: Preliminary Results of the Third Test Series of Nonmetal Materials Flammability Evaluation in SKOROST Apparatus on the Space Station Mir, in K.R. Sacksteder, ed.: *Fifth International Microgravity Combustion Workshop*, NASA CP–1999-208917, May 1999, pp. 47–50.

30. A.S. Melikhov, *et al.*: The Study of Polymer Material Combustion in Simulated Microgravity by Physical Modeling Method, in K.R. Sacksteder, ed.: *Fifth International Microgravity Combustion Workshop*, NASA CP–1999-208917, May 1999, pp. 361–364.

31. K.B. McGrattan, T. Kashiwagi, H.R. Baum, S.L. Olson: Effects of Ignition and Wind on the Transition to the Flame Spread in a Microgravity Environment. *Comb. and Flame*, vol. 106, 1996, pp. 371–391.

TABLE 1.1.—GROUND-TESTING RESULTS OF U.S.-PROVIDED MATERIAL FLAMMABILITY — LIMITING
OXYGEN CONCENTRATION (C_{lim}) AND LIMITING OXYGEN INDEX (LOI) COMPARISONS

Number	Material	C_{lim}, %, upward combustion		LOI, %, downward combustion	Material combustion pattern
		This re-port	(a)	(a)	
1	Low-density Polyethylene	17.1			Long (8-9 mm) melting zone; melt is transparent
2	High-density Polyethylene	17.2	18.0	18.0	Melting zone 5-6 mm; melt is transparent
3	PMMA	16.8	17.0	17.9	Melting zone 7-8 mm; melt is opaque
4	Delrin	11.2	12.0	17.3	Melts, forms a drop 5-6 mm diameter, melt is opaque
5	Nylon 6/6	18.9 (b)	22.0	29.0	Long (10-15 mm) melting zone
6	Polyurethane	19.8 (b)	27.0	28.0	Melts intensively
7	Glass-epoxy composite	18.0	17.0	26.5	When part of the material (binding agent) is burned out, a rigid frame (carcass) is formed in front of the flame.

ªHirsch and Beeson, testing at U.S. White Sands Test Facility, 1998
ᵇCombustion in air (C_{ox} = 21%), was unstable; C_{lim} was obtained with mica backplate 0.3 mm thick.

TABLE 1.2.—GROUND-TESTING RESULTS OF U.S.-PROVIDED MATERIAL
FLAMMABILITY — LIMITING VELOCITY (V_{lim}) DETERMINED IN
APPARATUSES WITH SUPPRESSED CONVECTION

Number	Material	V_{lim}, cm/sec		
		Narrow channel		Vertical combustion chamber
		C_{ox} = 21%	C_{ox} = 23%	C_{ox} = 21%
1	Low-density Polyethylene	16.9	6.8	-
2	High-density Polyethylene	8.3	3.6	4.5
3	PMMA	3.3	2.3	1.1
4	Delrin	0.5	0.3	1.1
5	Nylon 6/6	16.4	5.3	-
6	Rigid Polyurethane	15.5	4.7	-
7	Glass-epoxy composite	>25	>25	-

TABLE 1.3.—GROUND-TESTING RESULTS OF U.S.-PROVIDED
MATERIAL FLAMMABILITY — FLAME-SPREAD RATE (V_f)
IN NARROW CHANNEL APPARATUS

Material	Flow velocity in channel, cm/sec	V_f, mm/sec @ C_{ox}, percent:	
		21	23
Delrin	3	0.12	0.16
High-density polyethylene	10	0.52	0.60
PMMA	7	0.31	0.36

TABLE 1.4. GROUND-TESTING RESULTS OF U.S.-PROVIDED MATERIAL FLAMMABILITY — SKOROST APPARATUS, VERTICAL SAMPLE ORIENTATION, FLOW VELOCITY - 8 CM/SEC

Parameter	Material And Sample Shape					
	Delrin		High-density polyethylene		PMMA	
	cylinder	strip	cylinder	strip	cylinder	strip
V_r, mm/sec	0.20	0.35	0.25	0.30	0.25	0.30
τ_1, sec	130	85	50	65	65	55
τ_2, sec	115	100	55	75	30	25

V_r = Flame-spread rate

τ_1 = Time from ignition to flame front that covers half the sample length

τ_2 = Time from flow shutoff to flame extinguishment

TABLE 1.5.—PRELIMINARY SCHEDULE FOR MATERIAL-FLAMMABILITY EVALUATION IN SKOROST ON *MIR* (FLOW VELOCITY, CM/SEC).

Material	Ignition	Sample I		Sample II			Sample III			Sample IV		
		$l<1/2$	rest of the sample	$l<1/3$	$l<2/3$	rest of the sample	$l<1/3$	$l<2/3$	rest of the sample	$l<1/3$	$l<2/3$	rest of the sample
Delrin	2	2	0	2	0.5	0	1	0.5	0	4	0.5	0
PMMA	4	4	0	4	2	0	2	1	0	1	0.5	0
Polyethylene	10	10	0	10	8	6	8	6	4	6	4	2

l = fraction of sample length

TABLE 1.6.—ATMOSPHERIC CHEMICAL COMPOSITION MEASURED AT THE SKOROST OUTLET — FROM SPECIAL TESTING ON GROUND

Sample #	Conditions	Concentration of saturated hydrocarbons, mg/m^3	Concentration of unsaturated hydrocarbons, mg/m^3	Concentration of O_2 (% of total)	Concentration of CO_2 (% of total)
Delrin	background	0.6	0.3	20.3	0.4
"	combustion	4.5	0.2	20.2	0.3
Polyurethane	background	1.3	0.14	20.1	0.4
"	combustion	0.4	0.12	20.0	0.5
Nylon	background	0.4	0.16	20.3	0.3
"	combustion	1.1	0.1	20.5	0.2
High-density Polyethylene	background	0.6	0.12	20.3	0.3
"	combustion	0.7	0.11	20.3	0.4
PMMA	background	0.4	0.12	20.2	0.7
"	combustion	0.6	0.15	20.0	0.7
Glass-epoxy	background	0.4	0.13	20.3	0.7
"	combustion	0.7	0.1	20.2	0.7
Final reading	background	0.4	0.08	20.1	0.7

TABLE 2.1.—ACTUAL SCHEDULE FOR MATERIAL-FLAMMABILITY
EVALUATION IN SKOROST ON *MIR*

Material	Sample #	Flow Velocity, cm/sec				
		Ignition	First length of sample	Second length of sample	Third length of sample	Balance of zample
Delrin	1	2.0	1.0	0.0*	– – –	– – –
	2	4.0	1.0	0.5	0.0*	– – –
	3	4.0	2.0	0.3	0.0*	– – –
	4	4.0	7.0	0.3	0.0*	– – –
PMMA	5	2.0	2.0	0.0*	– – –	– – –
	6	2.0	1.0	0.5*	– – –	– – –
	7	2.0	8.5	0.5	0.0*	– – –
	8	2.0	4.0	0.75	0.5*	– – –
High-Density Polyethylene	9	8.5	8.5	0.0*	– – –	– – –
	10	8.5	4.0	2.0	1.0	0.0*
	11	8.5	2.0	1.0	0.5*	– – –
	12	8.5	1.0	0.5	0.3*	– – –

*This is the flow velocity and sample length where the flame extinguished eventually

TABLE 3.1.—SUMMARY OF TIME (τ_s) FROM FLOW SHUTOFF TO FLAME EXTINGUISHMENT FOR CYLINDRICAL SAMPLES IN
SPACE AND ON GROUND

Material	Delrin				PMMA				Polyethylene			
Sample number	1	2	3	4	5	6	7	8	9	10	11	12
τ_s, sec, in microgravity	130	24	13	19	11	a $V_{lim} = 0.5$ cm/sec	15	a $V_{lim} = 0.5$ cm/sec	10	0	a $V_{lim} = 0.5$ cm/sec	a $V_{lim} = 0.3$ cm/sec
τ_s, sec, on the ground	115				30				55			

ªFlame extinguished before flow shutoff, *i.e.*, $V_{lim} > V$.
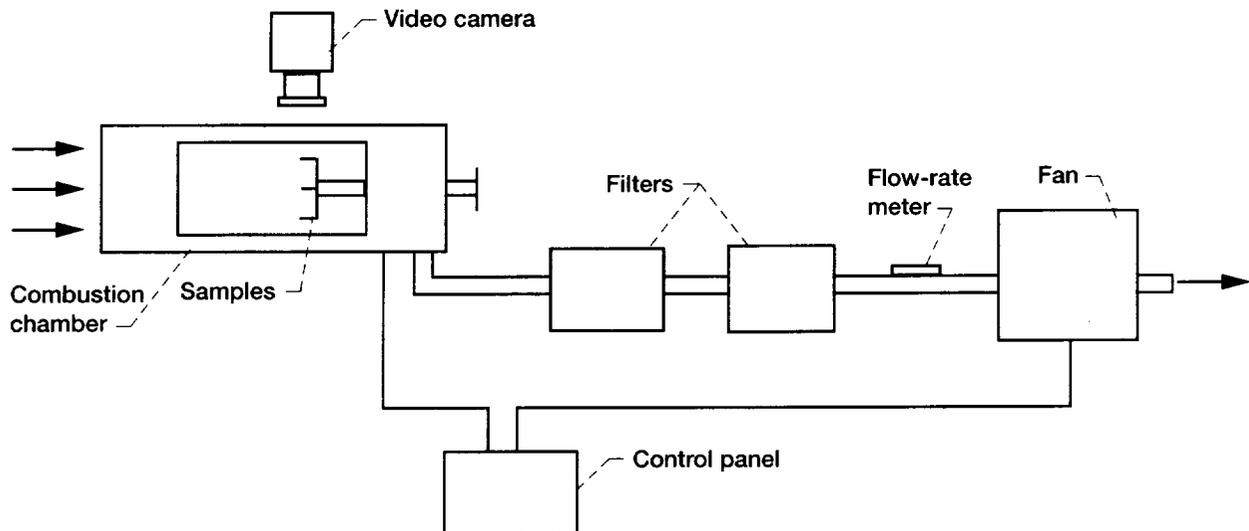
Figure 1.1.—Schematic of Experimental Facility *Skorost*.
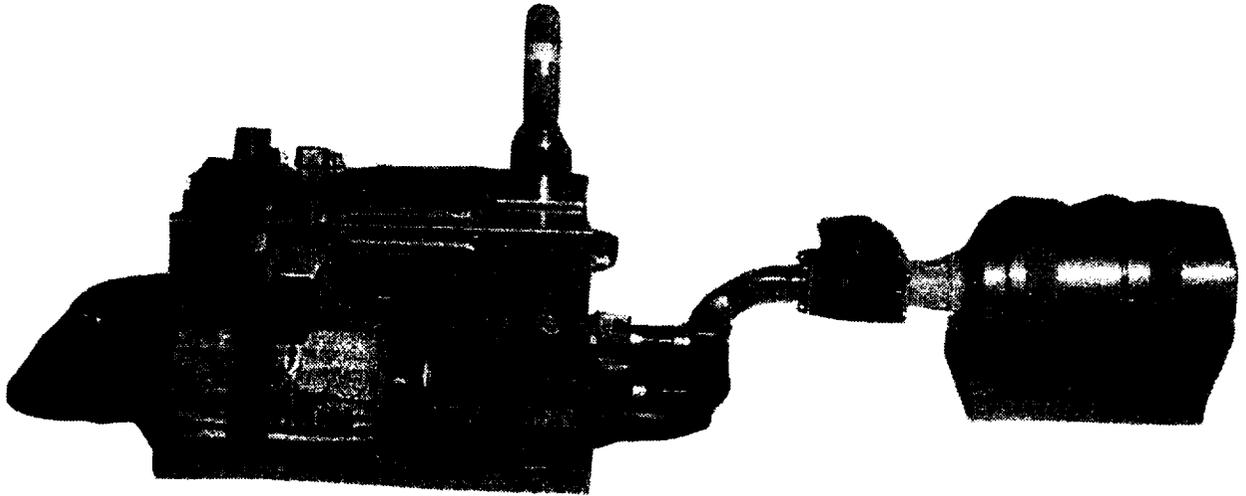
Figure 1.2.—General view of Experimental Facility *Skorost* (without control panel).
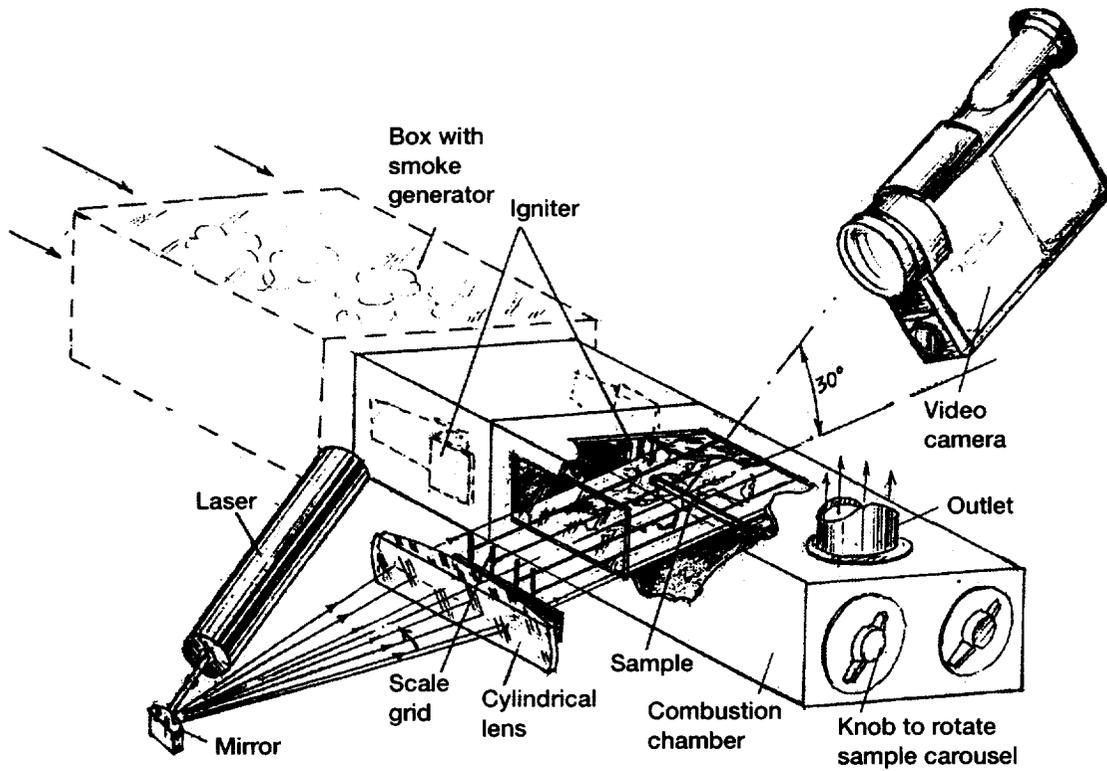
Figure 1.3.—Sketch of optical system to measure airflow velocity in Experimental Facility *Skorost* by smoke visualization.
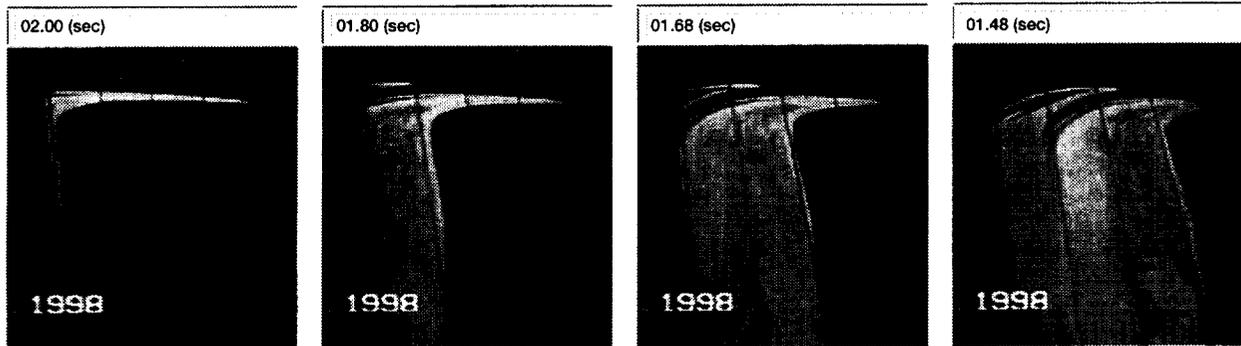
Figure 1.4.—Movement of smoke blobs in *Skorost* as visualized by laser illumination. Sequence is from right to left; grid lines are 1-cm apart. In this illustration, the velocity determined from smoke blobs is 6 cm/sec.
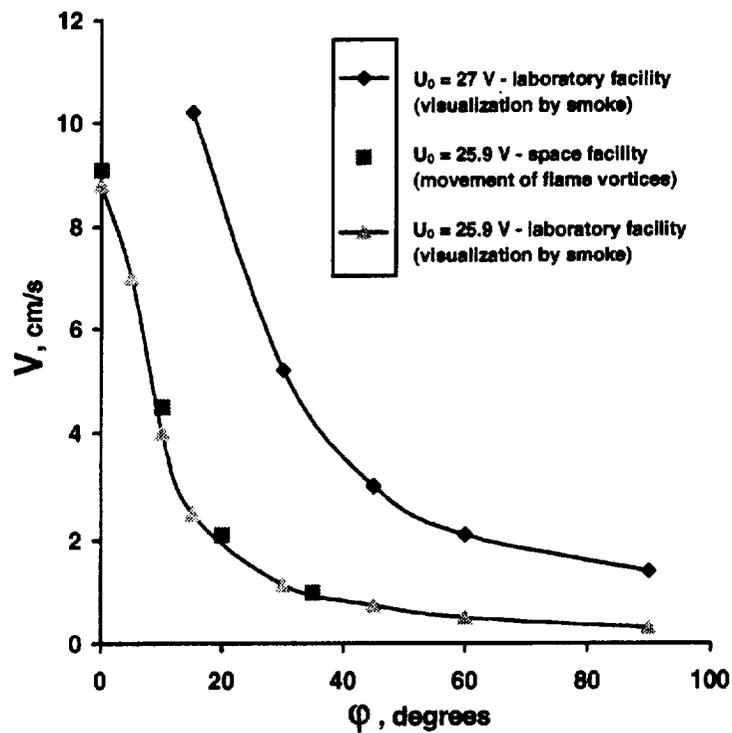
Figure 1.5.—*Skorost* air flow-velocity calibrations, based on ground measurements (smoke visualization) and space measurements (flame vortex drift).
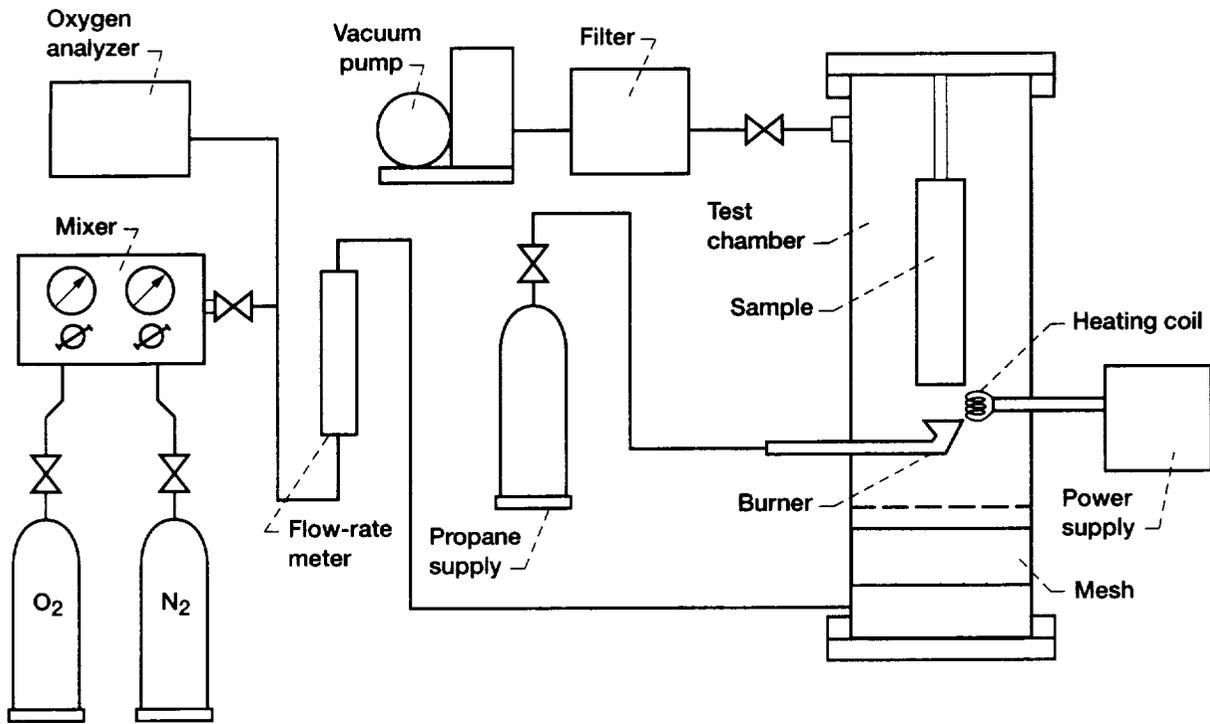
Figure 1.6.—Schematic of apparatus for the evaluation of limiting oxygen concentration (C_{lim}).
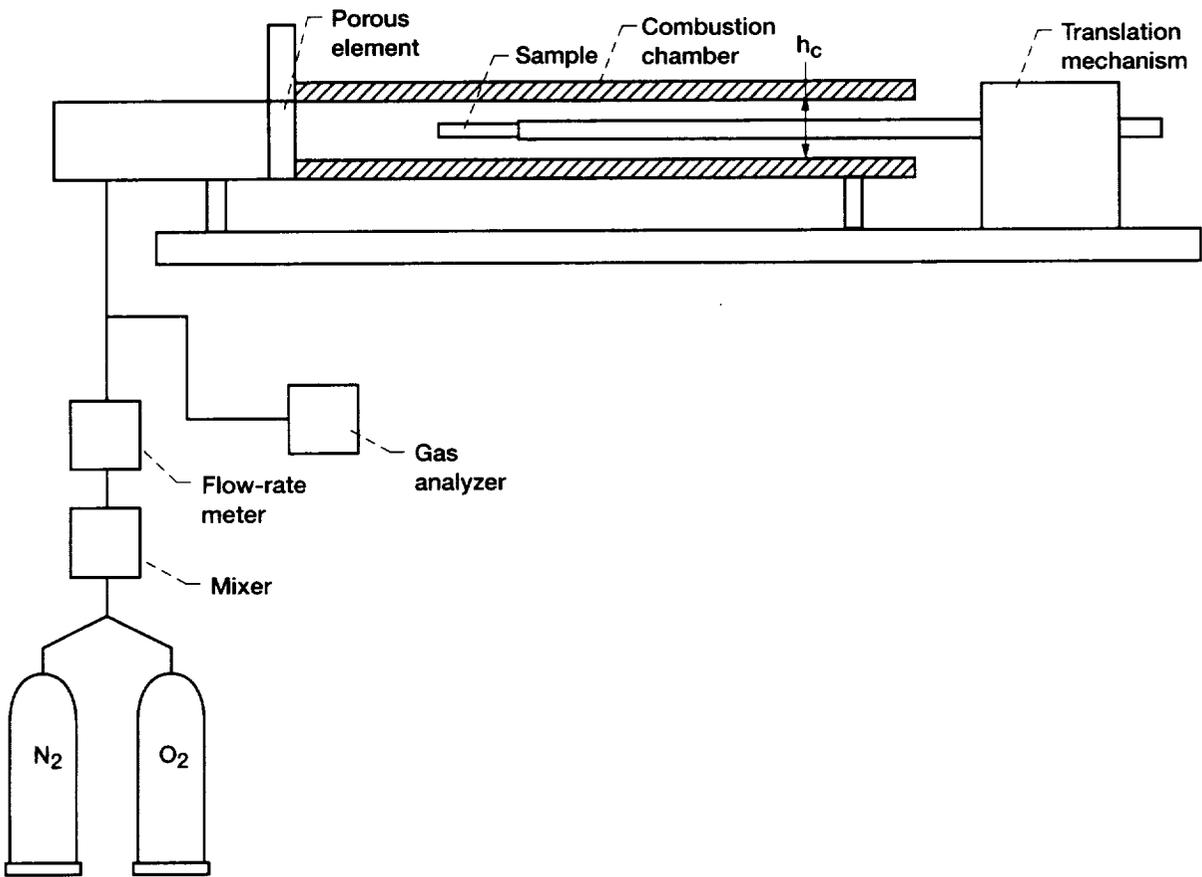
Figure 1.7.—Schematic of Narrow Channel apparatus.
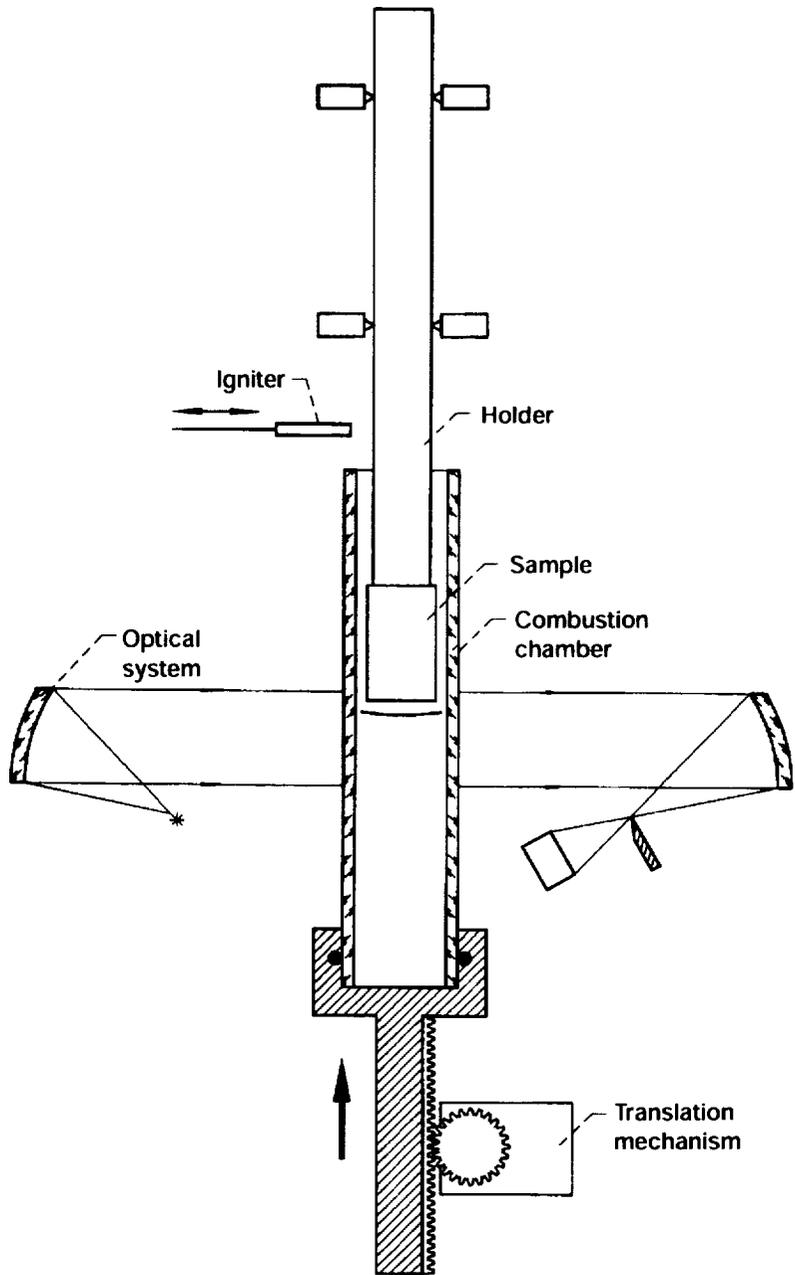
Figure 1.8.—Schematic of Vertical Combustion Chamber apparatus.
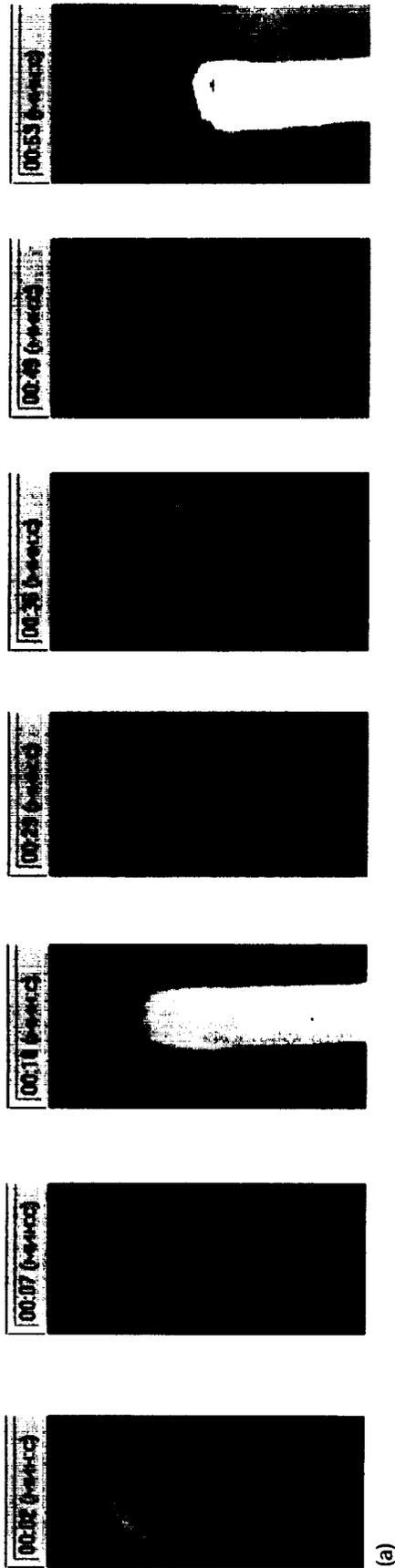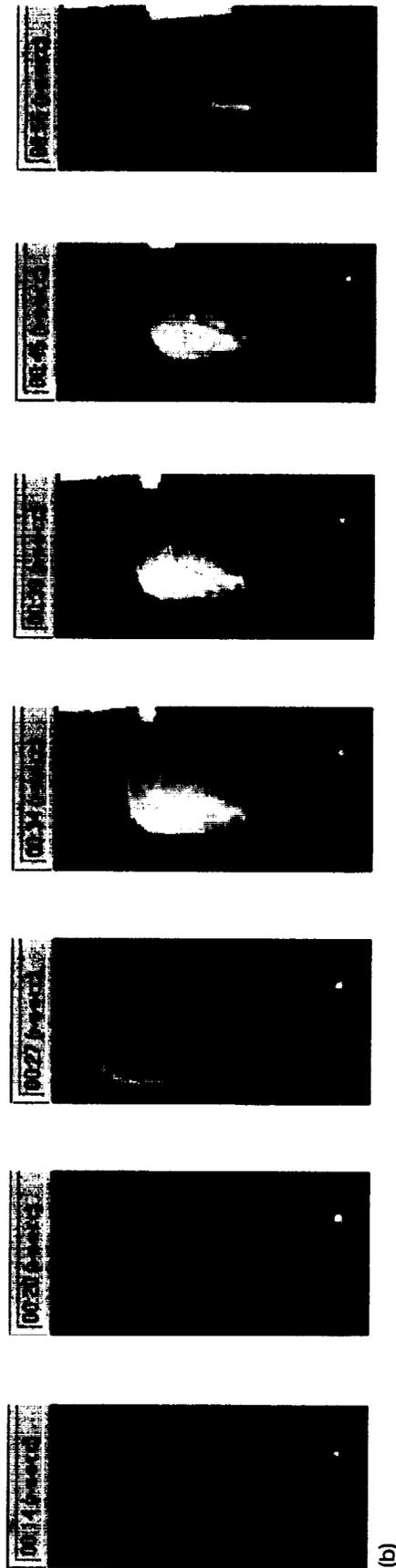
Figure 1.9.—Photographs of Delrin combustion in Experimental Facility *Skorost* operated on the ground in a vertical orientation. Elapsed times are from left to right, and they are indicated in min:sec. (a) Cylindrical sample. (b) Strip sample.

(a)

(b)
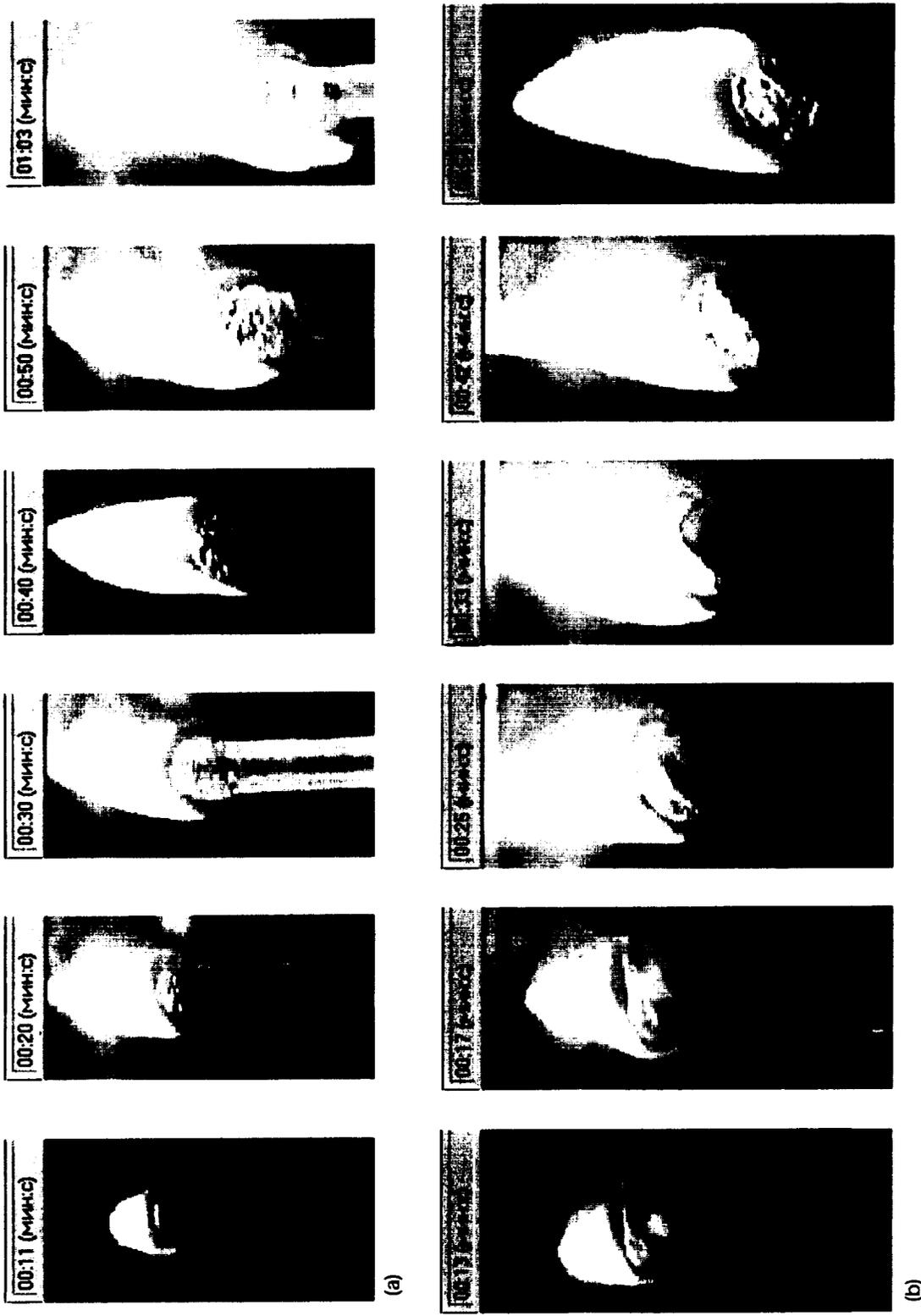
Figure 1.10.—Photographs of PMMA combustion in *Skorost* operated on the ground in a vertical orientation. Elapsed times are from left to right, and they are indicated in min:sec. (a) Cylindrical sample. (b) Strip sample.
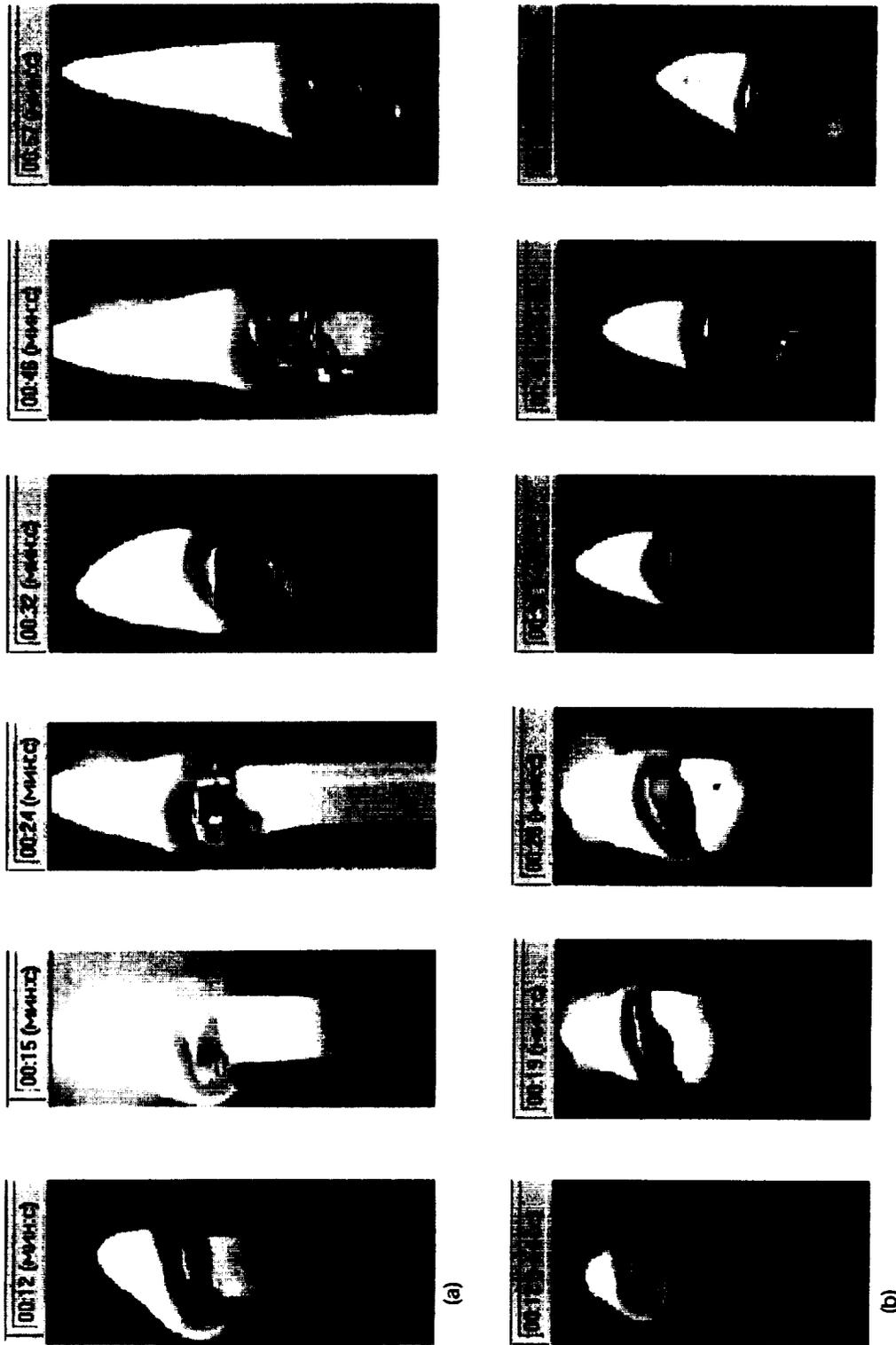
Figure 1.11.—Photographs of high-density polyethylene combustion in *Skorost* operated on the ground in a vertical orientation. Elapsed times are from left to right, and they are indicated in min:sec. (a) Cylindrical sample. (b) Strip sample.
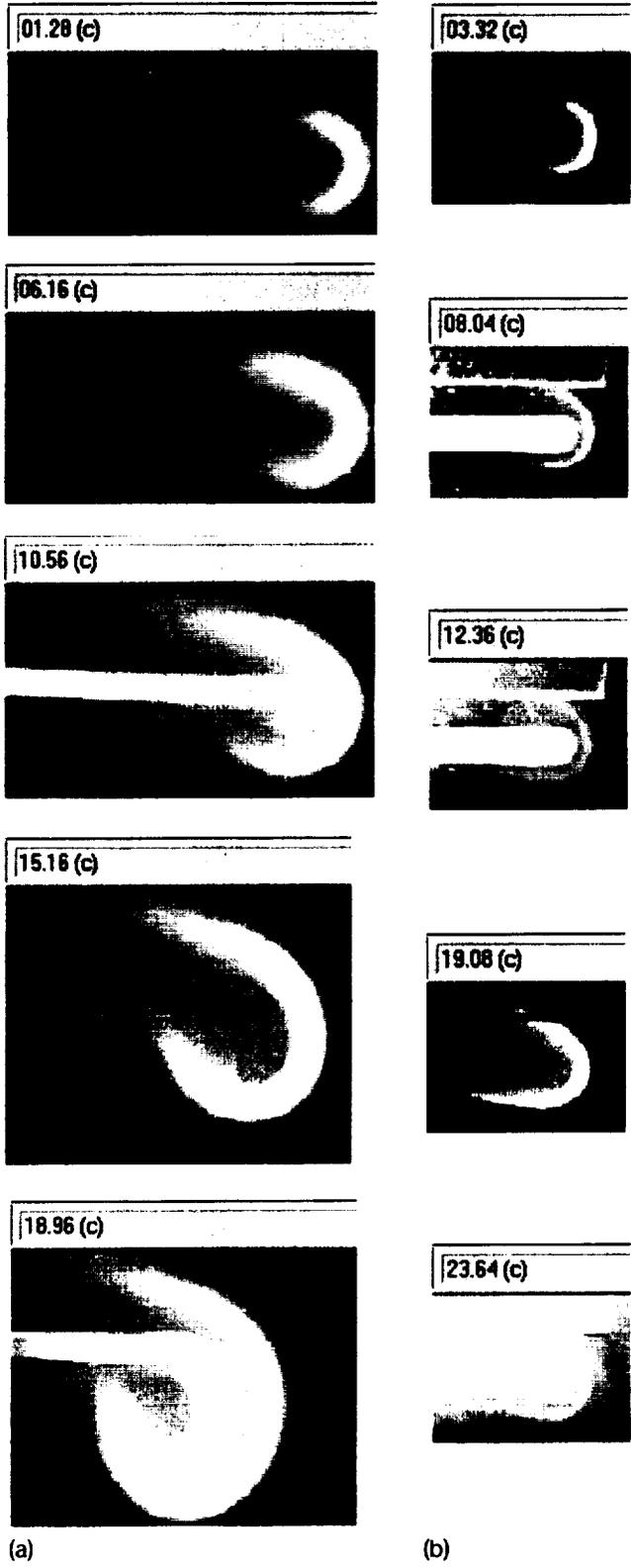
Figure 1.12.—Photographs of Delrin combustion in *Skorost*
on the ground in a horizontal orientation. Elapsed times
are from top to bottom, and they are indicated in sec.
(a) Strip sample. (b) Cylindrical sample.
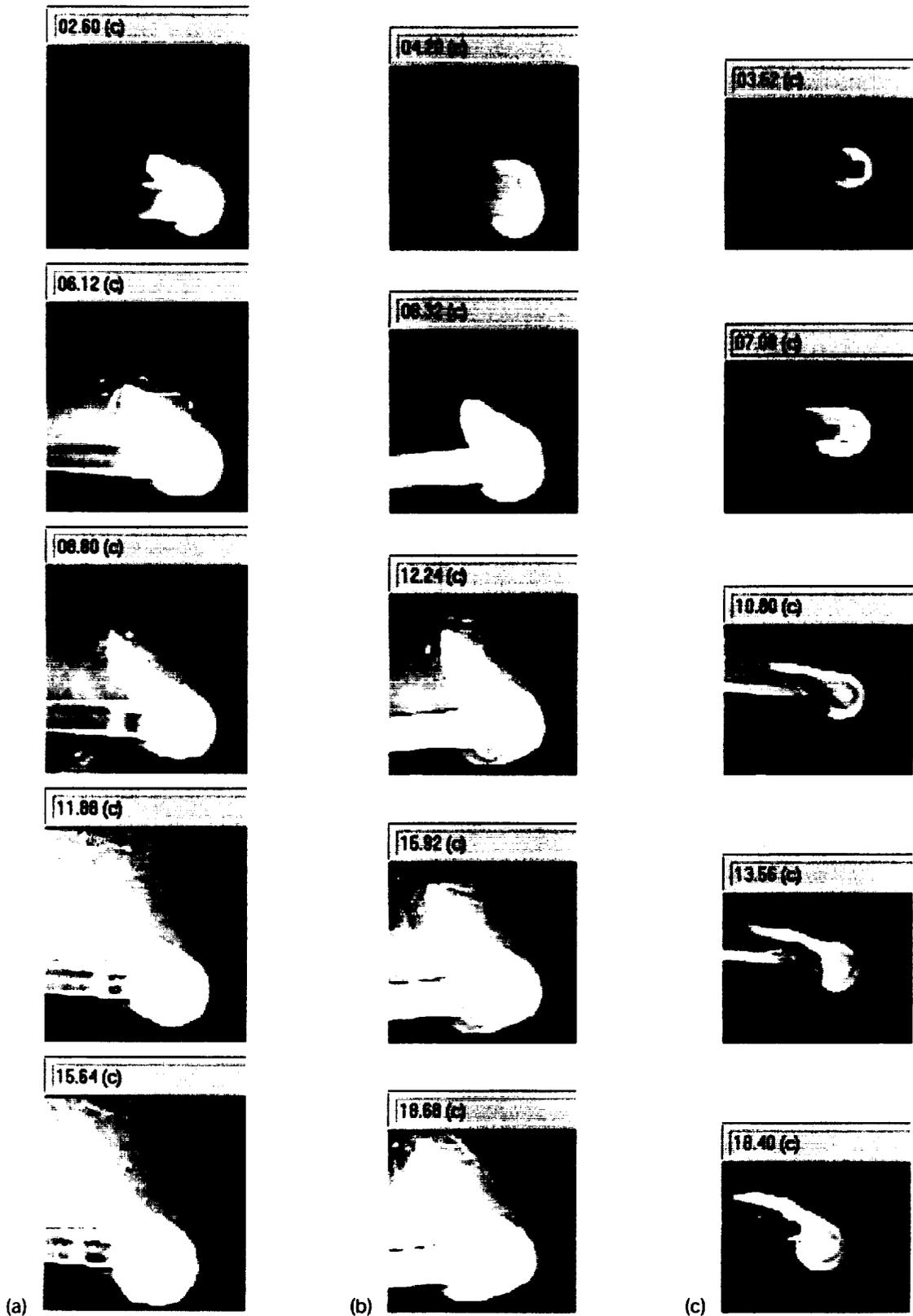
Figure 1.13.—Additional photographs of combustion in *Skorost* operated on the ground in a horizontal orientation. Elapsed times are from top to bottom, and they are indicated in sec. (a) PMMA cylindrical sample. (b) High-density polyethylene cylindrical sample. (c) High-density polyethylene strip sample.
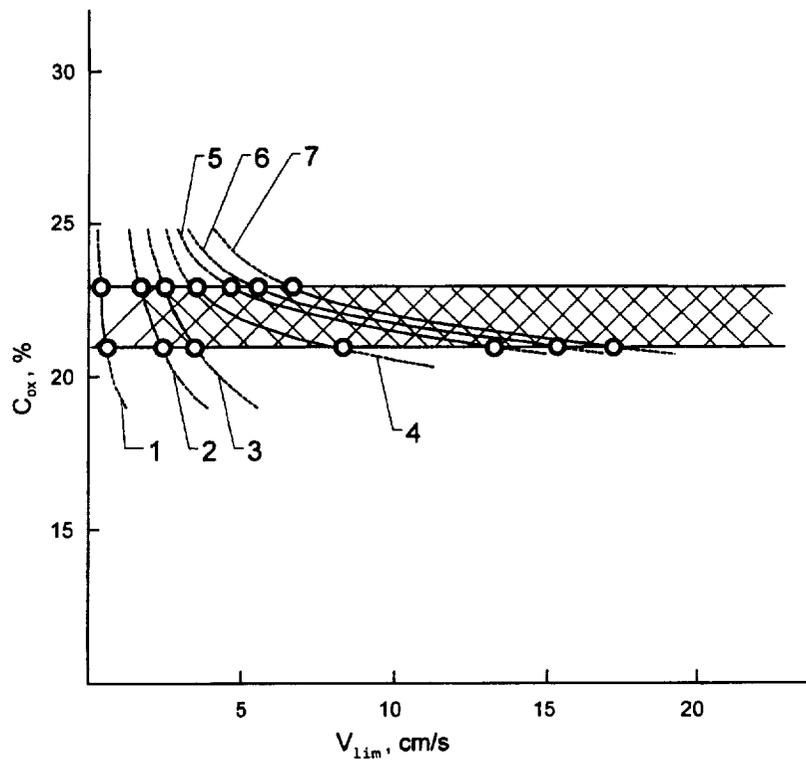
Figure 1.14.—Map of limiting flow velocity (V_{lim}) determined as a function of oxygen concentration (C_{ox}) from ground tests. Circles are data; cross-hatched region is expected range of C_{ox} for *Mir*. Fuels are 1–Delrin; 2–Russian PMMA; 3–U.S. PMMA; 4–high-density polyethylene; 5–polyurethane; 6–Nylon; 7–low-density polyethylene.
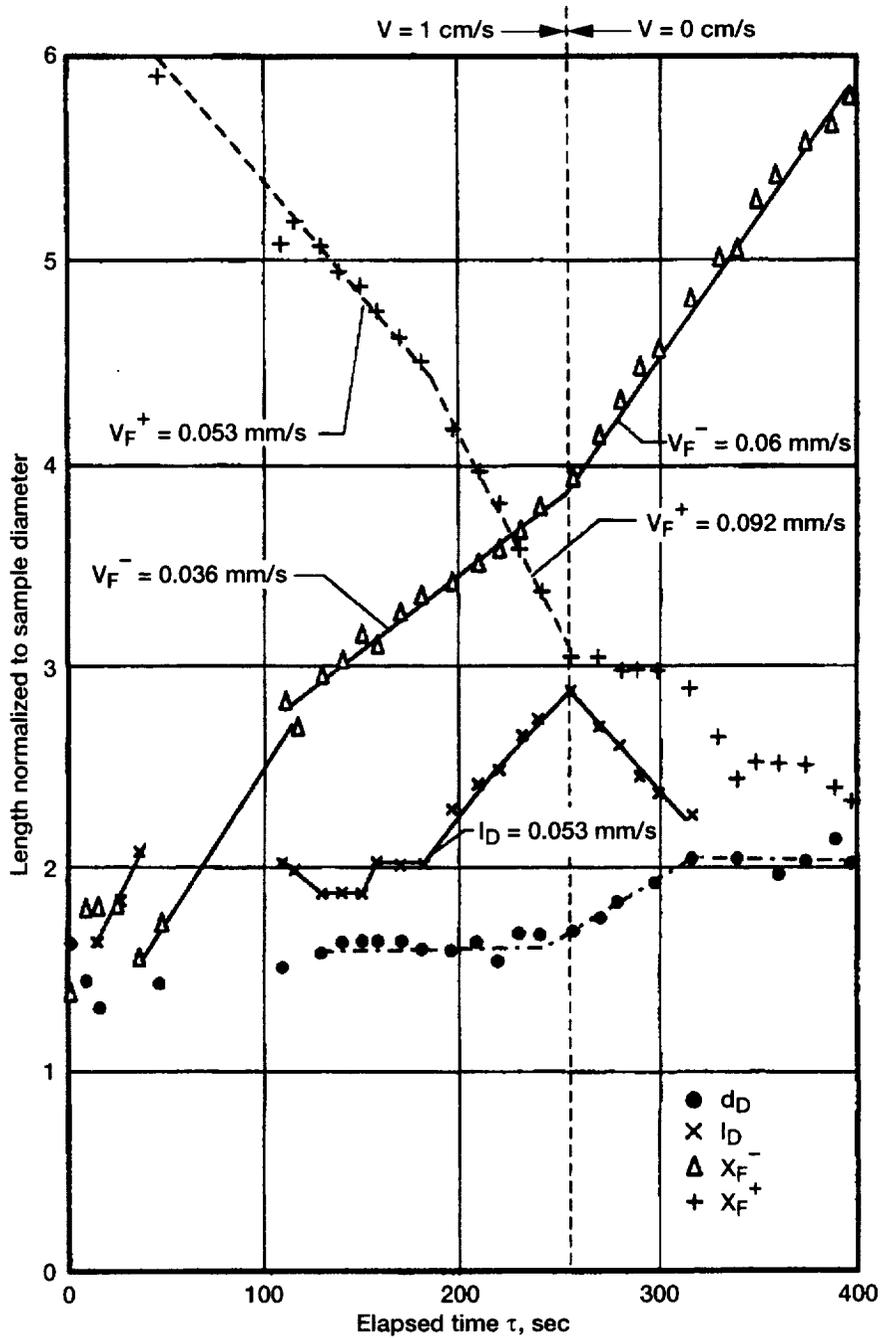
Figure 3.1.—The dynamics of Delrin sample #1 combustion with concurrent air flow in microgravity on Experimental Facility *Skorost*.
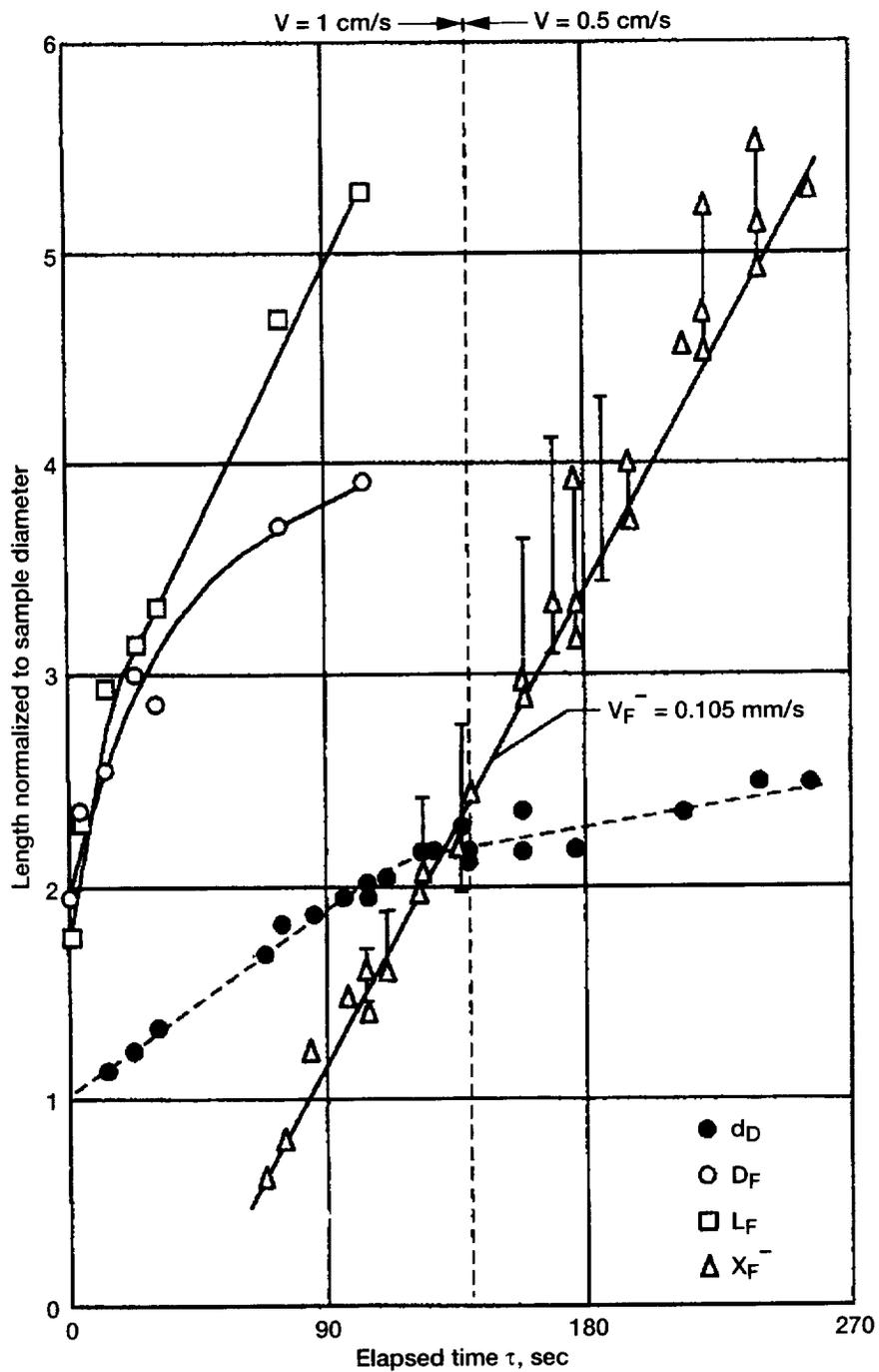
Figure 3.2.—The dynamics of Delrin sample #2 combustion with concurrent air flow in microgravity on *Skorost*.
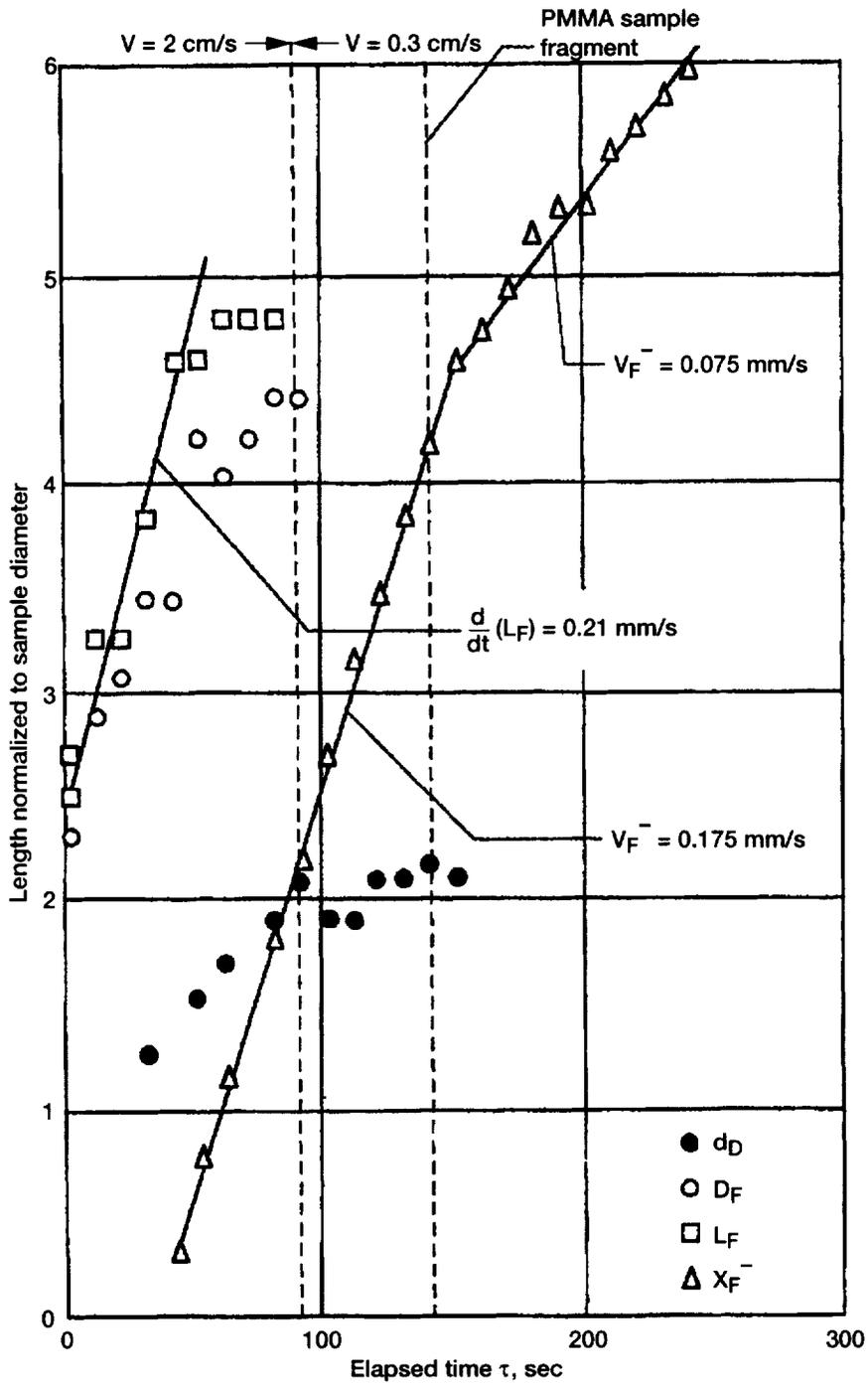
Figure 3.3.—The dynamics of Delrin sample #3 combustion with concurrent air flow in microgravity on *Skorost*.
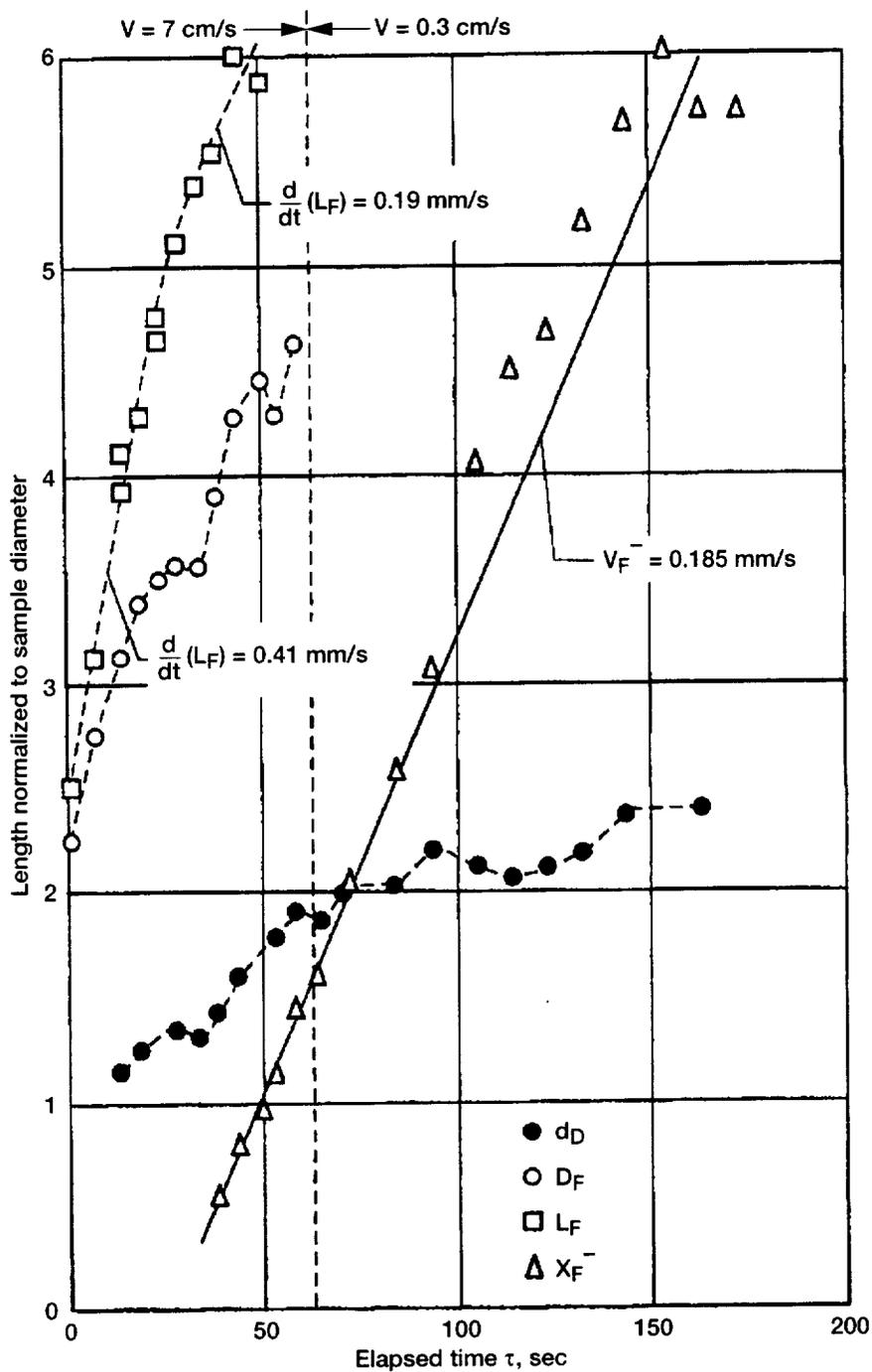
Figure 3.4.—The dynamics of Delrin sample #4 combustion with concurrent air flow in microgravity on *Skorost*.
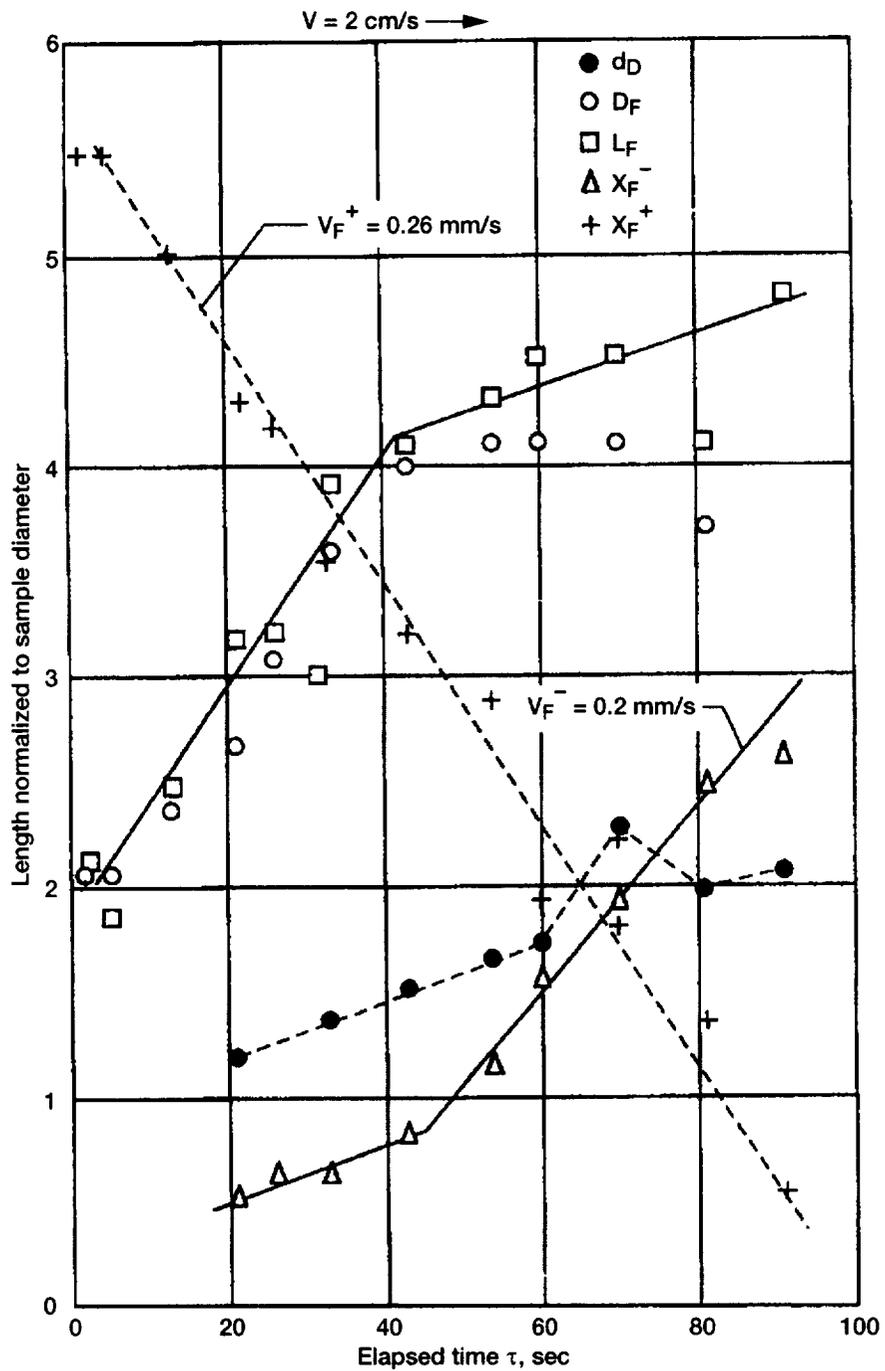
Figure 3.5.—The dynamics of PMMA sample #5 combustion with concurrent air flow in microgravity on *Skorost*.
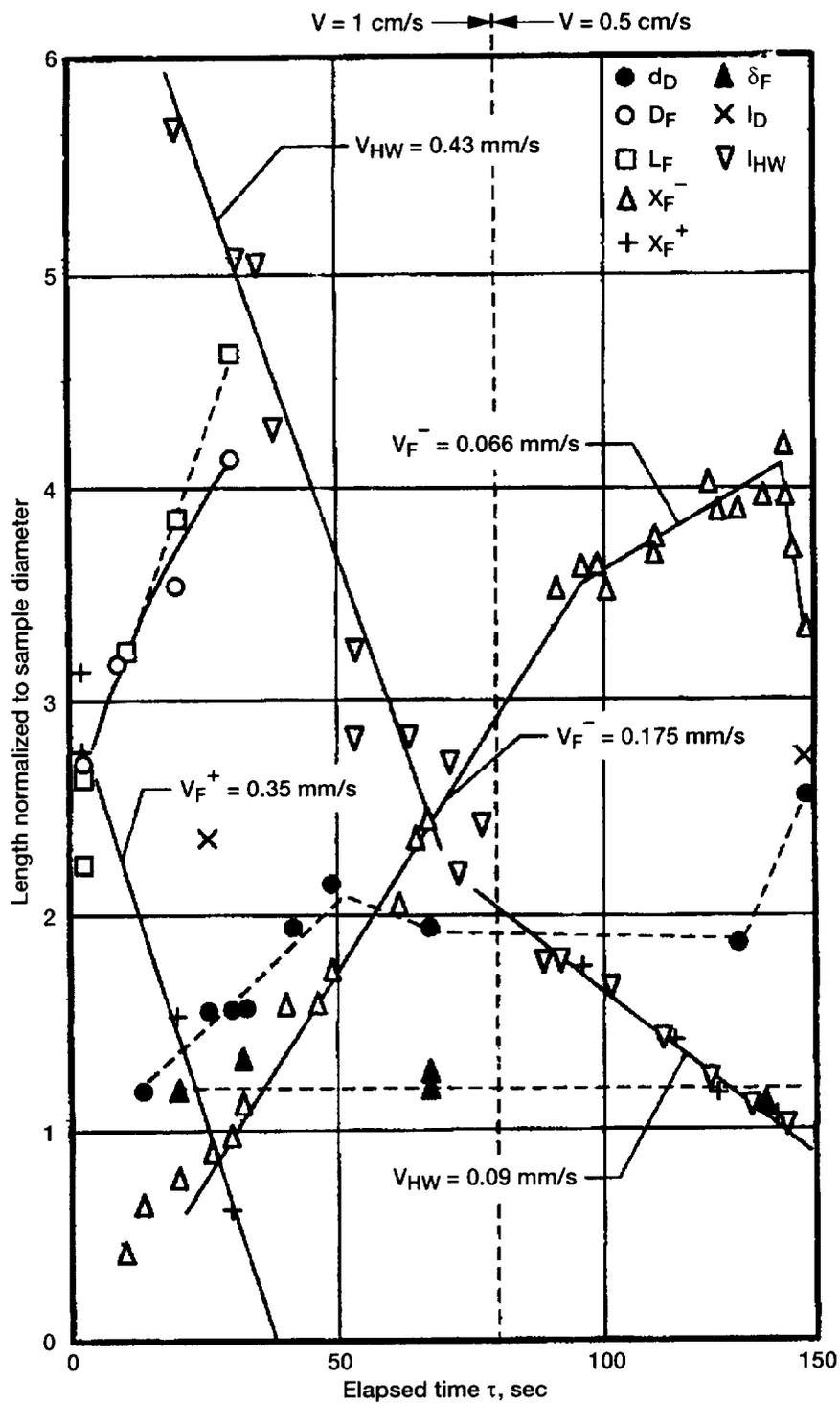
Figure 3.6.—The dynamics of PMMA sample #6 combustion with concurrent air flow in microgravity on *Skorost*.
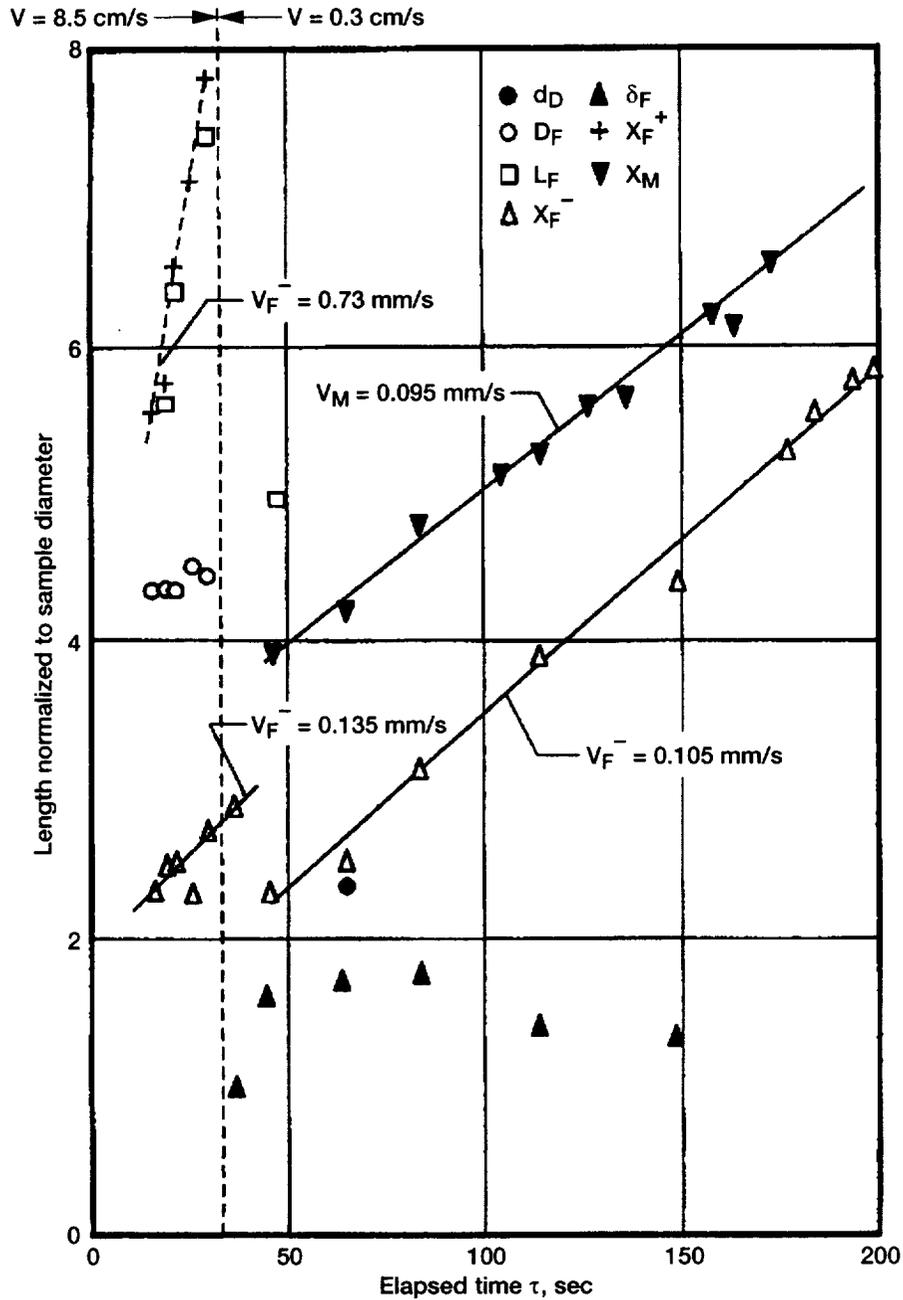
Figure 3.7.—The dynamics of PMMA sample #7 combustion with concurrent air flow in microgravity on *Skorost*.
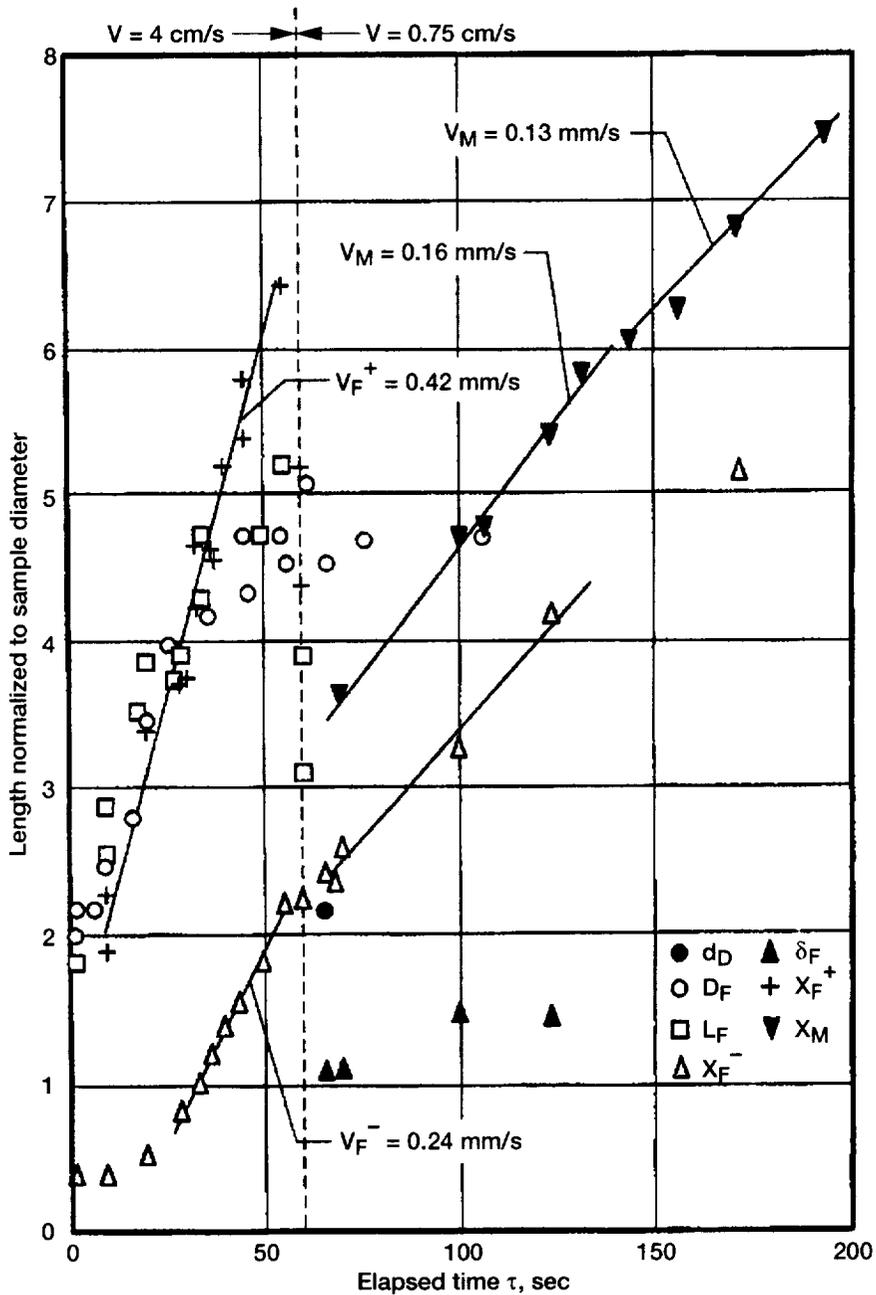
Figure 3.8.—The dynamics of PMMA sample #8 combustion with concurrent air flow in microgravity on *Skorost*.
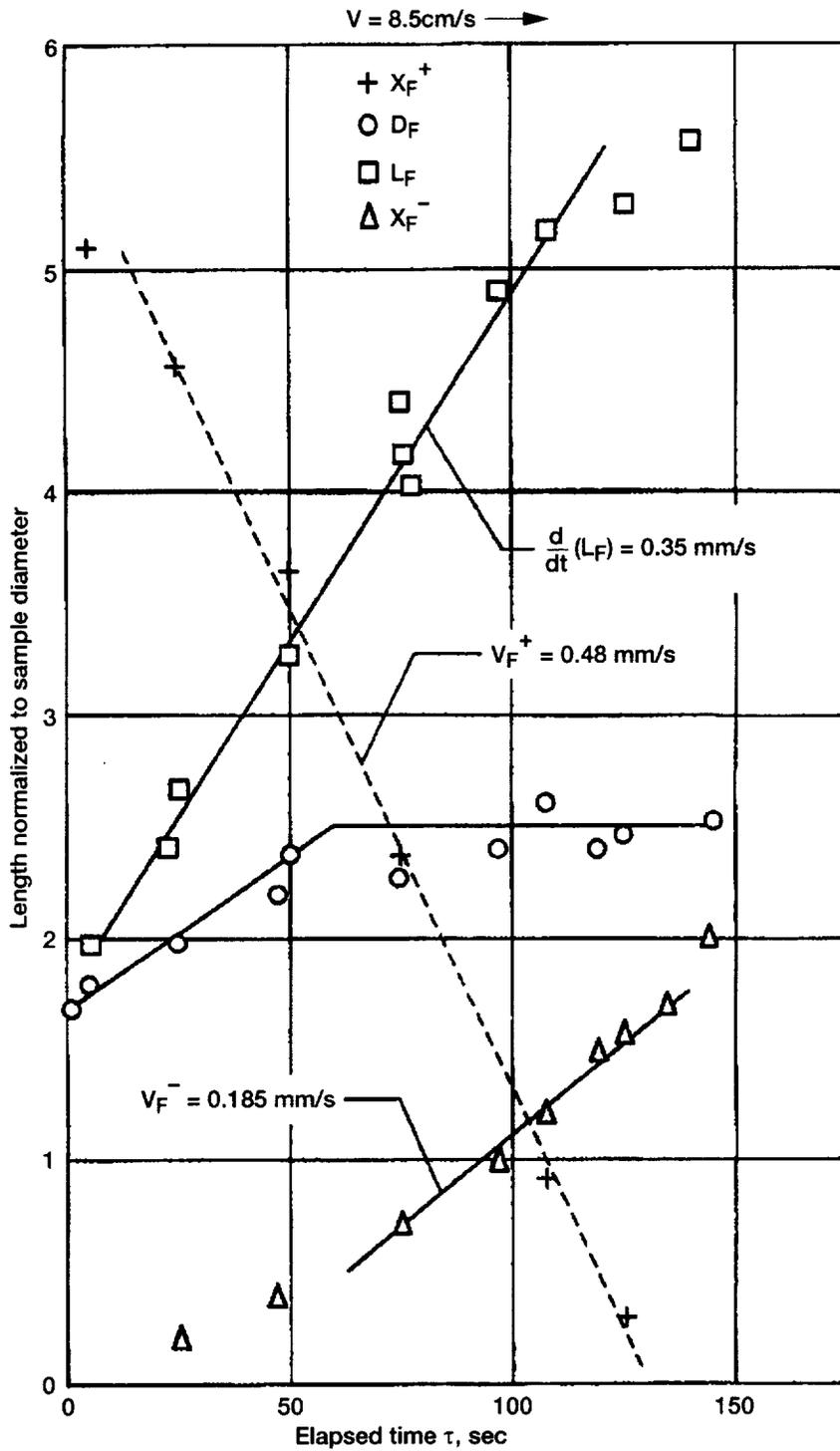
Figure 3.9.—The dynamics of High-Density Polyethylene sample #9 combustion with concurrent air flow in microgravity on *Skorost*.
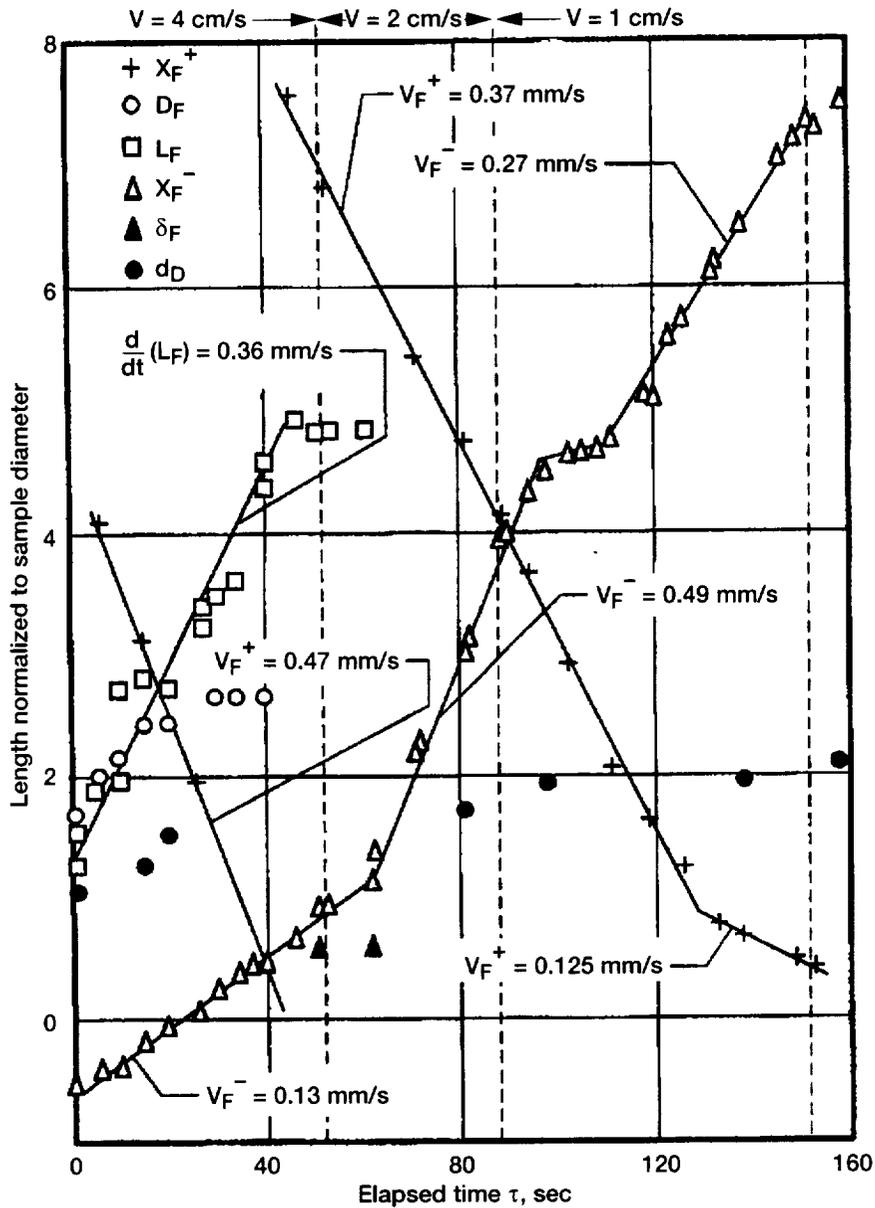
Figure 3.10.—The dynamics of High-Density Polyethylene sample #10 combustion with concurrent air flow in microgravity on *Skorost*.
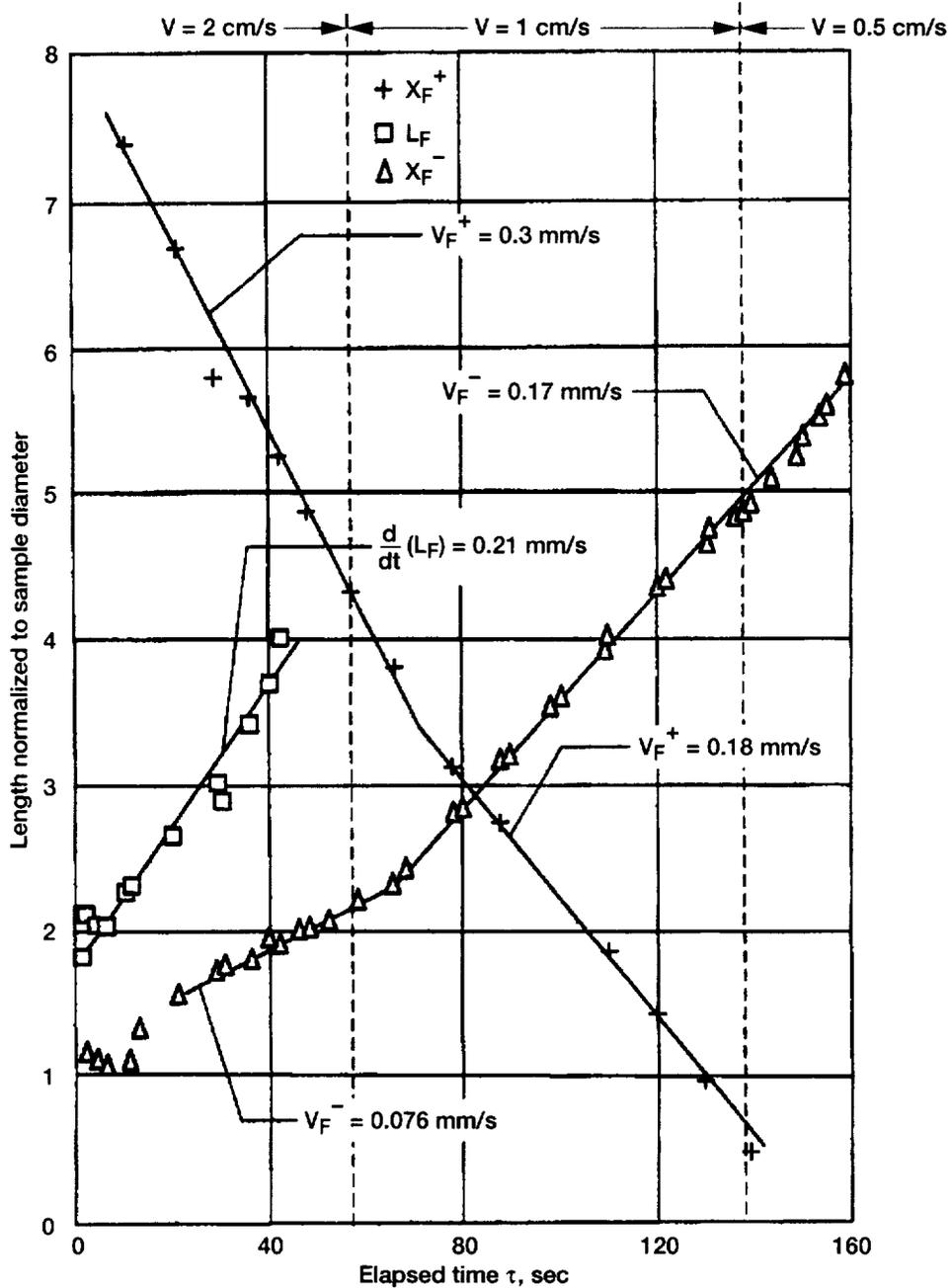
Figure 3.11.—The dynamics of High-Density Polyethylene sample #11 combustion with concurrent air flow in microgravity on *Skorost*.
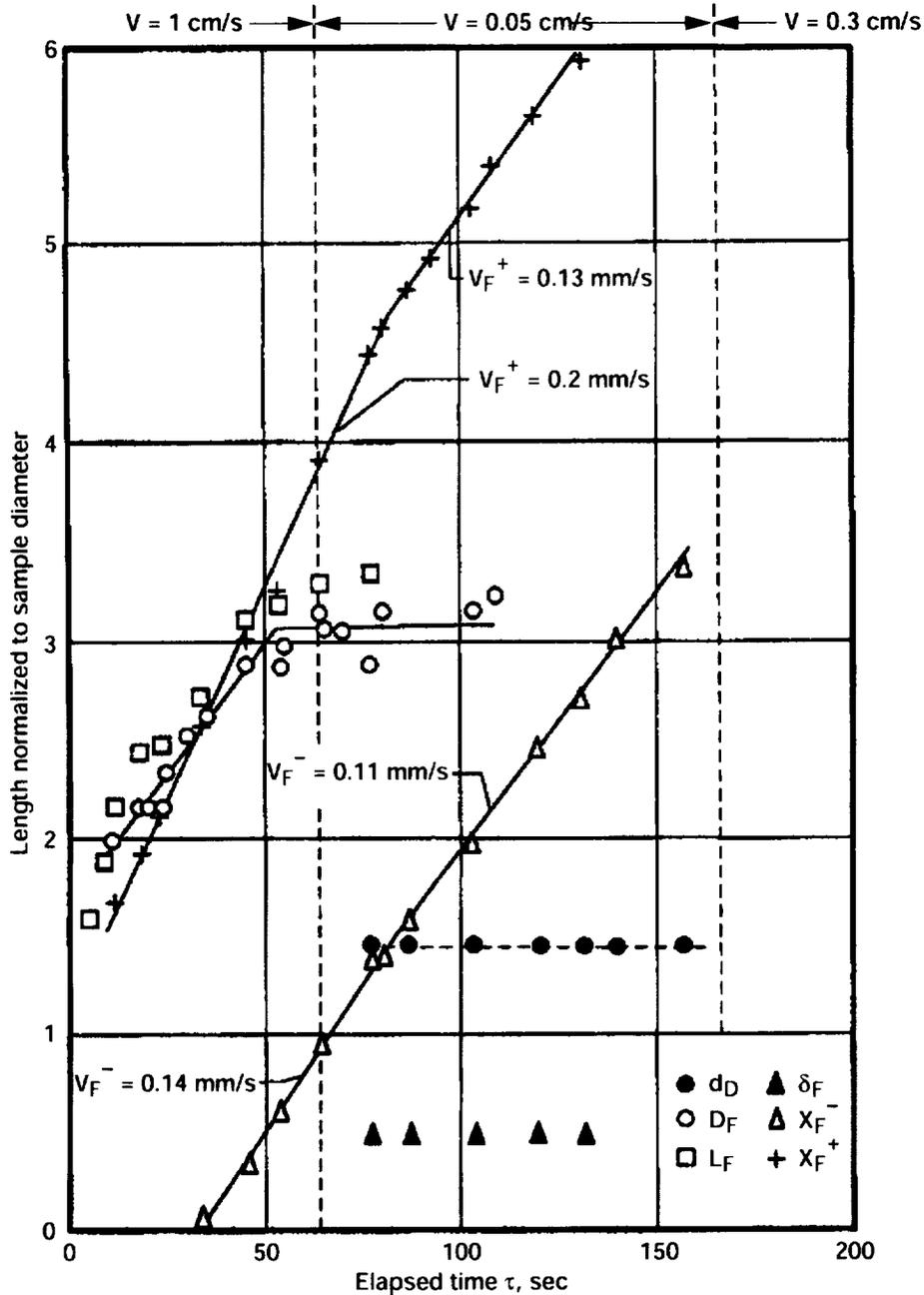
Figure 3.12.—The dynamics of High-Density Polyethylene sample #12 combustion with concurrent air flow in microgravity on *Skorost*.

Figure 3.13.—Photograph of formation of melt drop during combustion of Delrin sample #1 in microgravity with concurrent air flow of 1 cm/sec on Experimental Facility *Skorost*. Flame is almost invisible.

Figure 3.16.—Formation of melt drop during combustion of Delrin sample #4 in microgravity with concurrent air flow of 0.3 cm/sec on *Skorost*. Flame is nearly invisible.
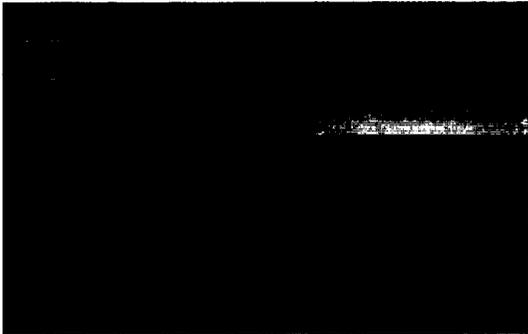
Figure 3.14.—Formation of melt drop during combustion of Delrin sample #2 in microgravity with concurrent air flow of 0.5 cm/sec on *Skorost*. Flame is almost invisible.

Figure 3.17.—Bright white spherical flame during combustion of PMMA sample #5 in microgravity with concurrent air flow of 2 cm/sec on *Skorost*.

Figure 3.15.—Strong blue flame during combustion of Delrin sample #4 in microgravity with concurrent air flow of 7 cm/sec on *Skorost*.

Figure 3.18.—Tiny melt drops in the heated portion of PMMA sample #5 (center) in microgravity on *Skorost*.
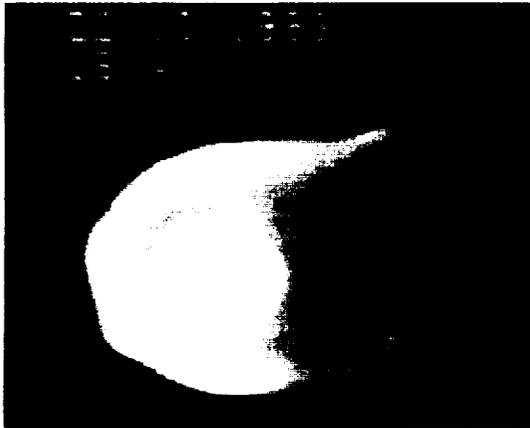
Figure 3.19.—Bright white flame during com-
bustion of PMMA sample #7 in microgravity
with concurrent air flow of 8.5 cm/sec on
Skorost.

Figure 3.20.—Bright white flame during combustion
of High-Density Polyethylene sample #9 in micro-
gravity with concurrent air flow of 8.5 cm/sec
Skorost.
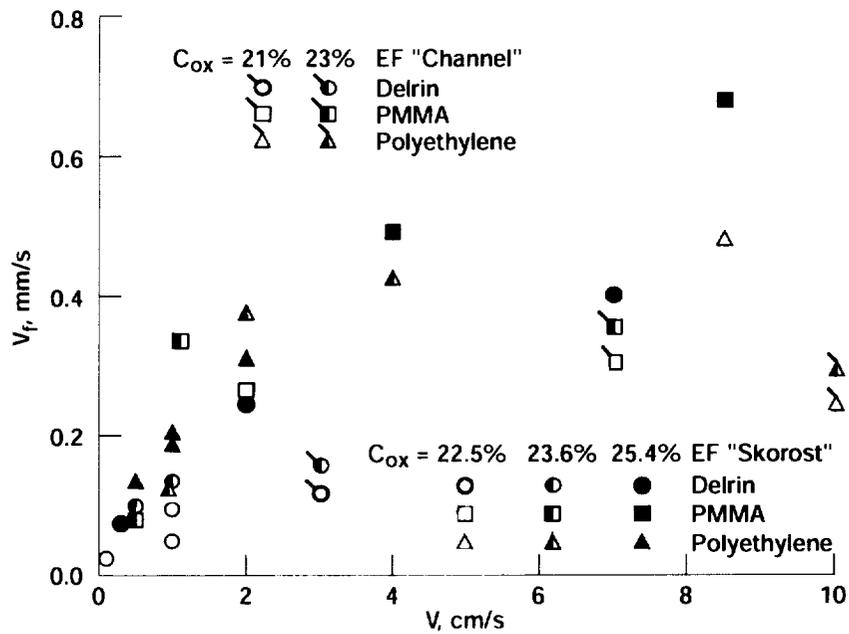
Figure 3.21.—Flame-spread rate (V_f^+) for test samples as function of con-
current flow velocity (V), measured on space on the *Skorost* apparatus
and on ground on the Narrow-Channel apparatus.

51
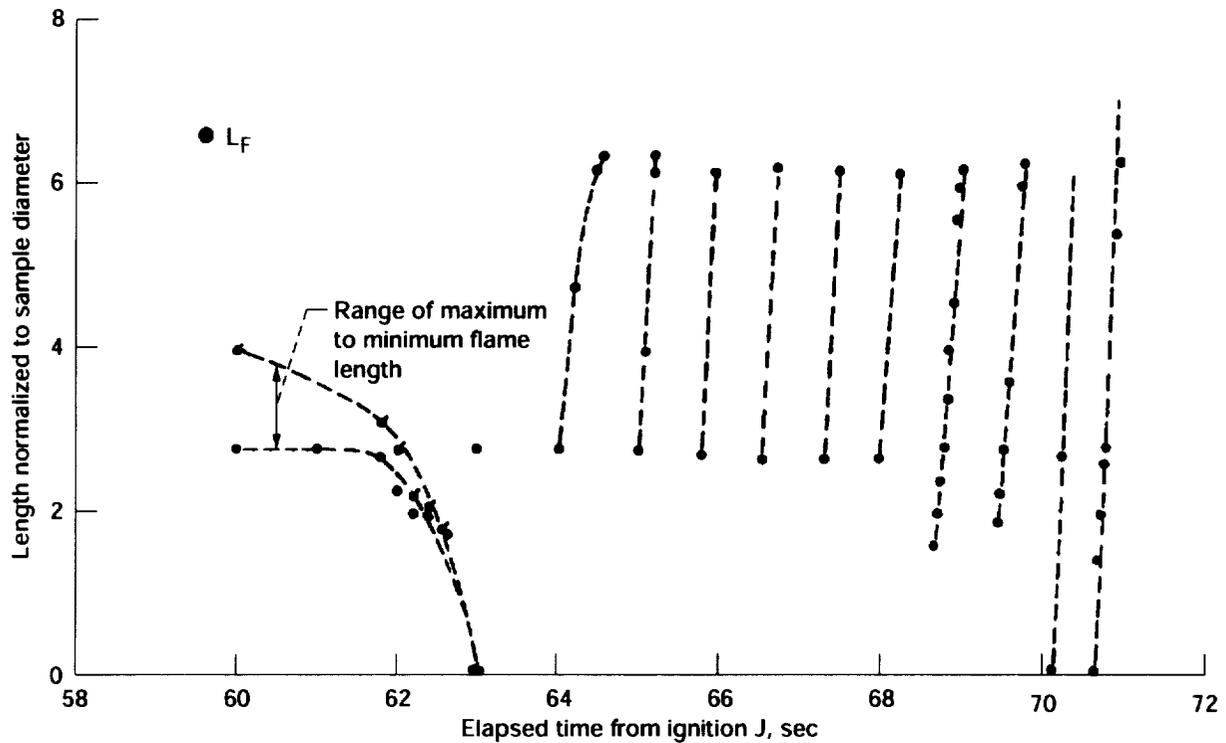
Figure 3.22.—White flame-length (L_F) decrease and subsequent blue flame-length fluctuations after fan turnoff at τ = 60 sec for High-Density Polyethylene sample #9 in microgravity on *Skorost*.

Figure 3.23.—Longitudinal flame oscillations during combustion of High-Density Polyethylene sample #9 in microgravity after flow shutdown on *Skorost*. Photograph illustrates minimum flame length.
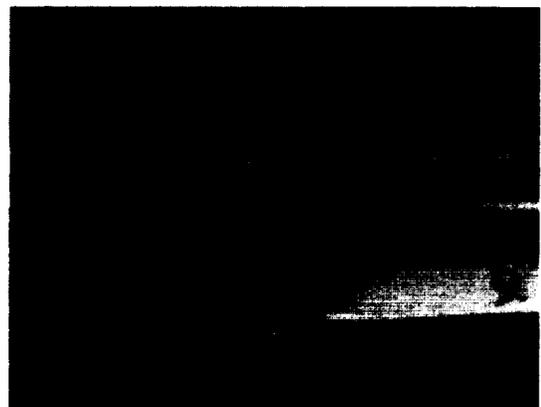
Figure 3.24.—Longitudinal flame oscillations during combustion of High-Density Polyethylene sample #9 in microgravity after flow shutdown on *Skorost*. Photograph illustrates maximum flame length.
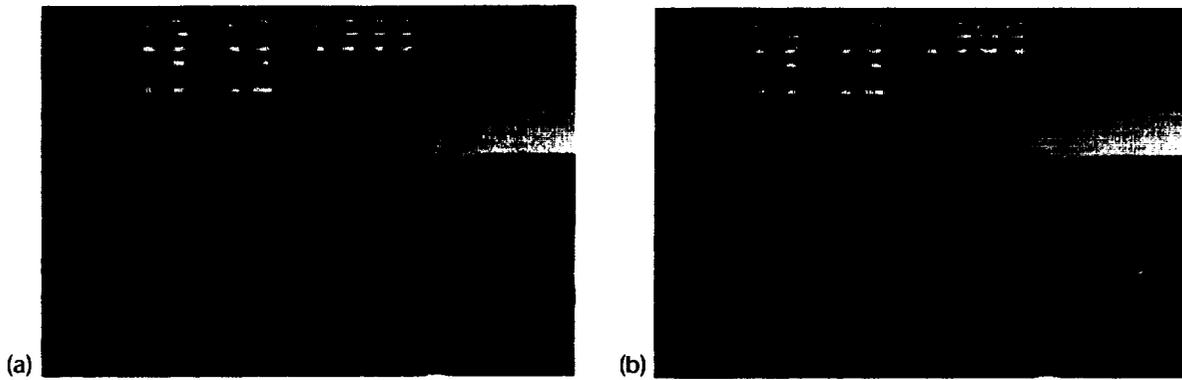
Figure 3.25.—Formation of flame tail from gaseous fuel ejection from bursting bubble in melt drop during combustion of Delrin sample #2 in microgravity with concurrent air flow of 0.5 cm/sec on *Skorost*. (a) Jet ejection. (b) Jet ignition after 0.04 sec.
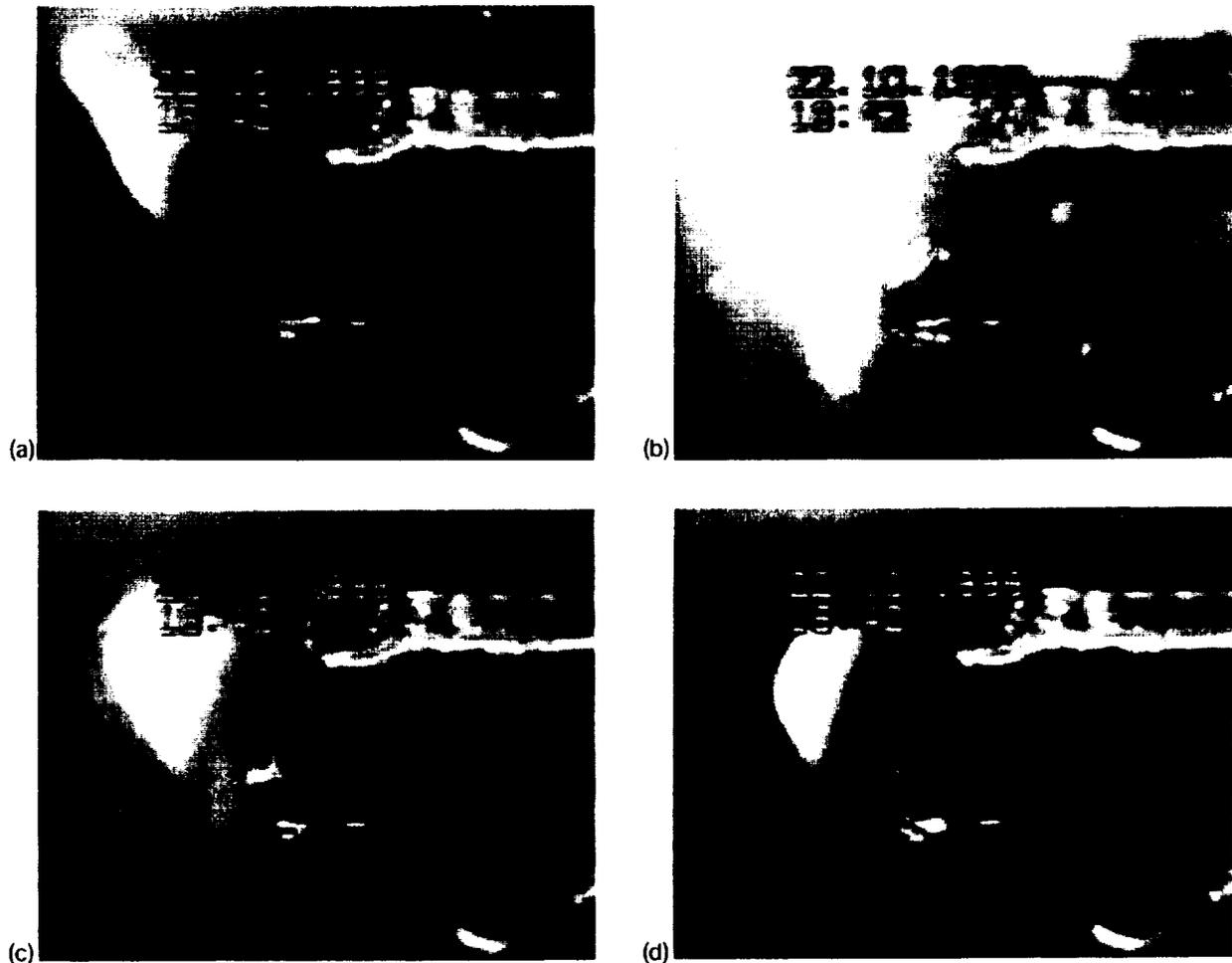
Figure 3.26.—Formation and decay of flame tail from gaseous fuel ejection from melt drop during combustion of PMMA sample #7 in microgravity with concurrent air flow of 0.5 cm/sec on *Skorost*. (a) Initial appearance, $\tau = 0$. (b) $\tau = 0.04$ sec. (c) $\tau = 0.12$ sec. (d) $\tau = 0.20$ sec.
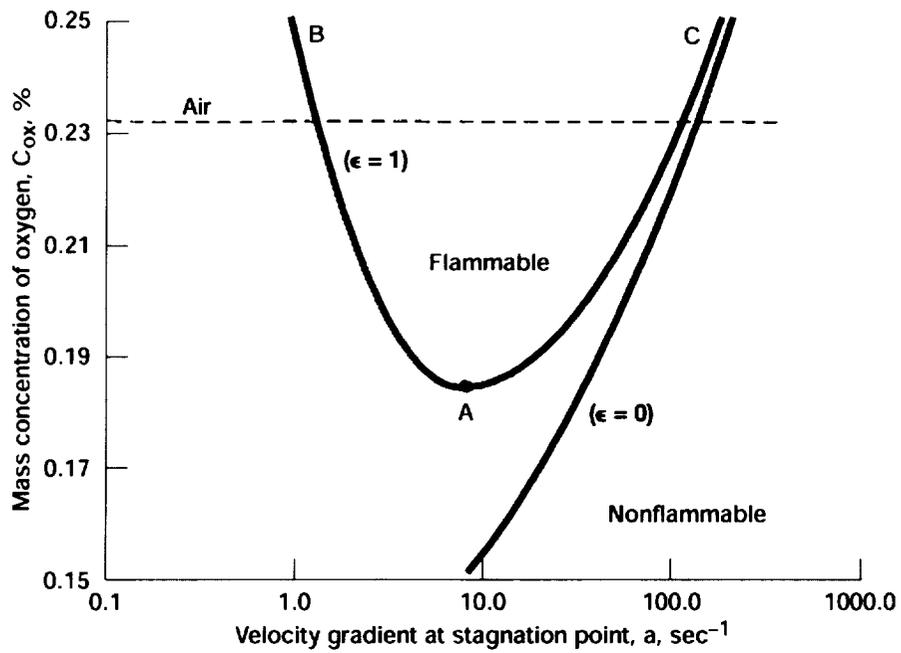
Figure 5.1.—Flammability map for PMMA samples for emissivity (ε) values of 0 and 1. Curve AB is locus for flame extinction due to quenching (radiation loss); curve AC is locus for flame extinction due to blowout (insufficient reaction time).

REPORT DOCUMENTATION PAGE

1. AGENCY USE ONLY (Leave blank)	2. REPORT DATE	3. REPORT TYPE AND DATES COVERED
	November 1999	Final Contractor Report

4. TITLE AND SUBTITLE

Experimental Verification of Material Flammability in Space

5. FUNDING NUMBERS

WU–398–95–0F–00
NAS3–97160

6. AUTHOR(S)

A.V. Ivanov, Ye.V. Balashov, T.V. Andreeva, and A.S. Melikhov

7. PERFORMING ORGANIZATION NAME(S) AND ADDRESS(ES)

Keldysh Research Center
Moscow, Russia

8. PERFORMING ORGANIZATION REPORT NUMBER

E–11932

9. SPONSORING/MONITORING AGENCY NAME(S) AND ADDRESS(ES)

National Aeronautics and Space Administration
John H. Glenn Research Center at Lewis Field
Cleveland, Ohio 44135–3191

10. SPONSORING/MONITORING AGENCY REPORT NUMBER

NASA CR—1999-209405

11. SUPPLEMENTARY NOTES

12a. DISTRIBUTION/AVAILABILITY STATEMENT

Unclassified - Unlimited
Subject Category: 27   Distribution: Nonstandard

This publication is available from the NASA Center for AeroSpace Information, (301) 621–0390.

12b. DISTRIBUTION CODE

13. ABSTRACT (Maximum 200 words)

The flammability in microgravity of three U.S.-furnished materials, Delrin, polymethylmethacrylate (PMMA), and high-density polyethylene, was determined using a Russian-developed combustion tunnel on Mir. Four 4.5-mm-diameter cylindrical samples of each plastic were ignited under concurrent airflow (in the direction of flame spread) with velocities from no flow to 8.5 cm/s. The test results identify a limiting air-flow velocity V_{lim} for each material, below which combustion ceases. Nominal values are V_{lim} <0.3 cm/s for Delrin, 0.5 cm/s for PMMA, and 0.3 to 0.5 cm/s for polyethylene. These values are lower than those obtained in prior ground testing. Nevertheless, they demonstrate that flow shutoff is effective for extinguishment in the microgravity environment of spacecraft. Microgravity test results also show that the plastic materials maintain a stable melt ball within the spreading flame zone. In general, as the concurrent flow velocity V decreases, the flame-spread rate V_F decreases, from an average (for all three materials) of V_F = 0.5-0.75 mm/s at V = 8.5 cm/s to V_F = 0.05-0.01 mm/s at V = 0.3-0.5 cm/s. Also, as V decreases, the flames become less visible but expand, increasing the probability of igniting an adjacent surface.

14. SUBJECT TERMS

Extinction; Fire safety; Flammability; Flammability limits; Flame propagation; Microgravity applications

15. NUMBER OF PAGES

62

16. PRICE CODE

A04

17. SECURITY CLASSIFICATION OF REPORT	18. SECURITY CLASSIFICATION OF THIS PAGE	19. SECURITY CLASSIFICATION OF ABSTRACT	20. LIMITATION OF ABSTRACT
Unclassified	Unclassified	Unclassified	